Lara Gião Fidalgo

Licenciada em Bioquímica

Sulfonate and Acetyl Derivatives of the Vasopressin Antagonist Tolvaptan: Reactivity Towards DNA and 2'-deoxynucleosides

Dissertação para obtenção do Grau de Mestre
em Química Bioorgânica

Orientador: Doutora Alexandra Maria Antunes, Investigadora Principal, CQE-IST
Elemento de Ligação Externa: Doutora Paula Cristina Branco, Professora Auxiliar, FCT-UNL

Júri:

Presidente: Doutora Ana Maria Lourenço
Arguente: Doutora Maria Matilde Marques
Vogal: Doutora Alexandra Maria Antunes

FACULDADE DE CIÊNCIAS E TECNOLOGIA
UNIVERSIDADE NOVA DE LISBOA

Dezembro 2015

Lara Gião Fidalgo

Licenciada em Bioquímica

Sulfonate and Acetyl Derivatives of the Vasopressin Antagonist Tolvaptan: Reactivity Towards DNA and 2'-deoxynucleosides

Dissertação para obtenção do Grau de Mestre
em Química Bioorgânica

Orientador: Doutora Alexandra Maria Antunes, Investigadora Principal, CQE-IST
Elemento de Ligação Externa: Doutora Paula Cristina Branco, Professora Auxiliar, FCT-UNL

Júri:

Presidente: Doutora Ana Maria Lourenço
Arguente: Doutora Maria Matilde Marques
Vogal: Doutora Alexandra Maria Antunes

FACULDADE DE CIÊNCIAS E TECNOLOGIA
UNIVERSIDADE NOVA DE LISBOA

Dezembro 2015

Sulfonate and Acetyl Derivatives of the Vasopressin Antagonist Tolvaptan: Reactivity Towards DNA and 2'-deoxynucleosides

Agradecimentos

Em primeiro lugar, gostaria de agradecer à minha orientadora, Dr.ª Alexandra Antunes, por me ter permitido desenvolver a tese de mestrado no seu laboratório, bem como às oportunidades de aprendizagem por ela proporcionadas. Quero também agradecer à Dr.ª Matilde Marques por toda a disponibilidade e ajuda prestadas.

Quero ainda agradecer à Faculdade de Ciências e Tecnologia da Universidade Nova de Lisboa, por todos os bons e maus momentos proporcionados e por todo o ambiente e profissionais qualificados que me permitiram crescer profissional e pessoalmente, ajudando a moldar a pessoa que sou hoje.

Seguidamente, quero agradecer aos meus colegas de laboratório Ana Godinho, Inês Martins, Catarina Charneira, Shrika Harjivan e aos "não tão" colegas de bancada Pedro Pinheiro, Ana Dias e João Nunes, por todo o conhecimento partilhado, paciência demonstrada, ajuda prestada, e palavras amigas. Quero ainda agradecer aos colegas do "Grupo V", Ivânia, Joana, Pedro, Sara e Tiago, por toda a boa disposição, companhia e ajuda prestadas.

Quero agradecer a todos os colegas e amigos, em especial aos que mais me apoiaram nesta jornada, sem os quais a mesma não teria sido possível, de seu nome: Catarina Correia, colega de bancada, amiga e muito mais e Alexander Van Halderen.

Às minhas meninas, Ana Inês, Raquel e Cláudia, por terem estado comigo durante os melhores piores seis anos da minha vida, um grande obrigada.

À minha "família" por terras algarvias, obrigada por todas as noites não dormidas, 2.º e 3.º jantares, pequenos almoços e demais refeições. Dizem que dos sete para cima é para a vida, então que assim seja, sempre mais e melhor.

Em último lugar, e sem dúvida o mais importante, quero expressar a minha gratidão à minha família, que ainda que longe, me mantiveram sempre por perto. À minha mãe, pela inspiração, força de vontade, perseverança, alegria e por tudo e mais alguma coisa. Às minhas irmãs, Íris e Patrícia, por estarem sempre presentes, ainda que em margens ou continentes diferentes. Aos meus avós, Hermínia e Fernando, por todo o incansável apoio e abastecimento de chocolates. Ao meu pai, por me ter incutido a paixão e rigor necessários a esta área. E ao Carlos, por todos os anos de amizade.

"*If Not Now, When?*" - **Incubus**

Resumo

O fármaco **tolvaptan** é um antagonista não peptídico dos recetores de arginina vasopressina V_2, utilizado para o tratamento de hiponatremia euvolémica e hipervolémica. No entanto, a utilização deste fármaco está associada a efeitos adversos graves, nomeadamente um elevado risco de lesões hepáticas, o que levou a *FDA (U. S. Food and Drug Administration)* a emitir um aviso quanto à sua toxicidade (*black box label warning*).

Estudos preliminares, em linhas celulares hepáticas, sugerem que o **tolvaptan** induz lesões no ADN sem intervenção da atividade metabólica de Fase I, por parte do citocromo P450 (CYP). Tendo em conta que as reações metabólicas de Fase II, envolvendo a sulfonação e acetilação do álcool secundário do **tolvaptan**, são acontecimentos plausíveis e não dependentes de catálise do CYP, a formação de adutos covalentes por reação destes **metabolitos de Fase II** com o ADN poderia explicar as lesões ao ADN observadas nas linhas celulares. Assim sendo, esta tese teve como objetivo a síntese dos derivados acetilado e sulfatado do **tolvaptan** (ou de modelos sintéticos destes) e o estudo da reatividade destes metabolitos com o ADN.

Uma vez que a análise de **adutos de ADN** envolve a hidrólise enzimática/térmica dos adutos com as nucleobases, seguida de análise por cromatografia líquida com deteção por espectrometria de massa (LC-ESI-MS) por comparação com adutos padrão, a primeira tarefa desta tese foi a preparação e caracterização dos adutos expectáveis da reação entre os metabolitos de Fase II do **tolvaptan** e os **2'-deoxinucleósidos**. Para tal, duas abordagens distintas foram seguidas: 1) biomimética, por reação dos derivados sulfatado e acetilado do **tolvaptan** com **2'-desoxinucleósidos**; e 2) não biomimética, envolvendo uma reação de acoplamento catalisada por paládio (0).

Na estratégia biomimética o primeiro passo consistiu na síntese e caracterização dos dois possíveis **metabolitos de Fase II** do **tolvaptan**. O **5'-*O*-acetilo- tolvaptan** foi sintetizado por reação com anidrido acético, com um rendimento de 80% e o derivado **5'-*O*-sulfonato-tolvaptan**, foi eficientemente preparado por reação com o complexo de trióxido de enxofre-piridina, com um rendimento de 89 %. O passo seguinte consistiu na reação dos metabolitos sintetizados com **2'-desoxinucleósidos,** com a finalidade de formar adutos padrão. No entanto, nenhum aduto foi identificado por análise de LC-ESI-MS destas reações. O único produto consistentemente identificado em todas as reações efetuadas em condições biomiméticas foi o produto resultante da eliminação dos grupos acetóxido e sulfóxido, com formação de uma ligação dupla.

Para a estratégia não biomimética, sintetizou-se o derivado 5'-cloro-**tolvaptan**, por reação do **tolvaptan** com cloreto de tionilo, seguido de uma reação de acoplamento, catalisada por paládio (0), entre este composto e a 3',5'-*O*-bis(*terc*butildimetilsilil)-2'-desoxiguanosina. Nesta estratégia, após desproteção dos grupos sililo, foi possível detetar por cromatografia líquida acoplada a espectrometria de massa de alta resolução (LC-ESI-HRMS) dois adutos: um despurinante e um não despurinante.

A reação dos dois possíveis metabolitos de Fase II do **tolvaptan** com o ADN foi também levada a cabo. No entanto, a análise por LC-ESI-HRMS da mistura obtida após hidrólise enzimática ou térmica, não permitiu a identificação de qualquer aduto. O que sugere que a lesão de ADN observada nas linhas celulares hepáticas não se deve à formação de adutos covalentes entre o ADN e os potenciais **metabolitos de Fase II** do **tolvaptan**, **5'-*O*-acetilo- tolvaptan** e **5'-*O*-sulfonato-tolvaptan**.

Palavras-chave: Tolvaptan, metabolitos de Fase II, adutos de ADN, 2'-desoxinucleósidos, 5'-*O*-acetilo-tolvaptan, 5'-*O*-sulfonato-tolvaptan.

Abstract

Tolvaptan is an orally effective nonpeptide arginine vasopressin (AVP) V_2-receptor antagonist, used in the treatment of clinically significant euvolemic and hypervolemic hyponatremia. Nonetheless, **Tolvaptan** was reported to be associated with a high risk of liver injury, prompting the U. S. Food and Drug Administration (FDA) to issue a black box label warning.

Whereas the mechanisms of **tolvaptan**-induced liver injury remain to be elucidated, preliminary results obtained in cytochrome P450 (CYP)-deficient liver cell lines have shown evidence of **tolvaptan**-induced DNA damage without the need for Phase I metabolism. Taking into consideration that Phase II sulfonation and/or acetylation of **tolvaptan**'s secondary alcohol are metabolically plausible events, the ultimate goal of this thesis was to study the reactivity of these putative **Phase II metabolites** towards DNA. Indeed, the covalent adducts thus afforded could explain the **tolvaptan**-induced DNA damage observed in CYP-deficient liver cell lines.

Since the identification of **DNA adducts** involves the hydrolysis to **2'-deoxynucleobase** adducts followed by liquid chromatography coupled with mass spectrometry (LC-ESI-MS) in comparison with adducts standards, the first step of this thesis was the preparation of **tolvaptan-DNA adduct** standards. Two distinct strategies were followed: 1) biomimetic, involving the reaction of the metabolic plausible sulfate and acetate **tolvaptan** metabolites with **2'-deoxynucleobases**; 2) non-biomimetic, involving a palladium-catalyzed coupling reaction.

For the biomimetic approach, the two metabolic plausible **Phase II metabolites** were first prepared: 1) **5'-*O*-sulfonate-tolvaptan** was prepared in 89 % yield upon tolvaptan sulfonation using sulfur trioxide-pyridine complex; 2) **5'-*O*-acetyl-tolvaptan** was prepared in 80% following tolvaptan acetylation with acetic anhydride and trimethylamine. The reaction of **5'-*O*-sulfonate-tolvaptan** and **5'-*O*-acetyl-tolvaptan** with 2'-deoxynucleobases (and nucleophilic amino acids) were subsequently undergone, with the ultimate goal of preparing adduct standards. However, only the product stemming from the elimination of sulfoxy and acetoxy groups was detected, upon LC-ESI-MS analysis of these reaction mixtures.

For the non-biomimetic strategy, the derivative 5'-chloro-**tolvaptan** was prepared upon reaction of **tolvaptan** with thionyl chloride, and subsequently coupled with 3',5'-*O*-bis(*tert*butyldimethylsilyl)-2'-deoxyguanosine, under palladium catalysis. Following deprotection, the LC-ESI-HRMS analysis of the reaction mixture allowed the identification of two covalent adducts, one non-depurinating and one depurinating.

The reaction of **5'-*O*-sulfonate-tolvaptan** and **5'-*O*-acetyl-tolvaptan** with DNA were also undergone. However, the LC-ESI-HRMS analysis of the hydrolysates obtained following enzymatic or thermic hydrolysis did not allow the identification of any **tolvaptan-DNA adduct**. This result suggests that the DNA damage observed in hepatic cell lines does not stem from the formation of **DNA adducts** with the metabolic plausible **Phase II metabolites**, **5'-*O*-sulfonate-tolvaptan** and **5'-*O*-acetyl-tolvaptan**.

Keywords: Tolvaptan, Phase II metabolites, DNA adducts, 2'-deoxynucleobases, 5'-*O*-acetyl- tolvaptan, 5'-*O*-sulfonate-tolvaptan.

Table of Contents

Index of Figures

Index of Tables

Abbreviations, Acronyms and Symbols

$[MH]^+$	Protonated Molecule	**GSH**	Glutathione
^{13}C NMR	Carbon 13 Nuclear Magnetic Resonance	**GST**	Glutathione *S*-transferase
^{1}H NMR	Proton Nuclear Magnetic Resonance	**HATs**	Histone acetyl transferases
AATase	Alcohol acetyltransferase	**HMBC**	Heteronuclear Multiple Bond Correlation
Ac	Acetyl	**HPLC**	High Pressure Liquid Chromatography
Acetyl-CoA	Acetyl coenzyme A	**HRMS**	High resolution mass spectra
APS	Adenosine-5'phosphosulfate	**HSQC**	Heteronuclear Single Quantum Coherence
Ar	Aromatic	***J***	Coupling constant
ATP	Adenosine-5'-triphosphate	**LC-ESI-HRMS**	Liquid Chromatography-High Resolution Mass Spectrometry
AVP	Arginine vasopressin	**LC-ESI-MS**	Liquid Chromatography-Mass Spectrometry
COSY	Homonuclear Correlation Spectroscopy	**m**	Multiplet
CYP	Cytocrome P450	***m/z***	Mass/charge ratio
d	Doublet	**MDR-4**	Multidrug resistance protein 4
dA	2'-deoxyadenosine	**Me**	Methyl
DCC	Dicyclohexylcarbodiimide	**MeCN**	Acetonitrile
dd	Duplet of duplets	**MeOH**	Methanol
dG	2'-deoxyguanosine	**MS**	Mass Spectrometry
dG•Si	3',5'-*O*-Bis(*tert*-butyldimethylsilyl)-2'-deoxyguanosine	**MsCl**	Methanesulfonyl chloride
DMF	*N,N*-dimethylformamide	**NAC**	*N*-acetyl-*L*-cysteine
DMSO	Dimethylsulfoxide	**$NaHCO_3$**	Sodium bicarbonate
DNA	Desoxyribonucleic acid (*ADN – ácido desoxirribonucleico)*	**NAL**	*N*-acetyl-*L*-lysine
DNAse	Deoxyribonuclease	**NAT**	*N*-acetyltransferase
e.e.	Ethyl ether	**OAT**	*O*-acetyltransferase
EDTA	Ethylenediaminetetraacetic acid	**PAP**	3'-phosphoadenosine 5'-phosphate
eq.	equivalent	**PAPS**	3'-Phosphoadenosine-5'-phosphosulfate
ESI	Electrospray Ionization	**PDE I**	5-exonuclease phosphodiesterase I
Et_3N	Triethylamine	**ppm**	Parts per million
FDA	Food and Drug Admnistration	**PTLC**	Preparative Thin Layer Chromatography

Py	Pyridine	**TBDMSCl**	*tert*-Butyldimethylsilyl chloride
r.t.	Retention time	**THF**	Tetrahydrofuran
rt	Room temperature	**TLC**	Thin Layer Chromatography
Rf	Retention factor	**TMS**	Tetramethylsilane
RM	Reactive metabolites	**TsCl**	*p*-toluenesulfonyl chloride
s	singlet	**TVP**	Tolvaptan
SAM	*S*-Adenosyl methionine	**TVP•Ac**	5'-*O*-acetyl -tolvaptan
SIADH	Syndrome of Inappropriate Antidiuretic Hormone	**TVP•SO_3^-**	5-*O*-sulfonate-tolvaptan
SO_3•DMF	Sulfur trioxide *N,N*-dimethylformamide complex	**UDPGA**	Uridine-5'-diphospho-α-D-glucuronic acid
SO_3•Py	Sulfur trioxide Pyridine complex	**UV**	Ultraviolet
SULT	Sulfotransferase	**Val-O-Et**	Ethyl Valinate
t	Triplet	**Vis**	Visible
TBAF	Tetrabutylammonium Fluoride	***δ***	Chemical Shift from TMS

1 Introduction

1.1 Tolvaptan

Vaptans, are a class of drugs that act by directly blocking the action of vasopressin at its receptors, competing for the active sites on cells meant for vasopressin binding, earning the title of vasopressin antagonists. The first FDA approved vaptan, in 2005, was the unselective vasopressin antagonist Conivaptan (**1**) (V_{1A}RA and V_2RA)[1, 2], but currently several other drugs of this class are either approved or in clinical trials (Figure 1.1): Mozavaptan (**2**), Tolvaptan (**3**), Lixivaptan (**4**).[3] In **table 1.1** it is summarized some of the features of these vaptans, including some of the adverse effects induced by these drugs.[3]

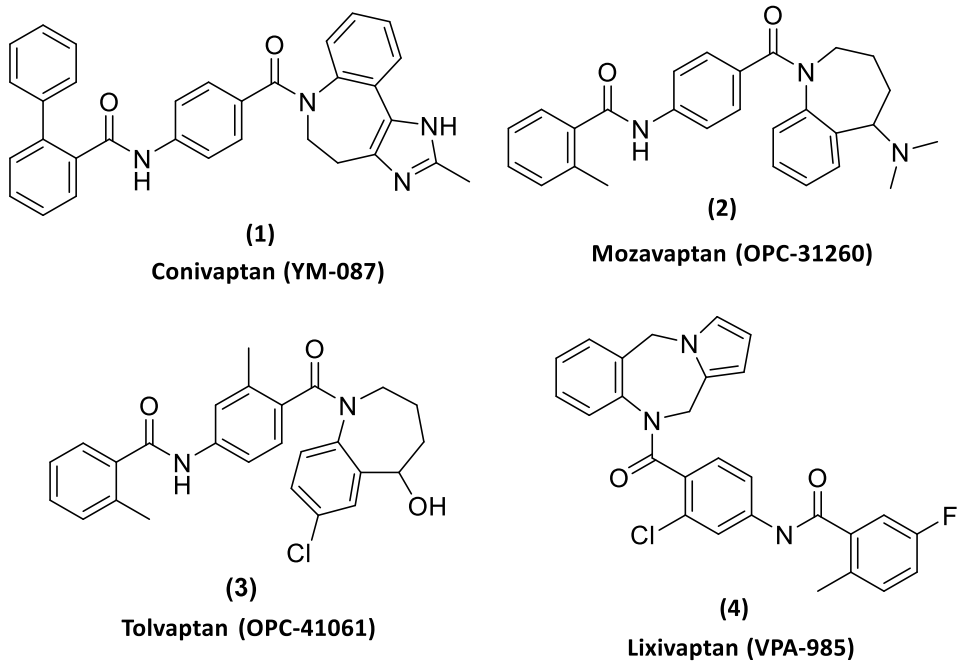

Figure 1.1 Vasopressin Receptor Antagonists (VRAs): nonselective V_{1a}/V_2 RA – Conivaptan (**1**); and selective V_2 RA – Mozavaptan (**2**), Tolvaptan (**3**), Lixivaptan (**4**).

Table 1.1 Summarized features of some Vaptans, including Tolvaptan.[1]

Drug	Conivaptan (1)	Mozavaptan (2)	Tolvaptan (3)	Lixivaptan (4)
Year	2005 (FDA)	2006 (in Japan)	2009 (FDA)	Phase III clinical trials (since May 2010)
Commercial Name	Vaprisol™	Physuline™	Samsca™	Cornerstone
Pharmaceutical	Astellas Pharma US	Otsuka Pharmaceutical	Otsuka Pharmaceutical	Cardiokine Biopharma
Receptor	V_{1a}/V_2	-	V_2	V_2
Rout of administration	IV	-	Oral	Oral
Urine Volume	↑	-	↑	↑
Urinary osmolality	↓	-	↓	↓
Urinary sodium excretion (24h)	↔	-	↔	↔ low doses ↑ high doses
Na_p	↑	-	↑	↑
Clinical development	Euvolemic or hypervolemic hyponatremia in hospitalized patients (only approved in the USA)	-	Hyponatremia due to SIADH (approved by EMA). Clinically significant hyponatremia (Na_p<125 mmol/L) or symptomatic hyponatremia unresponsive to fluid restriction (FDA approved)	Euvolemic or hypervolemic (Phase III) hyponatremia

↑ - Increase; ↓ - Decrease; ↔ - Unaltered

The vaptan, tolvaptan {*N*-{4''-[(7'-chloro-5'-hydroxy-2',3',4',5'-tetrahydro-1*H*-1-benzazepin-1'-yl)carbonyl]-3''-methylphenyl}-2-methylbenzamide, TVP**, 3, Figure 1.1**} is an orally effective nonpeptide arginine vasopressin (AVP) V_2-receptor antagonist. Whereas the molecule has an asymmetric center, the commercially available form is a racemate. Tolvaptan is used in the treatment of clinically significant euvolemic and hypervolemic hyponatremia including patients with heart failure, Syndrome of Inappropriate Antidiuretic Hormone (SIADH)[4] and several other diseases associated with volume overload.

In a recent large clinical trial, which tested the use of tolvaptan in patients with autosomal dominant polycystic kidney disease, tolvaptan was reported to be associated with a high risk of liver injury.[5] The severity of such side effects, which may lead to organ transplant or death, have prompt the U.S. Food and Drug Administration (FDA) to issue a black box label warning on tolvaptan.[6] According to this warning, tolvaptan should not be used for longer than 30 days and should not be used in patients with underlying liver disease, it also warns for hypersensitivity.

In terms of pharmacokinetics, tolvaptan is administered orally as a single dose in the morning, with a dosage limit between 15-60 mg/day. It is absorbed rapidly, with a maximum plasmatic concentration reached 2h after intake, and has a bioavailability of c.a. 56% and a half-life of 8h. In terms of distribution, tolvaptan primarily resides in the plasma rather than red blood cells and is about 98% bound to plasma proteins. Both enantiomers are stable in plasma and were found to be equally potent at the V_2 receptor in *in vitro* binding studies. However, following single dose, the concentrations of *S* (-) enantiomer is consistently higher in the plasma.[7]

Once in the liver, it is extensively metabolized by cytochrome P450 (CYP) 3A4. Consequently, its simultaneous use with CYP3A inducers and moderate CYP3A inhibitors should be avoided. Tolvaptan is excreted via urine [(40% metabolized, 1% unaltered) and feces (27% metabolized, 32% unaltered].[1]

Tolvaptan metabolism involves mainly dehydrogenation and hydroxylations reactions catalyzed by CYP3A4. Structural characterization of tolvaptan's metabolites allowed the identification of (**Figure 1.2**): **1**) At least three distinct monohydroxylated derivatives at the benzazepine ring, where at least two of them are deastereomers (**Figure 1.2 a**); **2)** A ketone derivative **5** resulting from the oxidation of the hydroxyl group at the 5'-position of tolvaptan (**Figure 1.2 b**); **3)** A metabolite resulting from the hydroxylation of the keto metabolite **5** (**Figure 1.2 c**); **4)** Four metabolites resulting from the cleavage of the benzazepine ring between positions 1 and 2 (**Figure 1.2 d**).[7]–[9]

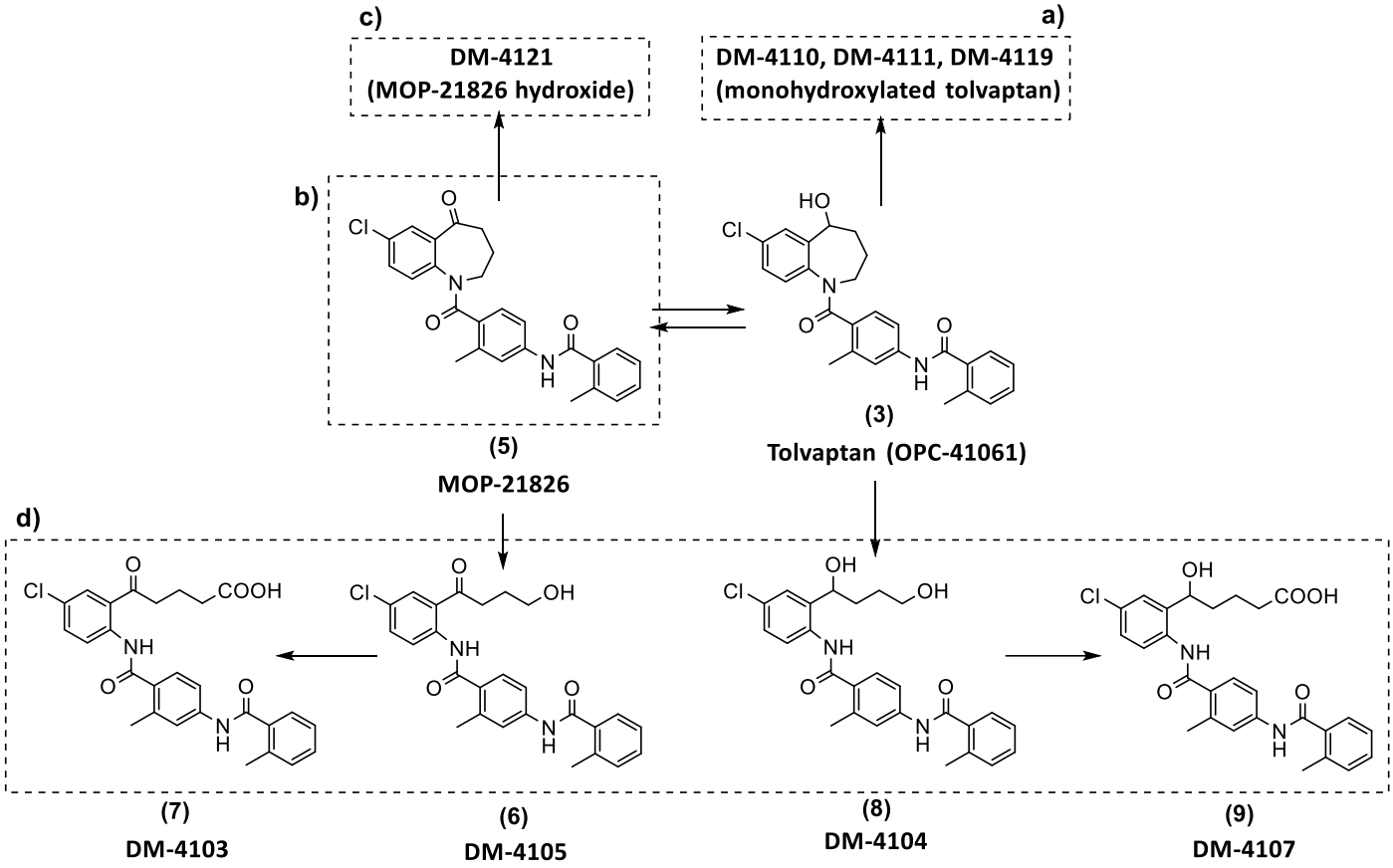

Figure 1.2 Schematic representation of proposed metabolic pathways of tolvaptan. a) hydroxylation of the benzazepine ring; b) oxidation of the hydroxyl group at 5' position; c) hydroxylation of metabolite 5; d) benzazepine ring cleavages.[8], [9]

Whereas the mechanisms of tolvaptan-induced liver injury remain to be elucidated, preliminary results obtained in CYP-deficient liver cell lines have shown evidence of tolvaptan-induced DNA damage without the need for Phase I metabolism (**Figure 1.3**). (JL Fang, FDA, personal communication) This result was the seed for the working hypothesis of this thesis. Taking into consideration that the Phase II sulfonation and/or acetylation of the hydroxyl group at the 5' position of tolvaptan are metabolically plausible events (and do not involve CYP catalysis), the ultimate goal of this thesis is to study the reactivity of these metabolic plausible Phase II metabolites towards DNA. Indeed, these metabolites, 5'-*O*-sulfonate-tolvaptan (TVP•SO_3^-, **10**) and 5´-*O*-acetyl-tolvaptan (TVP•Ac, **11**), as electrophiles bearing good leaving groups, could act as substrates to the nucleophilic groups of DNA bases. The covalent adduct afforded, could explain the tolvaptan-induced DNA damage observed by Fang.

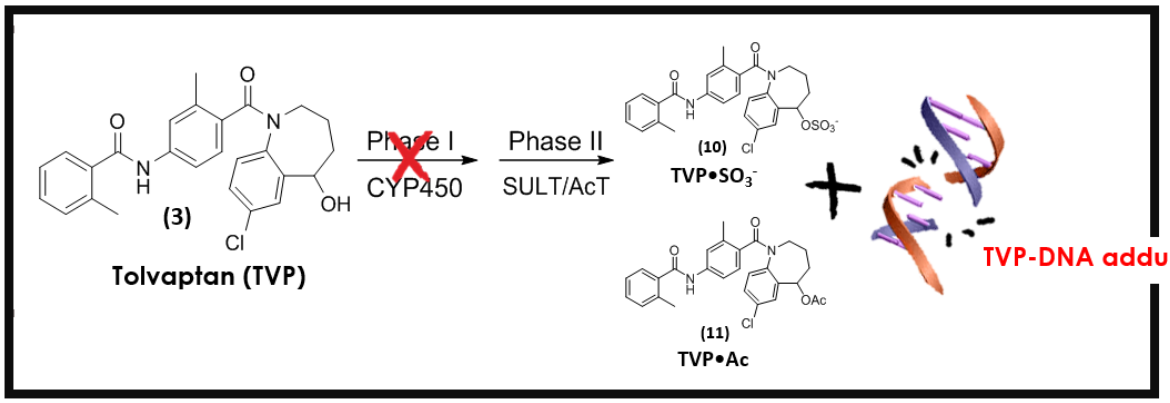

Figure 1.3 Potential mechanism of TVP-induced DNA damage.

1.2 Drug Metabolism

Metabolic biotransformations are usually subdivided in three stages: Phase I, II, and III. Phase I metabolism is typically associated with CYP reactions, mainly oxidative reactions, but non-CYP oxidations, like reductions and hydrolyses, are also included in this category. Phase II transformations are conjugative processes, where small, highly hydrophilic and endogenous groups, such as water-soluble endogenous sugars, salts or amino acids, are added to xenobiotics or endogenous chemicals. The Phase III systems consist of efflux pumps that exclude water soluble metabolites from the cell to the interstitial fluid, blood and ultimately the kidneys. The efflux pumps are also able of excluding drugs once they are absorbed from the gut, and likewise metabolites.[10], [11]

1.3 Phase II Conjugations

Phase II metabolism is defined as the attachment of minor, endogenous groups to the selected molecule. Phase II metabolism can follow Phase I metabolism, but not mandatorily. Hence, Phase II reactions can occur without previous Phase I transformations. Contrary to Phase I metabolism, in which introduction or exposure of functional groups occurs, there are no CYPs involved in Phase II reactions. Among the multitude of groups possible of being added, the three most common are: glucuronic acid, sulfonate and peptides (or amino acids).[10], [11]

Phase II conjugation reactions of hydroxyl, cyclic nitrogen, amino, and thiol groups present in the target molecule are carried out by specific enzymes, namely transferases. **Table 1.2** is the compilation of the different conjugation reactions and their correspondent participants.

Table 1.2 Phase II conjugation reactions and their intervenients.[11], [12]

Conjugate	Conjugated groups	Coenzyme form	Transferase enzyme
Glucuronide	-OH, -COOH, -NH_2, -NR_2, -SH, C-H	Uridine-5'-diphospho- α-D-glucuronic acid (UDPGA)	UDP – Glucuronosyltransferase
Sulfonate	-OH, -NH_2	3'-Phosphoadenosine-5'-phosphosulfate (PAPS) 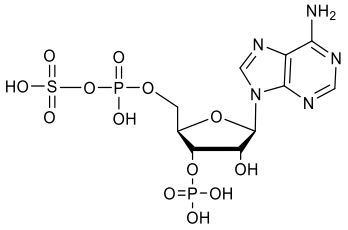	Sulfotransferase
Glycine and glutamine	-COOH	Activated acyl or aryl coenzyme A cosubstrate	Glycine *N*-acyltransferase; Glutamine *N*-acyltransferase
Glutathione	Ar-halogen, arene oxide, epoxide, carbocation	Glutathione (GSH)	Glutathione S-transferase (GST)
Acetyl	-OH, -NH_2	Acetyl coenzyme A (Acetyl-CoA) 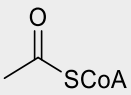	Acetyl-transferase
Methyl	-OH, -NH_2, -SH, heterocyclic N	*S*-Adenosyl methionine (SAM)	Methyl-transferase

Taking into account the tolvaptan chemical structure, the only Phase II reactions plausible of yielding electrophiles susceptible to bionucleophiles attack are sulfonation and acetylation of the hydroxyl group at the 5' position. Thus, only these two bioactivation routes will be further discussed in this thesis.

1.3.1 Sulfonate Conjugations

Sulfonation of xenobiotics is a Phase II metabolic mechanism that leads to increased molecular hydrophilicity, which is necessary for biliary excretion or efflux across the hepatic basolateral

membrane for subsequent renal clearance. Sulfonation, as a way of xenobiotic detoxification may occur directly on the parent compound or may follow Phase I oxidation.[13] However, hepatic sulfonation of xenobiotics can lead to the bioactivation of hepatotoxins, DNA-binding carcinogens (e.g. safrole), and prodrugs (e.g. minoxidil).

Sulfonate conjugations occur less frequently than glucuronidation, being the second most common Phase II reaction in mammals, presumably due to the limited availability of inorganic sulfates in mammals and due to the low number of chemical compounds which are suitable to undergo sulfonate conjugation (phenols, alcohols, arylamides, and *N*-hydroxy compounds).[11]

Sulfonate conjugation starts with an inorganic sulfate (**12)** that is converted into an organic form upon reaction with one molecule of adenosine-5'-triphosphate (ATP), catalyzed by ATP sulfurylase (**Figure 1.4**). The product formed, adenosine-5'phosphosulfate (APS, **13**), is then phosphorylated in an APS phosphokinase-catalyzed reaction to 3-phosphoadenoside-5'-phosphosulfate (PAPS, **14**). Finally, the target molecule (RXH) undertakes sulfotransferase-catalyzed sulfonation, with release of 3'-phosphoadenosine 5'-phosphate (PAP), resulting in a sulfonate-conjugate (**15**).[10], [11]

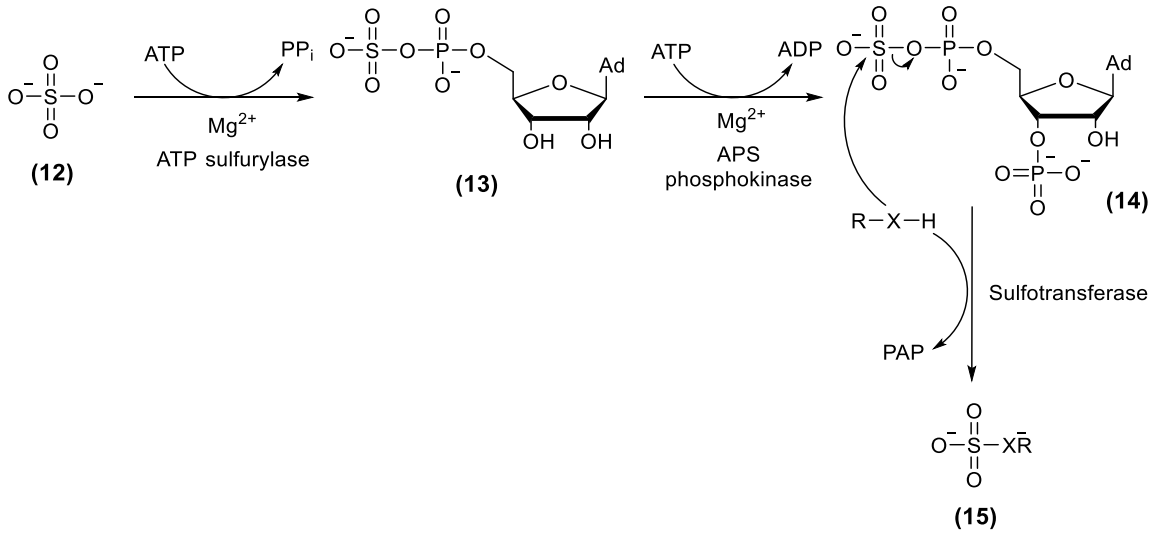

Figure 1.4 Schematic representation of sulfonate conjugation reactions (adapted from [11]).

Sulfonate conjugates, as in glucuronic acid conjugates, frequently present low pK_a values (< 1) due to the sulfonate moiety. Sulfonate conjugates have been shown to interact with the multidrug resistance protein 4 (MDR-4), an excretion protein, similar to MDR 2 and 3. However, these last two appear to play little or no role in the transport of sulfonation products.[13],[14]

Sulfonation enzymes have preference for phenols, although conjugations with aliphatic alcohols, amines and thiols may also occur.[15] Sulfonation predominates at low substrate concentrations, when there is less to diffuse into membranes, and with smaller, less lipid-soluble molecules[11], and

glucuronidation at high substrate concentrations, when sulfonation has been saturated either due to co-substrate depletion or enzyme saturation.[16]

Sulfonate conjugation is reversible; sulfonate conjugates may be desulfated by sulfatases, subsequently re-conjugated, deconjugated, etc., giving rise to the phenomenon of "futile cycling" between the parent compound and sulfonate metabolite.[16]

1.3.1.1 Cytosolic Sulfotransferases (SULT)

The class of cytosolic sulfotransferase (SULT) enzymes can be divided into three families: SULT1 [phenol sulfotransferase (PST) family], SULT2 [hydroxysteroid sulfotransferase (HST) family], and brain-specific SULT4.[17], [18] The SULT1 family is further subdivided into four subfamilies: SULT1A (phenolic-type xenobiotics), SULT1B (dopa/tyrosine and thyroid hormones), SULT1C (hydroxyarylamines), and SULT1E (estrogens); while the SULT2 family is subdivided into two subfamilies: SULT2A (neutral steroids/bile acids) and SULT2B (sterols).[19]–[22] Sulfonation of xenobiotics is primarily mediated by the SULT1A subfamily, which catalyzes sulfonation of hydroxyl groups and monoamine groups on phenolic-type molecules.[15], [22]

Humans express three isoforms of SULT1A: thermostable SULT1A1 and SULT1A2, which catalyze sulfonation of hydroxyl groups on phenolic-type molecules (sometimes referred to as PPST1 and P-PST2), and thermolabile SULT1A3.[23]–[25]

1.3.2 Acetyl Conjugations

Acetylations occur generally in molecules having primary amines, including aliphatic and aromatic amines, hydroxylamines (both the oxygen and the nitrogen can be acetylated), amino acids, sulfonamides, hydrazines, hydrazides, sulfhydryl and hydroxyl groups.[11] Acetyl conjugations, along with methylations, increase molecule's lipophilicity, a process thought to be aimed at deactivating the drug.[11], [26]–[28]

For us humans, acetylation is a major route for biological transformation of several arylamine and hydrazine type drugs, including for a number of well-known carcinogenic compounds present in cigarette smoke, and in the environment in general.

Acetyl conjugation is a two-step covalent catalytic process, known as a double displacement (ping-pong) mechanism. Initially, acetyl CoA acetylates an active site of an amino acid residue of the *N*-acetyltransferase (**16, Figure 1.5**), which is then followed by the transference of the acetyl group to the substrate (RXH).

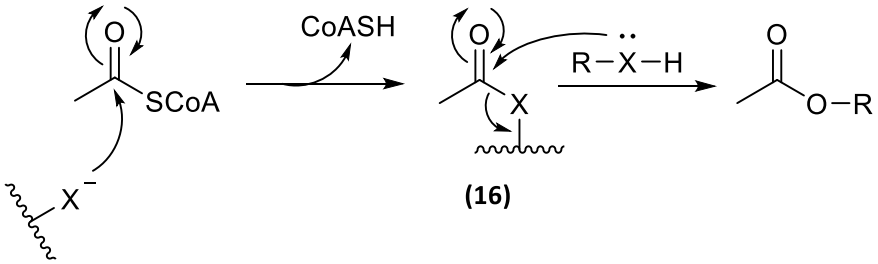

Figure 1.5 Schematic representation of acetyl conjugation reactions (adapted from [11]).

Reversible inhibitors of the process, such as salicylamide, have a similar structure to the substrates, whilst iodacetate and *N*-ethylmaleide, irreversible inhibitors, have a dissimilar arrangement.

1.3.2.1 Cytosolic *N*-acetyltransferases (NAT)

Acetyltransferases have a major role in the metabolic detoxication and bioactivation of different drugs, carcinogens and several other xenobiotics.[29] Additionally, they have a wide range of functions related to cell homeostasis. An example of that are histone acetyl transferases (HATs), which regulate DNA transcription by activating histone proteins through acetylation reactions. Another example is the hormone melatonin, which is regulated through acetyltransferases.

Aditionally, *N*-acetyltransferases can also have *O*-acetyltransferases and *N,O*-acetyltransferase activity. *N* to *O* transacetylation can also occur, which does not require the co-factor acetyl-CoA, i.e. the transfer of an acetyl group from an *N*-acetylated hydroxylamine (hydroxamic acid) to form an acetoxy product.[26]

The class of cytosolic *N*-acetyltransferase isoenzymes (NATs) can be divided into: *N*-acetyltransferase 1 (NAT1) and *N*-acetyltransferase 2 (NAT2), both polymorphic enzymes. NAT2 is mainly found in liver and intestine cells, while NAT1 appears to be ubiquitous. Human *N*-acetyltransferases 1 and 2 share 87% coding sequence homology.[27], [28], [30], [31]

NATs are involved in the metabolism of a variety of different compounds, some of which we are exposed on a daily basis. NAT1 and NAT2 have individual as well as overlapping substrate profiles. Substrates for NAT1 include compounds such as *p*–aminobenzoic acid, *p*–aminosalicylic acid, 2–aminofluorene and caffeine.[32] Human NAT2 is capable of metabolizing drugs such as hydralazine and endralazine (anti–hypertensive drugs), isoniazid (an anti–tuberculotic drug) and some sulphonamides (anti–bacterial drugs).[33]

1.4 Metabolism: Toxicity *vs* detoxification

Drug metabolism despite having as elemental objective the detoxification and excretion of xenobiotics, sometimes also converts them into toxic reactive metabolites (RM). These RM are often electrophilic species capable of reacting with bionucleophiles (proteins and DNA) affording covalent adducts that may be in the onset of toxic events, including immune-mediated responses, mutagenicity/carcinogenecity, hepatotoxicity (as described for TVP), renal toxicity, and cardiotoxicity. Indeed, the formation of a covalent adducts with proteins may modulate its activity and/or trigger immune responses. Likewise, should the DNA lesions remain un-repaired or undergo erroneous repair, the covalent modification of DNA by drugs (or their RM) can be at the onset of drug-induced mutagenic/carcinogenic processes.[11]

The link between drug metabolism, formation of reactive metabolites, covalent binding and irreversible damage to the organism are summarized in **Figure 1.6**. Conjugative detoxifying (UGTs, SULTs and GST/GSH) reactions of xenobiotics and their reactive metabolites are crucial to avert organ failure from high levels of covalent binding, and DNA repair is crucial to prevent carcinogenicity as a result of specific DNA binding of reactive metabolites. In terms of immune response, the sensitivity of each immune system may be the determinant factor of whether an immune response arises. Despite the fact that covalent binding is associated with the majority of toxicity routes, parent drug effects should not be discarded.[10], [11], [34]

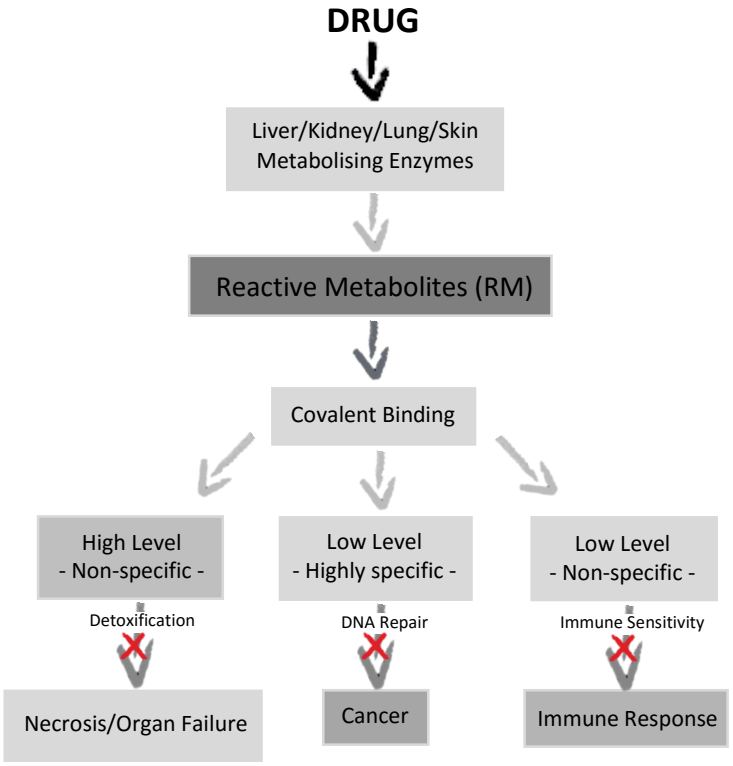

Figure 1.6 Connections between drug metabolism, formation of reactive metabolites, covalent binding and irreversible damage to the organism (adapted from [10]).

1.4.1 Bioactivation via Sulfonation

One of the representive examples where Phase II sulfonation of hydroxyl groups leads to a reactive metabolite, is the metabolite 12-sulfoxy-nevirapine (**17**, **Figure 1.7**) that was suggested to be in the onset of immune-mediated skin rashes induced by the anti HIV drug nevirapine (**18**).[35]–[38]

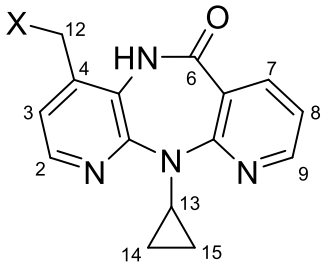

(17) X =OSO_3H; 12-Sulfoxy-NVP
(18) X = H; Nevirapine (NVP)

Figure 1.7 Structure of 12-sulfoxy-NVP metabolite (**17**) and nevirapine (**18**).

The *O*-sulfonation of the resulting metabolites from α-hydroxylation of the breast cancer drug tamoxifen (**19**, X= -N(CH_3)$_2$) and its product of *N*-desmethylation (*N*-desTAM, **19**, X= -NHCH_3), are additional examples of sulfonation leading to increased toxicity. Indeed, the sulfoxy derivatives **21**, are the electrophilic species that covalently bind to DNA, forming TAM-DNA covalent adducts (**Figure 1.8**), suggested to be in the onset of cancer events detected in rats treated with the parent drug.[39]–[41]

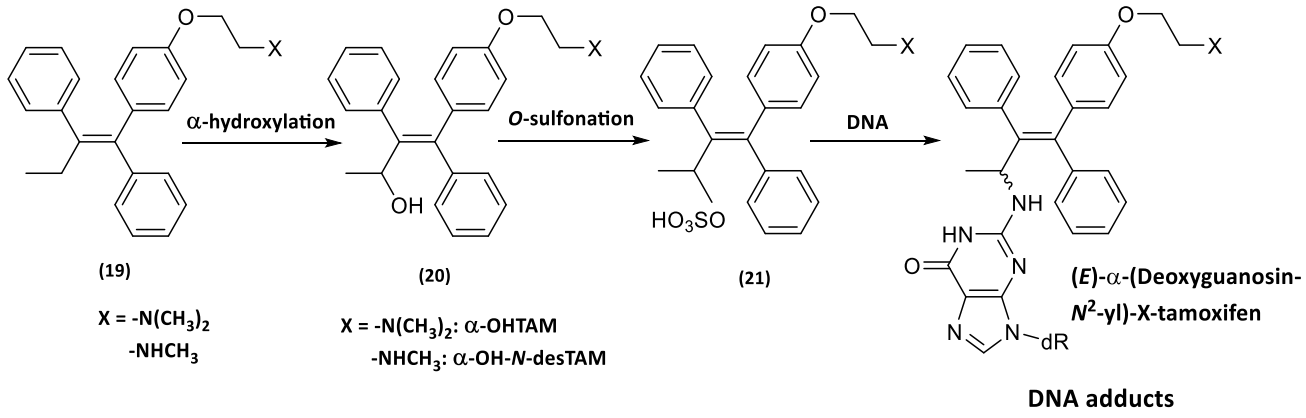

Figure 1.8 Schematic representation of *O*-sulfonation of α-hydroxylated TAM (α-OHTAM) and desmethylated TAM (α-OH-*N*-desTAM) and subsequent DNA adduct formation.[39]–[41]

7,12-Dimethylbenz[*a*]anthracene (**22**, DMBA) (**Figure 1.9**) undergoes CYP-mediated hydroxylation at the benzylic position, yielding the metabolite **23**. Sulfonation of this Phase I metabolite constitutes one additional example of bioactivation via Phase II. The sulfonate derivative **24** undergoes unimolecular nucleophilic reactions (S_N1) with DNA, involving the formation of the electrophilic carbonium ion **25** intermediate that leads to DNA binding and tumor formation.[28]

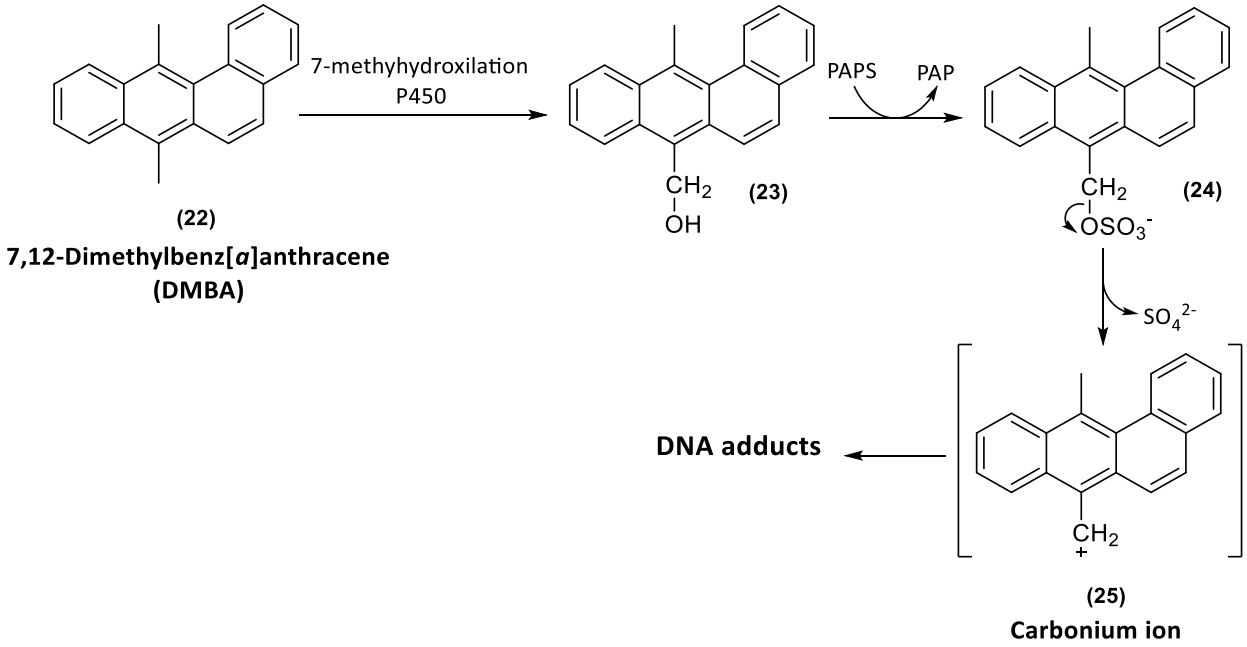

Figure 1.9 Bioactivation of the 7,12-dimethylbenz[a]anthracene (**22**) Phase I metabolite **23**, via Phase II sulfonation to **24**. The carbonium ion **25**, stemming from sulfate elimination from **24**, is suggested to be involved in the formation of DNA covalent adducts (adapted from [17]).

The bioactivation of the anti-cerebral-ischemia drug 3-*n*-butylphthalide (**26**, NBP), through the *O*-sulfonation of its major metabolite, 3-sulfoxy-NBP (**27**), constitutes one additional example of bioactivation via sulfonation. This bioactivation pathway was suggested to be involved in the NBP-induced moderate hepatotoxicity due to the identification of the adduct 3-*N*-acetylcysteine-NBP (**30**, 3-NAC-NBP) in human urine, which suggests the formation of the reactive metabolite 3-OH-sulfonate-NBP (**28**).[26]

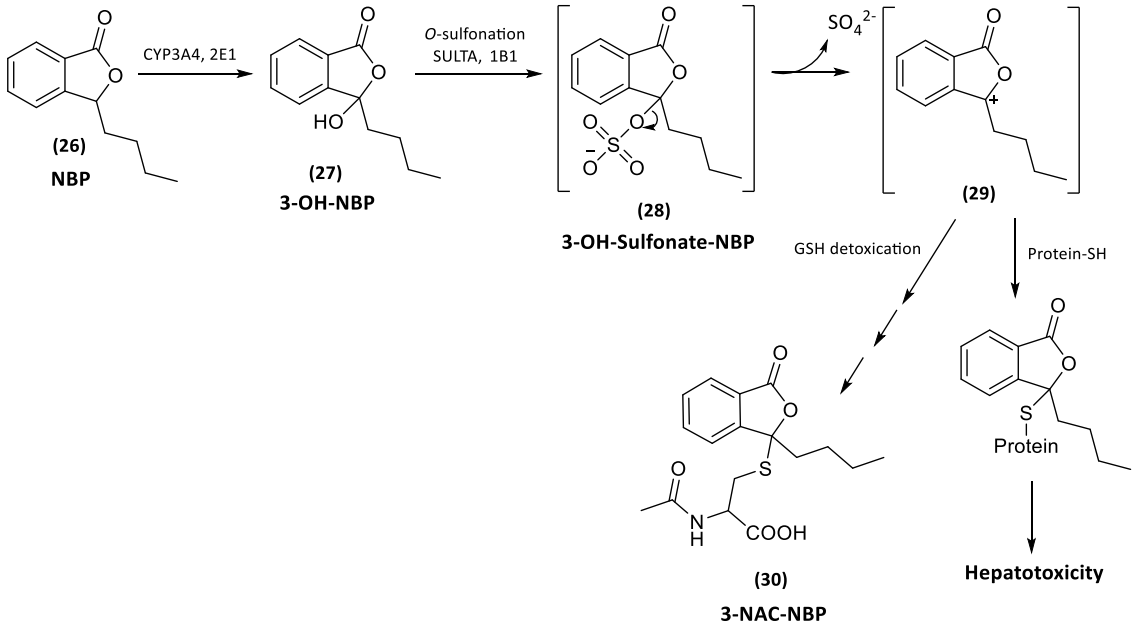

Figure 1.10 Proposed bioactivation pathway of 3-*n*-butylphthalide (26, NBP) via *O*-sulfonation of 3-hydroxy-NBP (27, 3-OH-NBP) (adapted from [15]).

The *O*-sulfonation of the *N*-hydroxy-2-acetylaminofluorene (**32**, *N*-hydroxy-2-AAF) is also a bioactivation pathway that leads to DNA adducts formation.

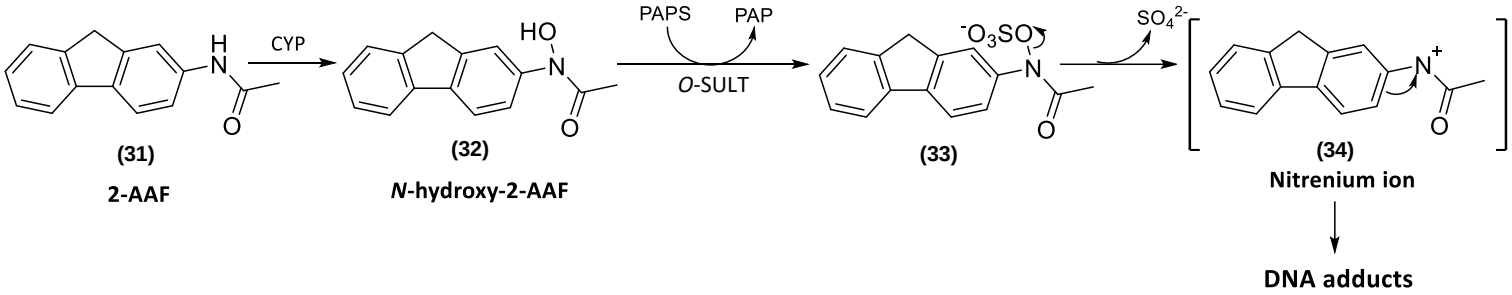

Figure 1.11 *O*-Sulfonation of *N*-hydroxy-2-AAF (**32**) and subsequent DNA adduct formation (adapted from [17]).

1.4.2 Bioactivation via acetylation

Acetylation constitutes a major bioactivation pathway of hydroxylamines and hydroxamic acids.

For example the rat carcinogen 2-hydroxylaminofluorene (2-AF, **35, Figure 1.12**), following Phase I *N*-hydroxylation to **36**, is *O*-acetylated by alcohol acetyltransferases (AATases) to **37**. The subsequent loss of acetoxy group leads to the formation of an electrophilic specie, the nitrenium ion **38**, capable of reacting with DNA.[28]

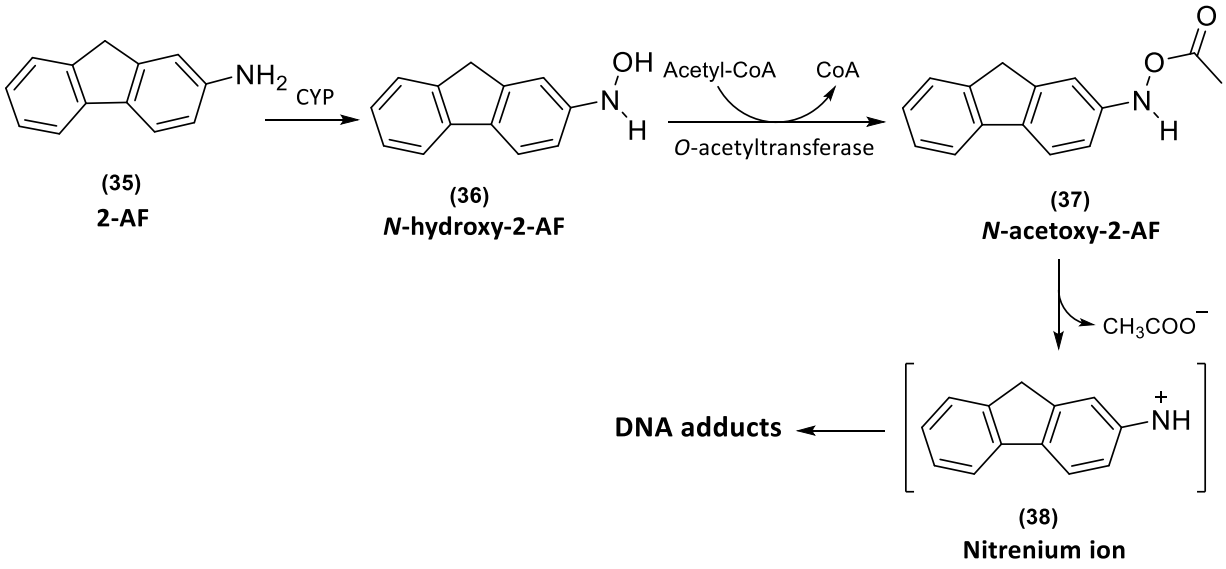

Figure 1.12 Schematic representation of *O*-acetylation of *N*-hydroxy-2-AF and subsequent DNA adduct formation (adapted from [17]).

1.5 Objectives

Taking into consideration the tolvaptan-induced DNA damage observed in CYP-deficient liver cell lines, we have hypothesized that tolvaptan could be directly bioactivated by Phase II mechanisms (sulfonation and/or acetylation) to electrophilic derivatives which could cause DNA damage via covalent adduct formation.

To test this hypothesis, the reactivity of the tolvaptan's plausible Phase II metabolites (tolvaptan sulfate and acetyl) with DNA was evaluated. Towards this goal, tolvaptan was converted into its metabolically plausible electrophilic derivatives (or their surrogates), using synthetic procedures that mimic metabolic Phase II activation pathways. The reactivity of these derivatives towards 2'-deoxynucleosides and DNA was evaluated upon analysis by liquid chromatography with mass spectrometry detection (LC-ESI-MS).

2 Results and Discussion

The main goal of this work is to gain insight into the ability of the metabolic plausible Phase II tolvaptan metabolites, 5'-*O*-sulfonate-tolvaptan (TVP•SO_3^-, **10**) and 5'-*O*-acetyl-tolvaptan (TVP•Ac, **11**), to yield DNA adducts. The identification of DNA adducts involves the enzymatic or thermal hydrolysis to individual deoxynucleosides, followed by liquid chromatography – mass spectrometry (LC-ESI-MS) analysis of adducts obtained, upon comparison with synthetic standards. Therefore, the first step of this thesis consisted on the preparation of potential synthetic standards of tolvaptan adducts formed with individual 2'-deoxynucleobases. Two distinct strategies were followed for the preparation of these standards:

1. Biomimetic Strategy: Reaction of tolvaptan's reactive metabolites (or their synthetic surrogates) with 2'-deoxynucleosides (deoxynucleobases).
2. Non-biomimetic strategy: Palladium-catalyzed coupling reaction of 5'-chloro-tolvaptan (**45**) with 3',5'-*O*-bis(*tert*butyldimethylsilyl)-2'-deoxyguanosine.

2.1 Synthesis of tolvaptan DNA adduct standards

2.1.1 Biomimetic Strategy

With the ultimate goal of preparing tolvaptan-DNA adduct standards, a biomimetic strategy was followed, which consisted on reacting 5'-*O*-sulfonate-tolvaptan (TVP•SO_3^-, **10**) and 5'-O-acetyl-tolvaptan (TVP•Ac, **11**), or their synthetic surrogates, with individual 2'-deoxynucleosides, namely 2'-deoxyadenosine (dA, **49**) and 2'-deoxyguanosine (dG) (**Figure 2.1**).

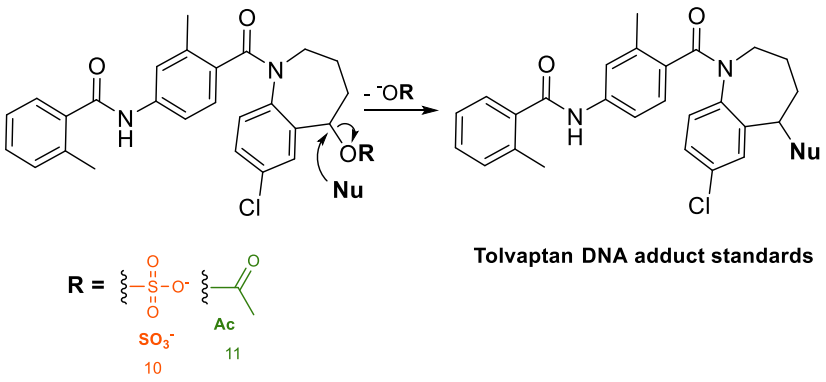

Figure 2.1 Proposed mechanism for the reactions between bionucleophiles and the tolvaptan electrophilic derivatives 5'-*O*-sulfonate-tolvaptan (TVP•SO_3^-, **10**) and 5'-*O*-acetyl-tolvaptan (TVP•Ac, **11**).

2.1.1.1 Synthesis of tolvaptan's reactive metabolites and synthetic surrogates

Taking into consideration that the anti-HIV drug nevirapine (**18**, NVP, **Figure 2.2**) share with tolvaptan a possible bioactivation pathway, involving the sulfonation of benzyl-like alcohol moieties, along with the successful use of 12-mesyloxy-NVP (**40**, **Figure 2.2**) as a synthetic surrogate of the reactive metabolite 12-sulfoxy-NVP (**17**) [35], the first task of this thesis was directed toward the preparation of the 5'-*O*-mesyl-tolvaptan (**42**) derivative. The preparation of 5'-*O*-sulfonate-tolvaptan (TVP•SO_3^-, **10**) and 5'-*O*-acetyl-tolvaptan (TVP•Ac, **11**) was subsequently undergone.

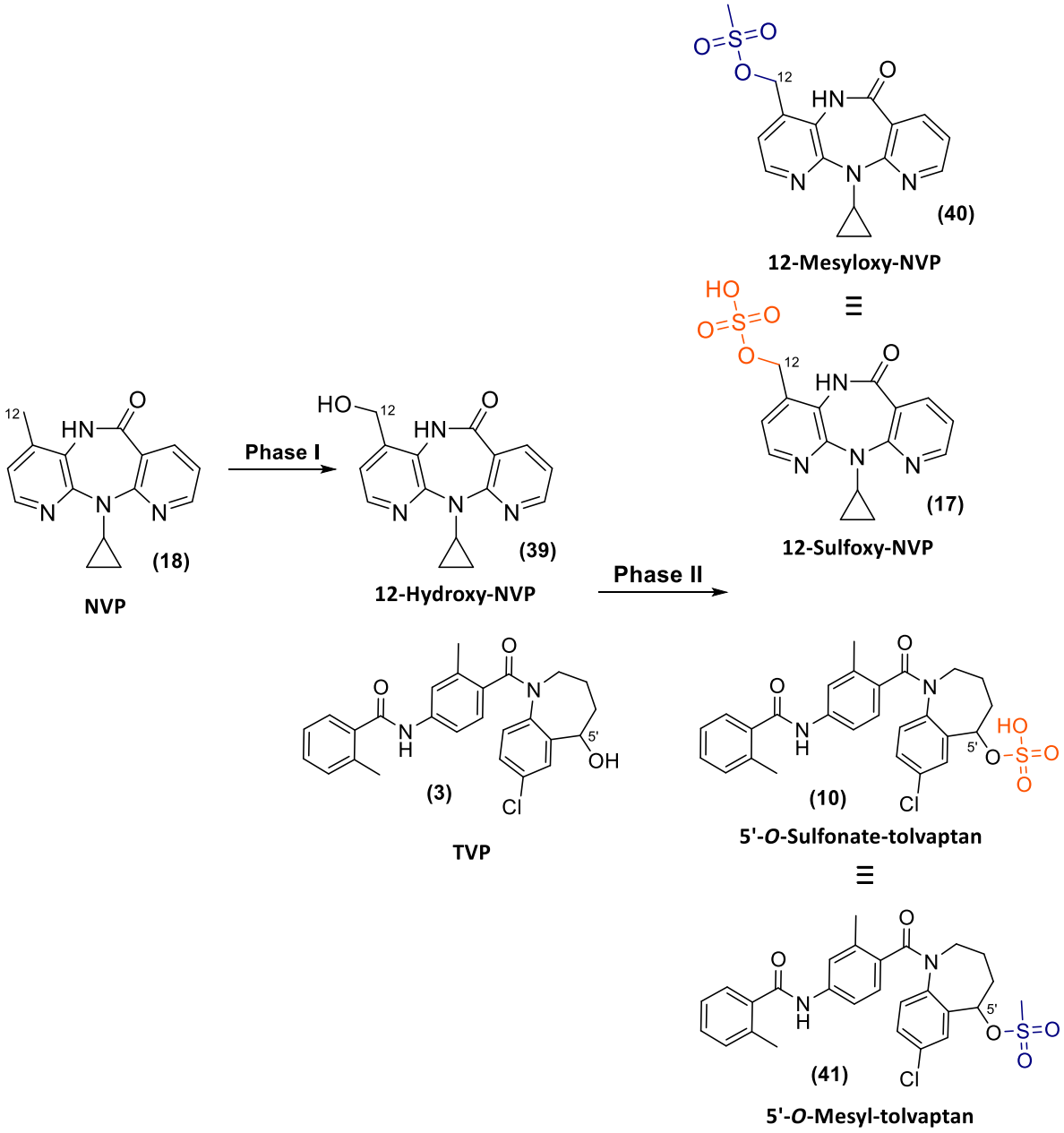

Figure 2.2 Potential similar bioactivation pathways of nevirapine (**18**) and tolvaptan (**3**).

2.1.1.1.1 Mesylation of Tolvaptan

The first synthetic methodology used for the mesylation of tolvaptan´s benzylic alcohol, was the one described for the preparation of 12-mesyloxy-NVP (**39**) from nevirapine (**18**), involving the use of 1.1 eq. methanesulfonyl chloride (MsCl) and triethylamine (Et_3N) in THF.[35] However, this strategy failed, as no product was observed upon thin-layer chromatography (TLC) and LC-DAD analysis of the reaction mixture. Subsequent reactions, using increased molar excess of reactants, were performed. The use of alternative solvents (DMF and acetone) and increased reaction times were also tested. Nonetheless, in all instances no evidence of 5'-*O*-mesyl-tolvaptan (**41**) formation was obtained. The increased stereochemical hindrance and/or decreased nucleophilic character of tolvaptan's secondary alcohol as compared with nevirapine's primary alcohol are reasonable explanations for the distinct behaviors of these two drugs under the tested mesylation conditions. Therefore, alternative conditions reported for the mesylation of hindered alcohols[26], [27] were tested, consisting in using pyridine as solvent and MsCl as the reagent. However, under these conditions, the only product obtained was **42** (**Figure 2.3**), stemming from mesyloxy group elimination. Indeed, when the reaction mixture was analyzed by liquid chromatography with mass spectrometry detection with electrospray ionization (LC-ESI-MS) under positive ionization mode, it was possible the identification of a compound eluting at retention time (rt) c.a. 31.0 min, displaying in the MS spectrum two signals at *m/z* 431 and 433, compatible with the protonated molecule of **42**, with ^{35}Cl and ^{37}Cl, respectively.

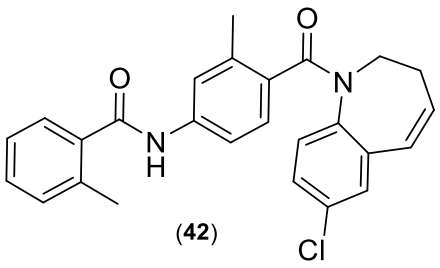

(**42**)

Figure 2.3 Structure of tolvaptan's elimination product **42**.

Other attempts, aimed at improving the nucleophilic character of tolvaptan's hydroxyl group, were also performed. The first approach consisted on adding an initial step, for the formation of the alkoxide derivative (e.g. upon reaction with sodium hydride), followed by reaction with MsCl **(Figure 2.4)**. The LC-ESI-MS analysis of this reaction mixture showed two signals: one eluting at c.a. 29.0 min, whose mass spectrum exhibited two signals at *m/z* of 529 and 527 in 1:3 ratio, compatible with the protonated molecules $[^{37}Cl\text{-}MH]^+$ and $[^{35}Cl\text{-}MH]^+$ of tolvaptan mesylated derivative **41**; the other

eluting at rt c.a. 31.0 min, that displayed in the mass spectrum two signals at m/z 433 and 431, compatible with the protonated molecule of the elimination product **42**, $[^{37}Cl\text{-}MH]^+$ and $[^{35}Cl\text{-}MH]^+$.

Despite the evidence obtained for the mesylation of tolvaptan, the isolation of this derivative was only accomplished when the sodium alkoxide was precipitated (following reaction of tolvaptan with sodium in THF) and then subsequently reacted with MsCl without any solvent. However, when this derivative was reacted with *N*-acetyl-cysteine (NAC), the only product obtained was **43 (Figure 2.5)**, stemming from the nucleophilic attack of NAC to the secondary amide's carbonyl of tolvaptan **(Figure 2.5,** compound **43)**. Taking into consideration that no product was formed upon reaction of tolvaptan with NAC, the formation of compound **43** can only be explained if mesylation occurred at the amide moiety of tolvaptan.

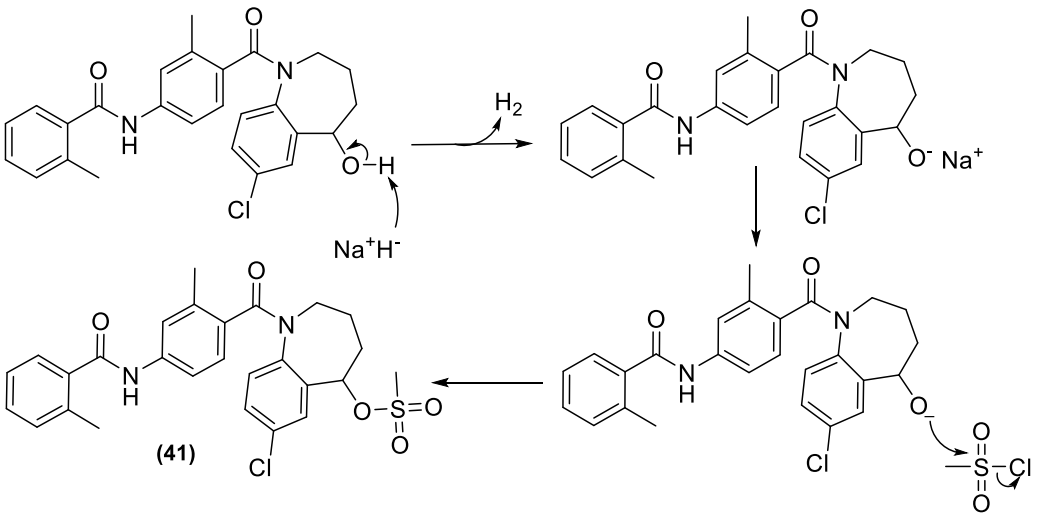

Figure 2.4 Schematic representation of the synthetic strategies used for the formation of tolvaptan derivative **41.**

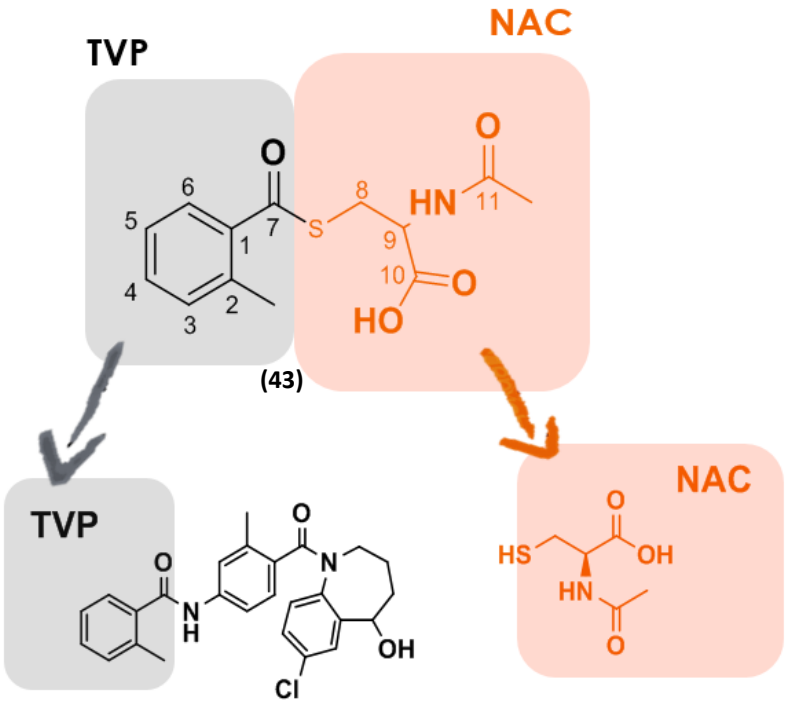

Figure 2.5 Structure of the covalent adduct **43** obtained by reaction of NAC with product obtained upon tolvaptan's mesylation.

The first spectroscopic evidence for the formation of this adduct was obtained by ^{1}H NMR, where beside NAC's signals it was noticeable the existence of only four aromatic protons and one methyl group. The three-bond correlations observed in the ^{1}H-^{13}C HMBC spectrum, between the prochiral protons at position C-8 of NAC's moiety and the carbonyl carbon of the tolvaptan moiety, were decisive for structural assignment (**Figure 2.6**).

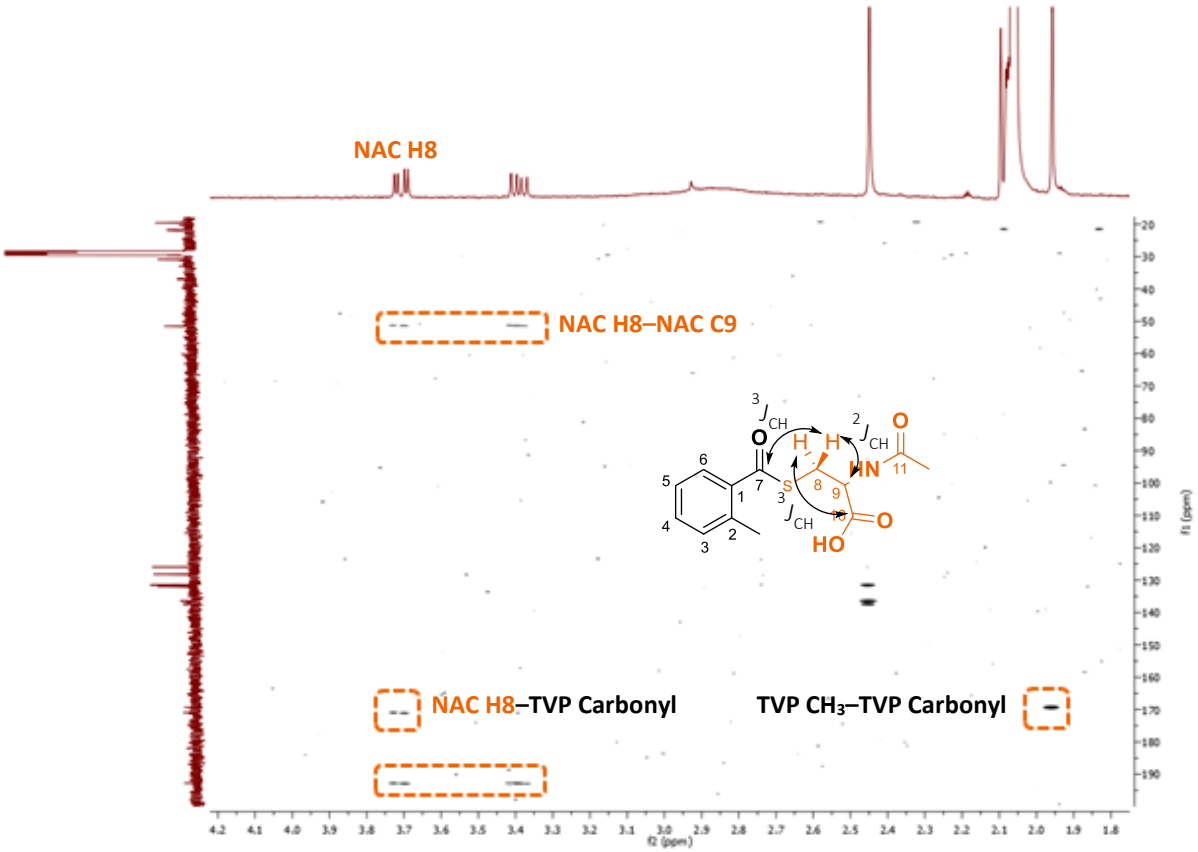

Figure 2.6 Expanded region of the ^{1}H-^{13}C HMBC spectrum recorded for adduct **43**, displaying the connectivities between the geminal NAC-H8 protons and the carbonyl carbon of the tolvaptan moiety.

The identification of this adduct suggests that if sulfonation at the amide position occurs *in vivo*, it could constitute one additional pathway for DNA and protein damage.

2.1.1.1.2 Synthesis of 5'-*O*-sulfonate-tolvaptan (10)

Some of the most widely used chemical sulfonation conditions involve the use of reagents such as sulfuric acid, dicyclohexylcarbodiimide (DCC) combined with sulfuric acid and sulfur trioxide–amine complexes, such as sulfur trioxide–*N*,*N*-dimethyl formamide (SO_3-DMF) and sulfur trioxide–pyridine (SO_3-Py) complexes.[42]

Since DMF is a weaker base than pyridine, the partial positive charge on the sulfur atom of the complex SO_3-DMF is expected to be greater when compared with pyridine complex. Consequently, higher yields are expected from the nucleophilic attack on SO_3-DMF.[42] Therefore, sulfonation with SO_3-DMF was first attempted. However, when the reaction mixture was analyzed by TLC and LC-DAD no evidence of 5´-*O*-sulfonate-tolvaptan (**10**) formation was obtained. In contrast, the use of SO_3-Py complex revealed to be efficient on the sulfonation of tolvaptan's secondary alcohol. Multiple

experimental conditions were tested towards the optimization of this sulfonation reaction, including the number of equivalents of SO_3-DMF used, the time and temperature of reaction.

The optimized tolvaptan sulfonation conditions involved the addition of SO_3•Py (5.0 eq) to a solution of anhydrous tolvaptan in pyridine, followed by stirring at 60˚C for 7 h (**Figure 2.7)**. 5'-*O*-sulfonate-tolvaptan (TVP•SO_3^-, **10**) was obtained as a translucent light beige oil, with 89 % yield, following semi-preparative HPLC purification.

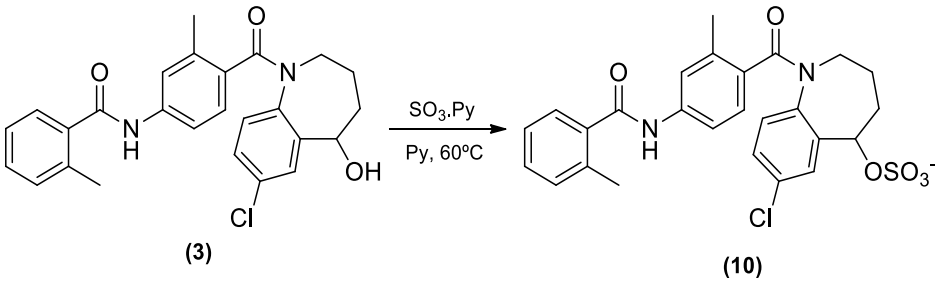

(3) (10)

Figure 2.7 Representation of optimized experimental conditions for the formation of 5'-*O*-sulfonate-tolvaptan (**10**).

2.1.1.1.3 Synthesis of 5'-*O*-acetyl-tolvaptan (11)

The *O*-acetylation of tolvaptan, was efficiently accomplished upon reaction with an excess of acetic anhydride and triethylamine in acetonitrile (MeCN) at 50˚C for 5 h. This reaction involves the nucleophilic attack from the electronegative oxygen of the hydroxyl group towards the electrophilic carbon of acetic anhydride (**Figure 2.8**). Following deprotonation of the positively charged alcohol under alkaline conditions, the rearrangement of the anion occurs with the loss of an acetate anion, yielding the acetoxy moiety.

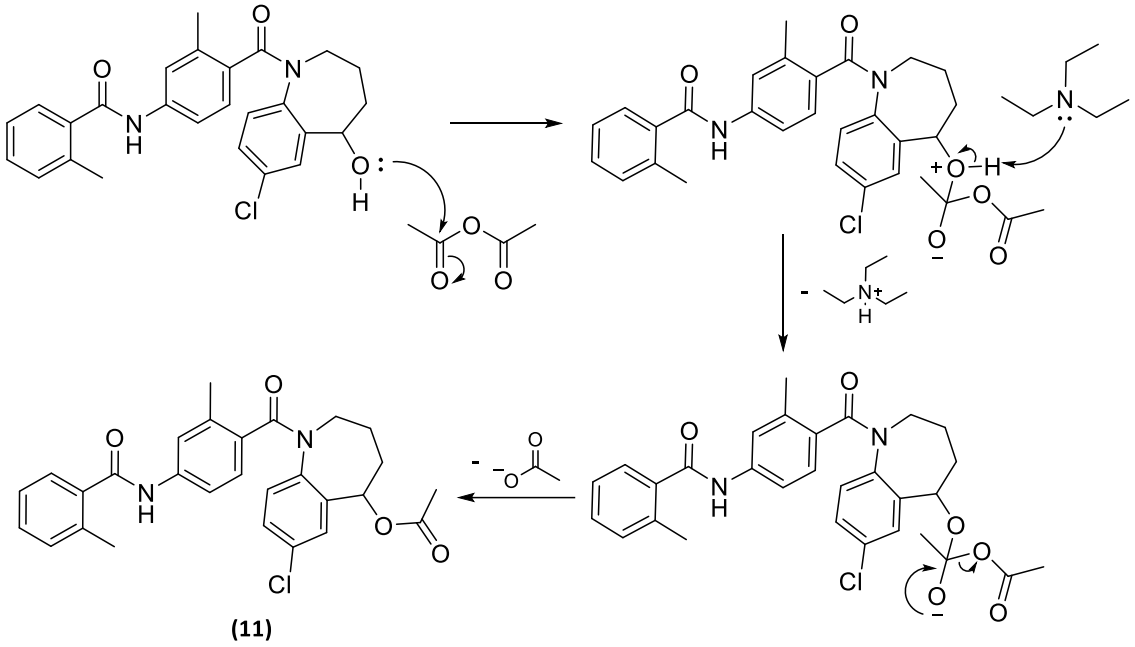

Figure 2.8 Representation of the acetylation reaction of tolvaptan with acetic anhydride.

2.1.1.1.5 Structural Characterization of tolvaptan's derivatives

The first evidence for the formation of tolvaptan derivatives referred in the previous subsections was always obtained upon comparison of the ^{1}H and ^{13}C NMR acquired with tolvaptan's spectra.

Interestingly, despite the commercially obtained product exhibited a single chromatographic signal, when analyzed by LC-DAD, a very complex ^{1}H NMR spectrum was obtained showing duplication of resonances. Nonetheless, the duplicated resonances gradually collapsed upon heating between 30˚ to 60°C (**Figure 2.10**), which suggests that the sample consisted of a mixture of two readily interconvertible conformers. The observed changes were reversible upon cooling to room temperature. Therefore, similar behavior was anticipated from tolvaptan derivatives. The assignment of all ^{1}H NMR and ^{13}C NMR resonances was based on the correlations observed in ^{1}H-^{13}C HSQC, ^{1}H-^{13}C HMBC and ^{1}H-^{1}H COSY spectra (**Table 2.1**).

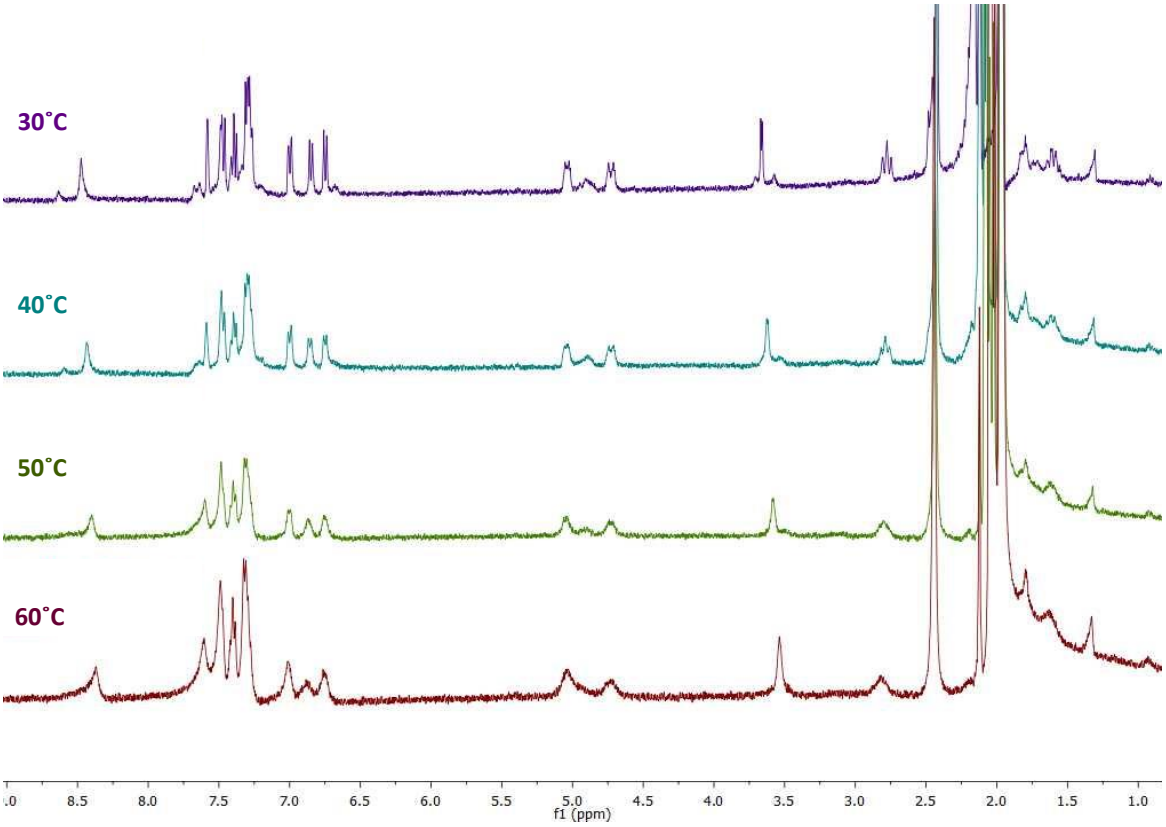

Figure 2.9 Variable temperature ^{1}H NMR experiments of tolvaptan (**3**).

As expected, and similarly to what was observed with tolvaptan, the ^{1}H and ^{13}C NMR spectra of derivatives **10** and **11** also showed duplicated resonances, evidencing the existence of conformers in solution. When compared with tolvaptan, the ^{1}H NMR spectra for 5'-*O*-sulfonate-tolvaptan (**10**) and 5'-*O*-acetyl-tolvaptan (**11**), showed the disappearance of the signal corresponding to the OH proton and the downfield shift of resonances corresponding to the proton adjacent to the hydroxyl group (at position 5') (**Figure 2.11**). The same effect is observed in the ^{13}C NMR resonances (**Table 2.1**), which is fully compatible with the addition of an electron withdrawing group to the hydroxyl moiety.

Table 2.1 Summarized ^{1}H and ^{13}C NMR resonances, and high resolution mass spectrometry (HRMS) data obtained for tolvaptan (**3**), 5'-*O*-sulfonate-tolvaptan (**10**) and 5'-*O*-acetyl-tolvaptan (**11**).

Compound	**(3)** 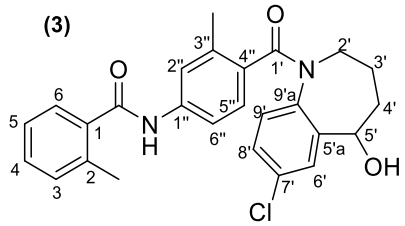	**(10)** 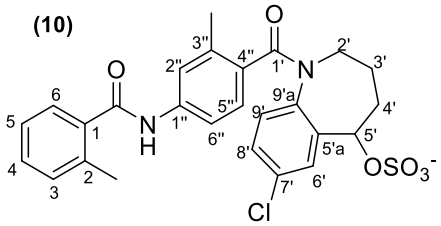	**(11)** 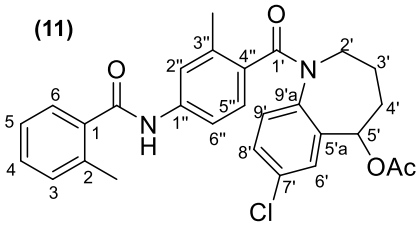
Position	^{1}H NMR δ (ppm) / ^{13}C NMR δ (ppm)	^{1}H NMR δ (ppm) / ^{13}C NMR δ (ppm)	^{1}H NMR δ (ppm) / ^{13}C NMR δ (ppm)
2, 3'' (CH_3)	2.43 / 18.8	2.42-2.43 / 18.9 2.09 / 19.0	2.42 / 18.8 1.99-2.00 / 19.1 2.20 / 20.3
CH_2	1.81, 2.08 / 25.8 1.61, 2.20 / 35.4 2.79, 4.72 / 46.3	1.72-1.78 / 25.4 1.68-1.68, 2.38-2.39 / 33.1 2.83, 4.67-4.70 / 45.8 4.89-4.91 / 47.2	1.75-1.83, 2.06-2.14 / 25.1 2.36-2.37 / 29.8 1.73-1.74, 2.11-2.14 / 31.5 2.82-2.87 / 45.7 4.70-4.74 / 46.0
OH	3.67 / -	- / -	- / -
5'	5.04 / 70.2	5.57-5.59 / 75.5 5.37-5.43 / 78.4	6.04-6.07 / 72.4 5.97-5.98 / 75.5
Ar	7.27 / 116.0 7.48 / 121.2 7.59 / 125.0 7.29 / 125.7 6.85 / 126.7 7.00, 7.45 / 127.0 6.75 / 129.3 7.39 / 129.9 7.31 / 130.8	7.06-7.08, 7.16 / 116.3 7.57, 7.72 / 121.0 7.26-7.30, 7.53-7.54 / 125.7 7.46-7.48 / 127.1 7.00 / 127.3 6.77 / 129.4 7.36-7.37 / 130.0 6.69 / 130.1 7.28 / 130.8	7.02-7.06, 7.23-7.24, 7.66-7.69 / 116.0 7.66-7.69, 7.51-7.55 / 121.0 7.26-7.32 / 125.6 7.02-7.06, 7.40-7.44, 7.45-7.47 / 127.3 6.80 / 129.8 7.37-7.39 / 129.9 7.33-7.35 / 130.7
NH	8.46 / -	8.65 / -	8.50 / -

ArCquat	-	-	-	132.0, 132.4, 136.0, 136.6, 136.7, 138.6, 139.2, 142.4	-	131.8, 132.7, 136.0, 136.6, 137.0, 139.0, 139.4, 140.0,
C=O	-	-	-	168.3, 169.1	-	168.2, 168.8, 169.9
HRMS (ESI) *m/z*	449.1601 [^{35}Cl-MH]$^+$, 451.1647 [^{37}Cl-MH]$^+$		531.1173 [^{37}Cl-MH]$^+$, 529.1197 [^{35}Cl-MH]$^+$		493.1732 [^{37}Cl-MH]$^+$, 491.1751 [^{35}Cl-MH]$^+$	
MS/MS *m/z*	-		431.1519 [$C_{26}H_{24}{}^{35}ClN_2O_2$]$^+$, 433.1498 [$C_{26}H_{24}{}^{37}ClN_2O_2$]$^+$, 252.1014 [$C_8H_7O$]$^+$		431.1533 [$C_{26}H_{24}{}^{35}ClN_2O_2$]$^+$,433.1513 [$C_{26}H_{24}{}^{35}ClN_2O_2$]$^+$, 252.1023 [$C_8H_7O$]$^+$	

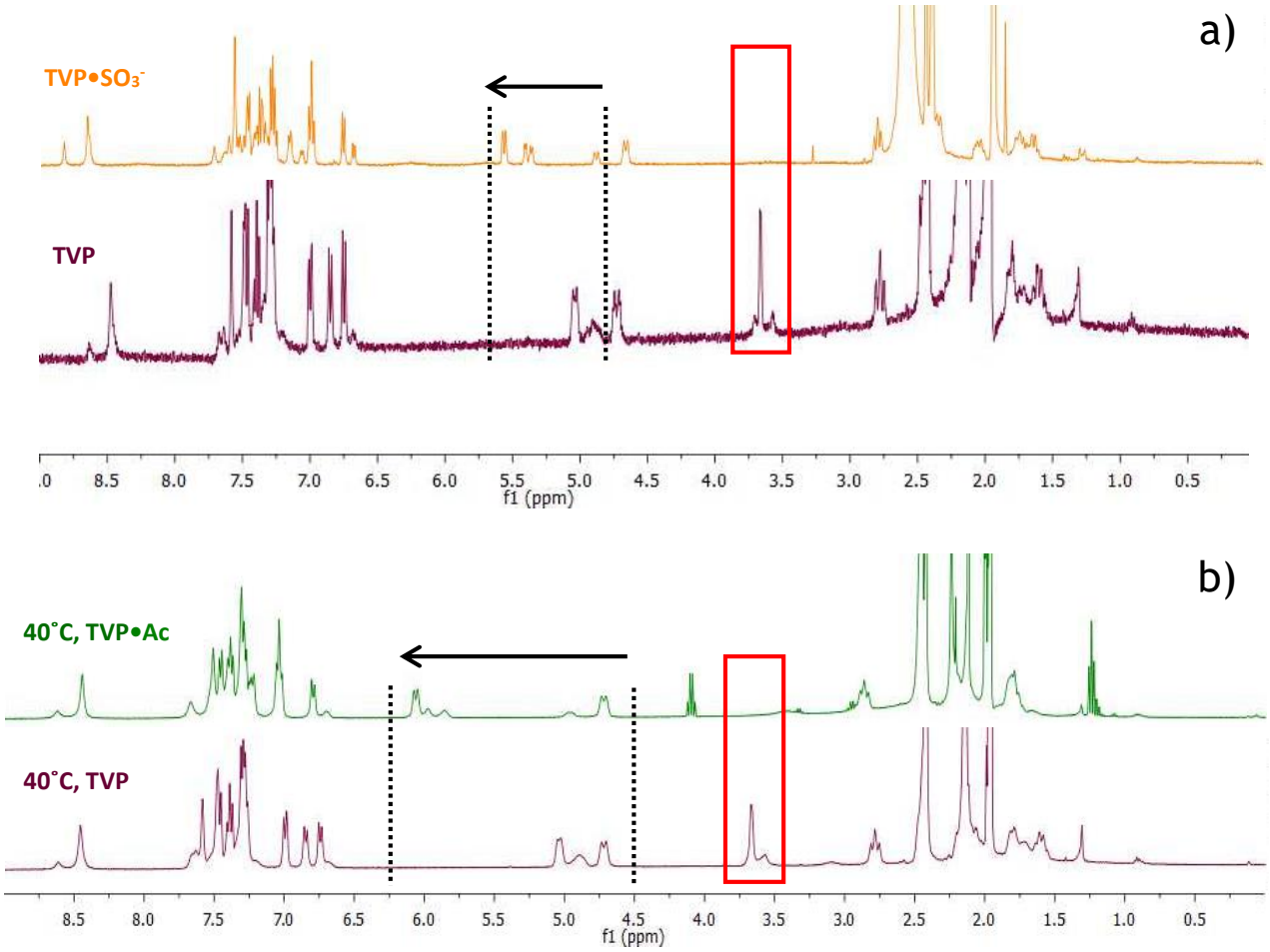

Figure 2.10 Comparison between the ^{1}H NMR spectra of tolvaptan with: a) 5'-*O*-sulfonate-tolvaptan (**10**); and b) 5'-*O*-acetyl-tolvaptan (**11**).

Based on the ^{1}H NMR data obtained for 5'-*O*-sulfonate-tolvaptan (**10**) (**Figure 2.11 a)**), it is visible low-field shift from the resonance of proton at the 5' position on tolvaptan, from 5.25 to 5.75 ppm, when compared with tolvaptan. This proton signal presents a correlation in the ^{1}H-^{13}C HSQC spectrum with the tertiary carbons at 75.46 ppm and 78.45 ppm, corresponding to the two conformations of **10**. These ^{13}C NMR signals present also a downfield shift when compared with the corresponding C-5' of tolvaptan (at 70.16 ppm), confirming the presence of OSO_3^- group. When compared with tolvaptan, the ^{13}C NMR spectrum of 5'-*O*-acetyl-tolvaptan (**11)** presents two new carbons corresponding to the acetyl moiety, namely a methyl carbon at 20.3 ppm, which correlates to three methyl protons in the ^{1}H-^{13}C HSQC spectrum, and a carbonyl carbon at 169.9 ppm.

When analyzed by reversed phase LC-DAD, 5'-*O*-acetyl-tolvaptan (**11)** was detected with rt = 34.8 min (**Figure 2.12**), differing from the starting material, tolvaptan, which was detected at rt = 30.0 min. This is fully compatible with the lower polarity of the tolvaptan acetate when compared with tolvaptan.

In contrast, tolvaptan sulfate eluted before tolvaptan with a rt = 23 min, as expected by the increased polarity upon sulfonation.

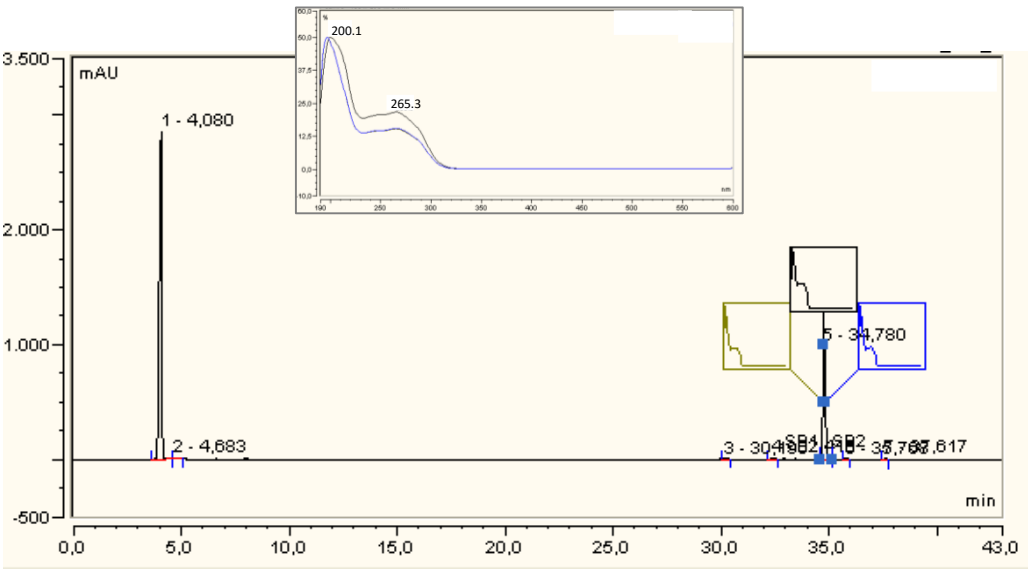

Figure 2.11 LC-DAD chromatogram and UV/Vis profile of 5'-*O*-acetyl-tolvaptan (**11**).

Definitive structural evidence of 5'-*O*-sulfonate-tolvaptan and 5'-*O*-acetyl-tolvaptan formation were obtained upon high resolution mass spectrometry analysis with electrospray ionization, LC-ESI-HRMS. Indeed, when 5'-*O*-acetyl-tolvaptan was analyzed in the positive ion mode two signals at *m/z* 493.1732 and 491.1751 were detected, showing the isotopic distribution expected for a molecule with one chlorine substituent, corresponding to the protonated molecules with ^{37}Cl and ^{35}Cl, respectively. Likewise, also in positive mode, the protonated molecule of 5'-*O*-sulfonate-tolvaptan showed two signals at *m/z* 531.1173 $[^{37}Cl\text{-}MH]^+$ and 529.1197 $[^{35}Cl\text{-}MH]^+$. When analyzed by tandem mass spectrometry (MS/MS), both molecules originated a similar fragmentation pattern showing at *m/z* 252.1023(14), respectively, the fragment ion stemming from the loss of the benzazepine moiety, and at *m/z* 431.1533(19), respectively, the fragment ion stemming from the elimination reaction of acetoxy and sulfoxy groups from the protonated molecules (**Figure 2.13)**.

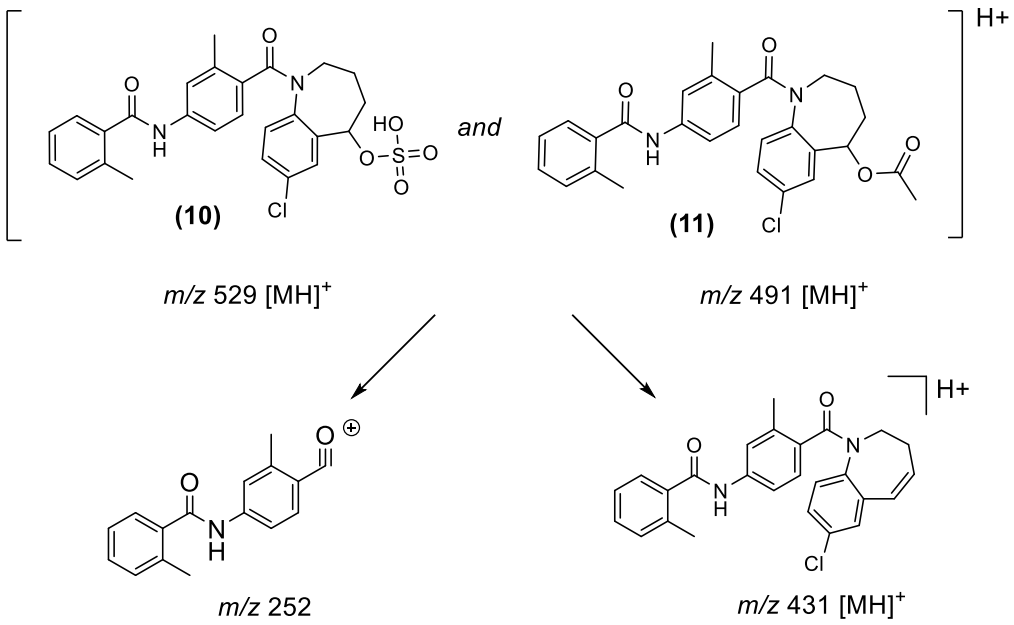

Figure 2.12 Proposed fragmentation mechanism, upon tandem mass spectrometry analysis (MS/MS) of 5'-*O*-sulfonate-tolvaptan (**10**) and 5'-*O*-acetyl-tolvaptan (**11**).

2.1.1.2 Reaction of tolvaptan's metabolic plausible reactive metabolites with deoxynucleobases and amino acids

Reactions of tolvaptan's metabolically plausible reactive metabolites, 5'-*O*-sulfonate-tolvaptan and 5'-*O*-acetyl-tolvaptan, with 2'-deoxyguanosine (dG) and 2'-deoxyadenosine (dA), were conducted at 37 °C in THF/DMF/water, using 0.2 molar excess of electrophile (**Figure 2.1**). However, and despite the Antunes *et al.*[35] success on the preparation of multiple nevirapine DNA adduct standards using similar conditions, following LC-ESI-MS analysis of reaction mixtures, no evidence of adduct formation was observed. Subsequent attempts, using an increased molar excesses of the deoxynucleobase, also failed.

Taking into consideration that covalent adducts formed between electrophilic metabolites and proteins are frequently implicated in the onset of drug-induced toxic events[36], [43], [44] we have subsequently investigated whether putative tolvaptan reactive metabolites could react with amino acids bearing nucleophilic side chains. Indeed, despite the fact these electrophilic metabolites did not react with dG and dA, a distinct behavior could be obtained upon reaction with highly nucleophilic amino acids such the thiol-containing cysteine. Reactions of 5'-*O*-sulfonate-tolvaptan and 5'-*O*-acetyl-tolvaptan with NAC (*N*-acetyl-L-cysteine), NAL (*N*-acetyl-L-lysine) and ethyl valinate (mimicking the *N*-terminal valine of hemoglobin) were conducted at 37˚C in 50 mM phosphate buffer (pH 7.4)/THF (5:1) using a 4 molar excess of the nucleophile [36]. However, once again, no adduct was identified upon LC-

ESI-MS analysis of reaction mixtures. In fact, the only product detected in all reactions of 5'-*O*-sulfonate- tolvaptan and 5'-*O*-acetyl- tolvaptan with 2'-deoxynucleobases and amino acids, exhibited a signal at *m/z* 431 and 433, compatible with the formation of **42**.

To obtain definitive proof of **42** formation, a standard of compound was synthesized, by reacting tolvaptan with a molar excess of methanesulfonic acid, at 50˚C, followed by PTLC purification (**Figure 2.13**). Compound **42** was identified with rt c.a. 31.0 min, displaying in the MS spectrum two signals at *m/z* 431 and 433, compatible with the protonated molecule of the structure containing, ^{35}Cl and ^{37}Cl, respectively. The rt and fragmentation patterns of this standard were identical to the ones observed in the reactions of **10** and **11** with bionucleophiles.

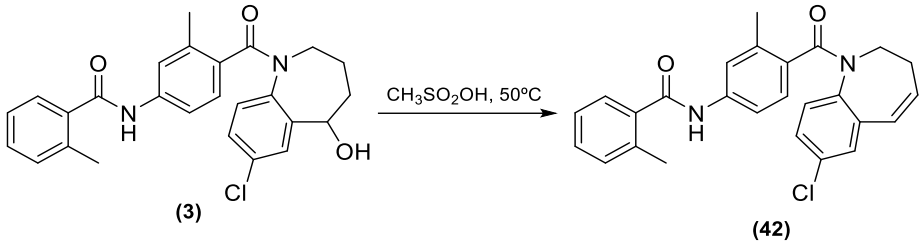

Figure 2.13 Formation of the synthetic standard of **42**, upon reaction of tolvaptan with methanesulfonic acid.

Whereas **42** was not obtained as a pure compound, it was noticeable upon NMR analysis the presence of only two methylene carbons at 32.1 ppm and 45.7 ppm (instead of three, as in tolvaptan) (**Figure 2.14**). Additional signals are also observed in the downfield region of the spectra, compatible with the existence of a double bound in the benzazepine ring.

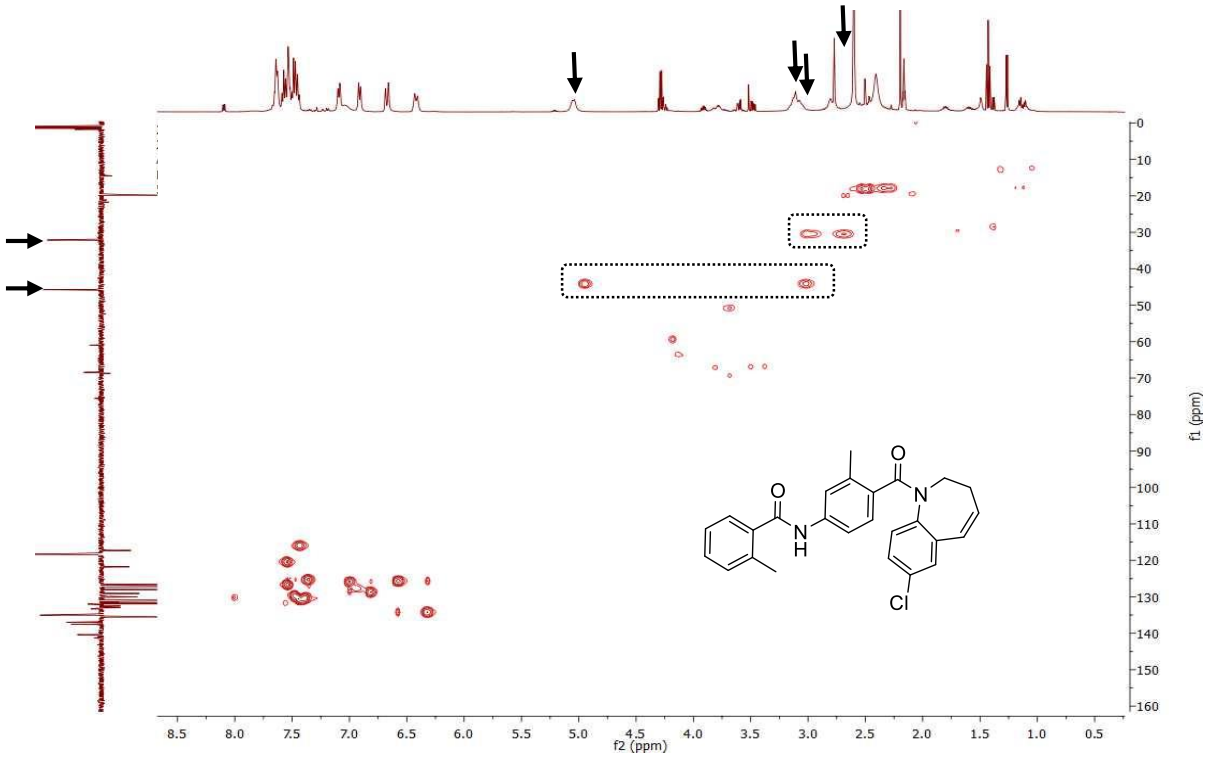

Figure 2.14 ^{1}H-^{13}C HSQC NMR spectrum of tolvaptan's derivative **42**.

The fragmentation pattern obtained upon tandem mass spectrometry analysis is fully compatible with the structure described (**Figure 2.15**).

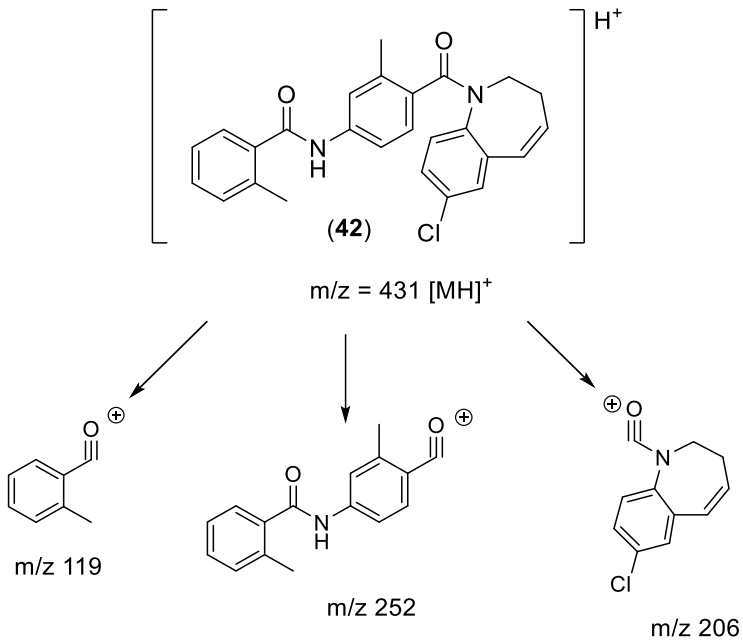

Figure 2.15 Proposed fragmentation pattern of tolvaptan's derivative **42**.

The preparation of this synthetic standard allowed the definitive identification of **42** in the reactions of **10** and **11** with bionucleophiles. This suggests that if formed *in vivo* **10** and **11** can lead to the formation of **42**. In fact, taking into consideration that the formation of the epoxides (Phase I reaction) from olefinic derivatives, are frequently implicated in drug-induced toxic events[45], the *in vivo* formation of **42** may have some toxicological role.

2.1.2 Non-biomimetic strategy: Palladium-catalyzed coupling reaction of 5'-chloro-tolvaptan (43) to 2'-deoxynucleobases

Antunes *et al.*[35, 46] reported the synthesis of multiple nevirapine covalent adducts by an adaptation of the Buchwald-Hartwig strategy of Pd-catalyzed C-N bond formation (**Figure 2.16**). This strategy consisted on heating for 1h a suspension of a brominated derivative of nevirapine, 12-Bromo-NVP (20 mg, 58 µmol, **44**) with tris(dibenzylideneacetone)dipalladium (0) [$Pd_2(dba)_3$] (5 mg, 5.8 µmol) ,3',5'-bis-*O*-(*tert*-butyldimethylsilyl)-2'-deoxynucleoside (87 µmol) and cesium carbonate (28 mg, 87 µmol, $CsCO_3$). The deprotection of the silyl protecting group was accomplished upon addition of tetrabutylammonium fluoride.

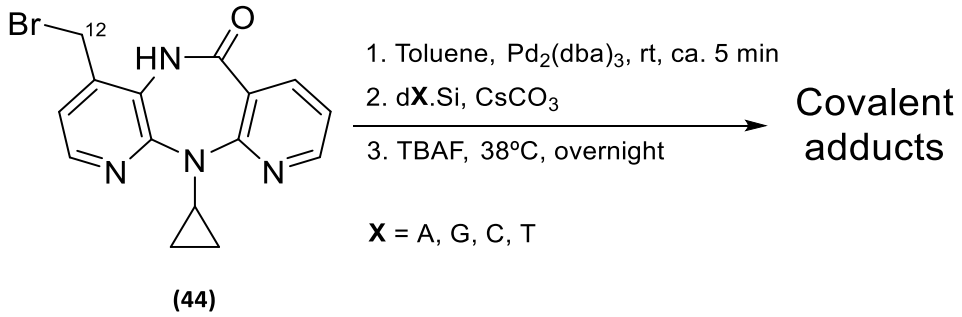

(44)

Figure 2.16 Strategy used by Antunes *et al.*[35, 46] for the formation of covalent adducts between 12-Bromo-NVP (**44**) and dX•Si, X = A, G, C, T.

These results prompt us to explore a similar methodology for the preparation of tolvaptan covalent adduct standards.

2.1.2.1 Synthesis of 5'-chloro-tolvaptan (45)

The first step of this strategy consisted on the preparation of 5'-chloro-tolvaptan (**45**) upon substitution of the hydroxyl group at the position C-5' of the benzazepin ring by a chlorine atom. This substitution was needed, since the synthetic strategy to be used for the formation of adduct standards,

involves the oxidative addition of palladium (0) to C-X substrates (X = halogen and pseudohalogen).[47, 48]

General procedures for alcohol chlorination make use of concentrated HCl, $SOCl_2$, PCl_5, PCl_3 and $POCl_3$, strongly acidic and corrosive reagents, which often require heating for the reaction to take place [49]. However, the chlorination of benzyl alcohols can be achieved by softer conditions that include the use of PPh_3/CCl_4, a variation of the Mitsunobu reaction, silyl chlorides upon catalysis, and specifically for benzylic alcohols, sulfonyl chlorides, like methanesulfonyl chloride (MsCl) and *p*-toluenesulfonyl chloride (TsCl), along with an organic base.[50]

The optimized condition for the formation of 5'-chloro-tolvaptan (TVP•Cl, **45**), involved refluxing tolvaptan in thionyl chloride, leading to the formation of this derivative as a translucent light beige oil (**Figure 2.17**).

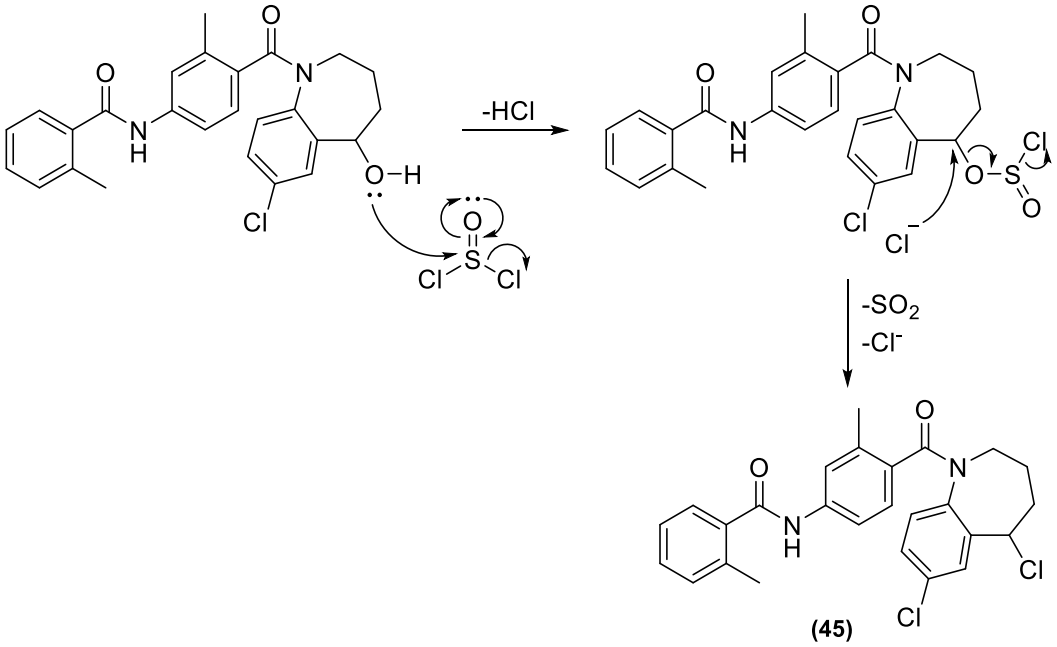

Figure 2.17 Mechanistic representation of tolvaptan chlorination reaction with thionyl chloride.

Despite the fact compound **45** was not obtained as a pure derivative, through analysis of the ^{1}H-^{13}C HSQC spectrum (**Figure 2.18**), it is noticeable the downfield shift of C-5' of **45** when compared with tolvaptan (from 63.6 and 67.7 ppm to 70.2 ppm), which is compatible with the substitution of a hydroxyl group by a chlorine atom.

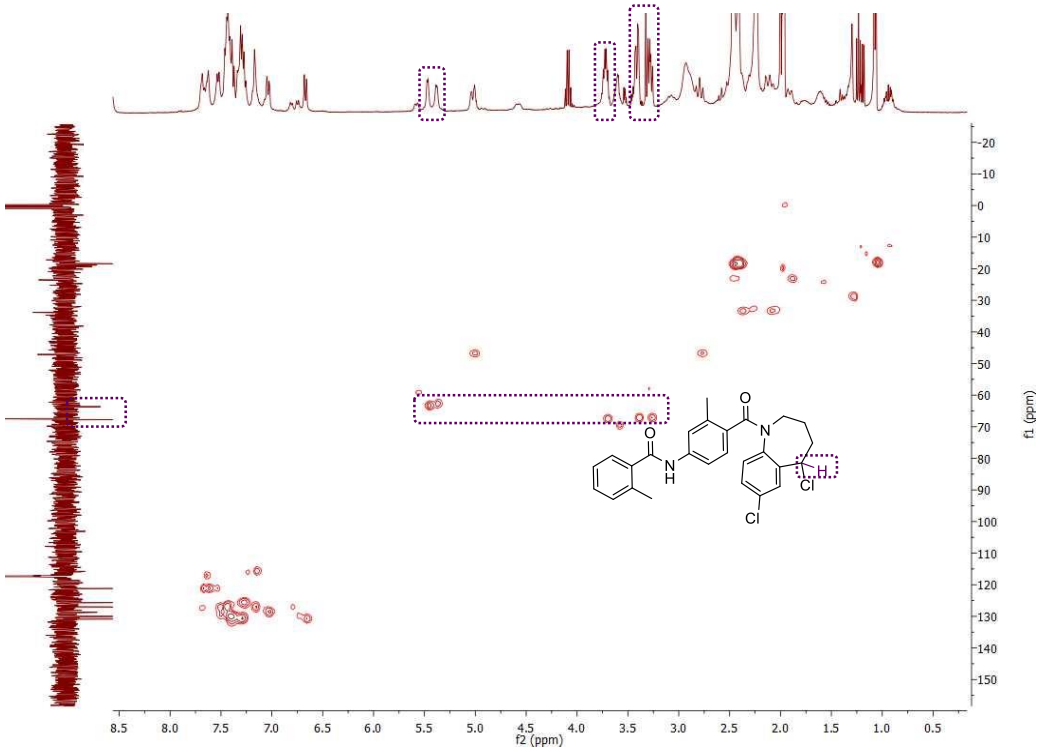

Figure 2.18 ^{1}H-^{13}C HSQC spectrum of the mixture containing compound **45.**

The mixture was also analyzed by LC-ESI-MS, and the full scan spectrum (**Figure 2.19**) of product eluting at rt = 25.0 min, displays at *m/z* 467, 469 and 471 signals compatible with the protonated molecules of 5'-chloro-tolvaptan (**45**) $[MH]^+$, $[MH+2]^+$ and $[MH+4]^+$, with the isotopic distribution expected for a molecule containing two chlorine atoms. A fragment ion is also obtained at *m/z* 431 and 433, compatible with the loss of HCl from the protonated molecule of **45**. It was also detected in the reactional mixture the elimination product **42**, with *m/z* 431, 433 also having the appropriate chlorine isotopic pattern for a molecule with one chlorine.

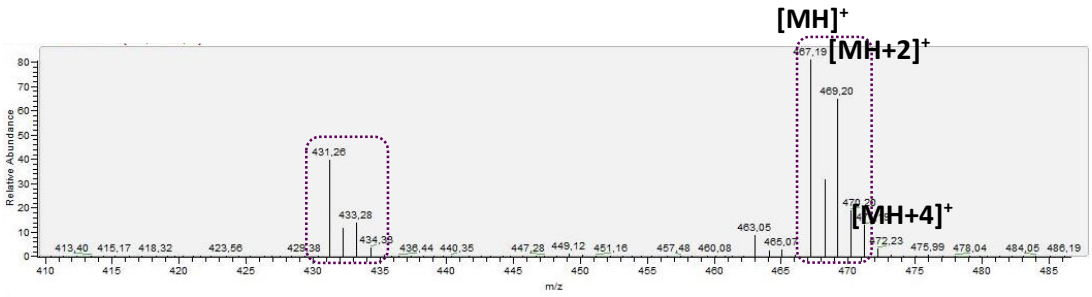

Figure 2.19 Mass spectrum obtained upon LC-ESI-MS analysis of 5'-chloro-tolvaptan (**45**) displaying the signals corresponding to the protonated molecules $[MH]^+$, $[MH+2]^+$ and $[MH+4]^+$ along with the fragment ion at *m/z* 431, 433 corresponding to the loss of HCl from the protonated molecule.

2.1.2.2 Coupling reaction

The palladium-mediated coupling of compound **45** with 3',5'-*O*-Bis(*tert*-butyldimethylsilyl)-2'-deoxyguanosine (dG•Si, **46**) (**Figure 2.20**) was subsequently performed. Towards this goal, a suspension of chlorinated tolvaptan (**45**) (1.0 eq.) in toluene (144.0 µL) was added tris-(dibenzylideneacetone)dipalladium (0) [$Pd_2(dba)_3$] (0.1 eq.), the mixture was stirred at r.t. for 10 min., whereupon a solution of dG•Si (1.5 eq.) and $CsCO_3$ (1.5 eq.) in toluene (144.0 µL) was added. The resulting mixture was stirred at 90˚C for 3.5 h and was monitored by TLC. Following cooling to r.t. tetrabutyl ammonium fluoride (TBAF) (5.0 eq.) was added and the resulting solution was stirred at c.a. 38˚C, for 1.5 h. The reaction mixture obtained was analyzed by LC-ESI-HRMS.

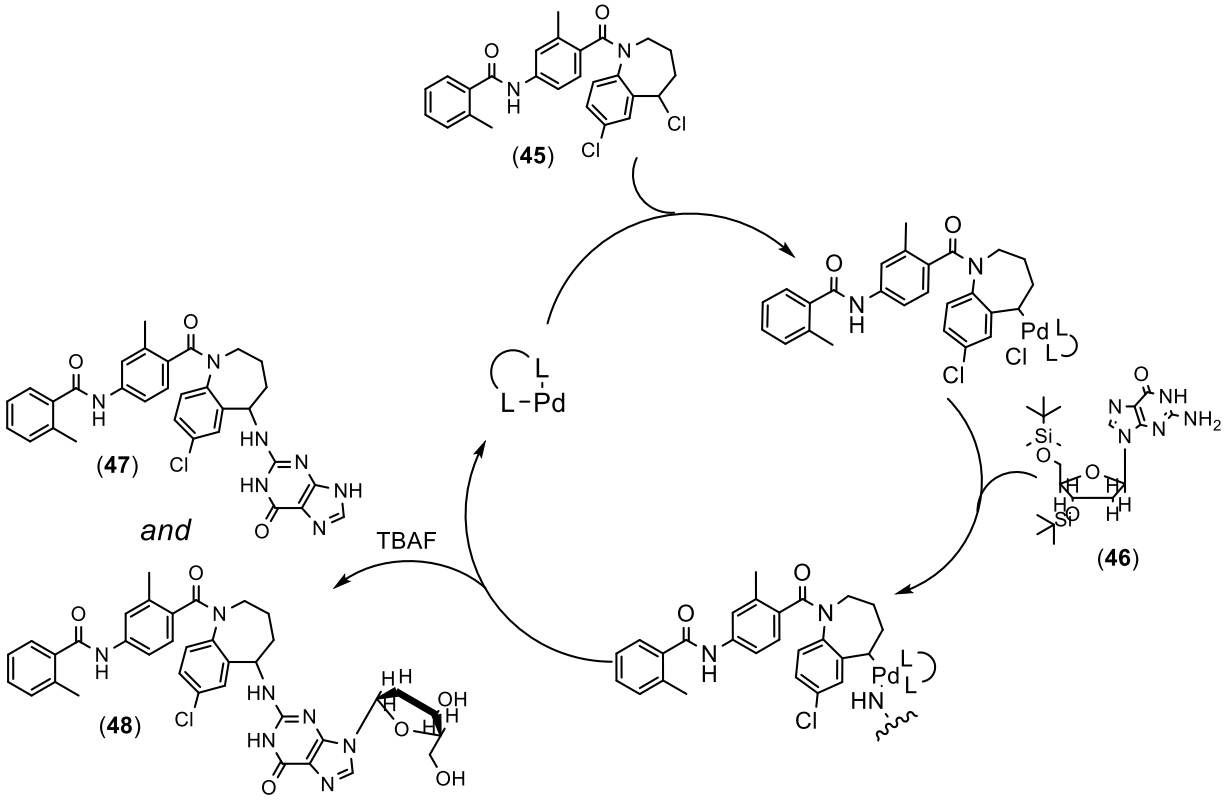

Figure 2.20 Schematic representation of palladium-catalyzed coupling reaction of 5'-chloro-tolvaptan (**45**) to dG•Si (**46**), followed by cleavage of the silylated protection groups with tetrabutylammonium fluoride.

In order to accept an experimentally measured accurate mass value, the same has to have an associated mass measurement error comprised within pre-determined standard values. The mass measurement error (or accuracy) of a single reading can be calculated as described in **Equation 1**, were Δm_i can take positive or negative values, and m_i stands for experimental individual measurement and

m_a for true value (exact mass). Since the mass analyzer operated was a Q-TOF from Bruker Daltonics, a mass peak can be accurately mass measured to < 5 ppm with an external calibration.[51], [52]

$$\Delta m_i = \frac{(m_i - m_a)}{m_a} < 5\ ppm \qquad \textbf{(1)}$$

The LC-ESI-HRMS full scan analysis allowed the identification of two signals with *m/z* 582.2000 (**Figure 2.21 a)**) and *m/z* 698.2469 (**Figure 2.21 b)**), compatible with formation of non-depurinating (TVP.dG, **48**) and depurinating (TVP.G, **47**) adducts, respectively. These signals present a m*ass* measurement error of $|\Delta m_i| = 2.76 < 5.00$ ppm and $|\Delta m_i| = 2.56 < 5.00$ ppm, respectively. The MS/MS analysis of these adducts, constituted further evidence of their formation, namely displaying the fragment ion at *m/z* 152, characteristic of the protonated molecule of guanine (**Figure 2.22**). However, the MS/MS fragment ions identified do not clarify the position where the covalent bond formation between tolvaptan's C-5' position and the nucleobase occurred.

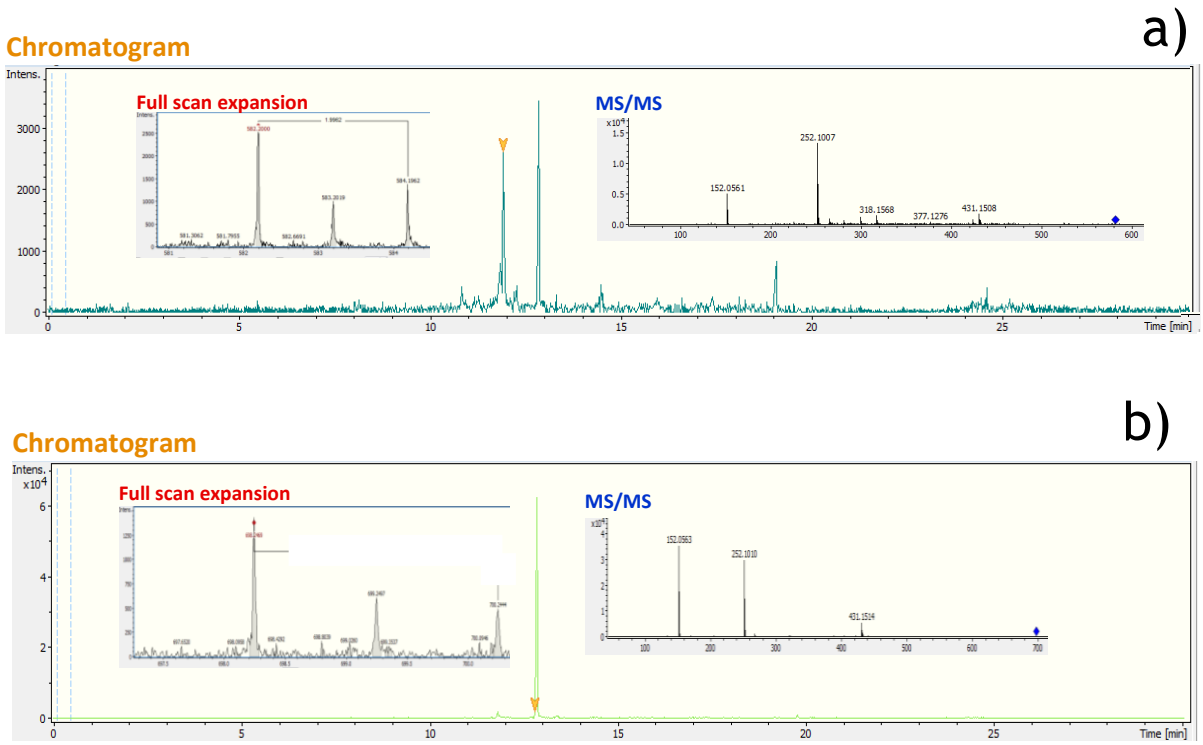

Figure 2.21 HPLC-ESI-HRMS chromatograms and mass spectra of TVP.G and TVP•dG and adducts with *m/z*: a) 582.2000 and b) 698.2469.

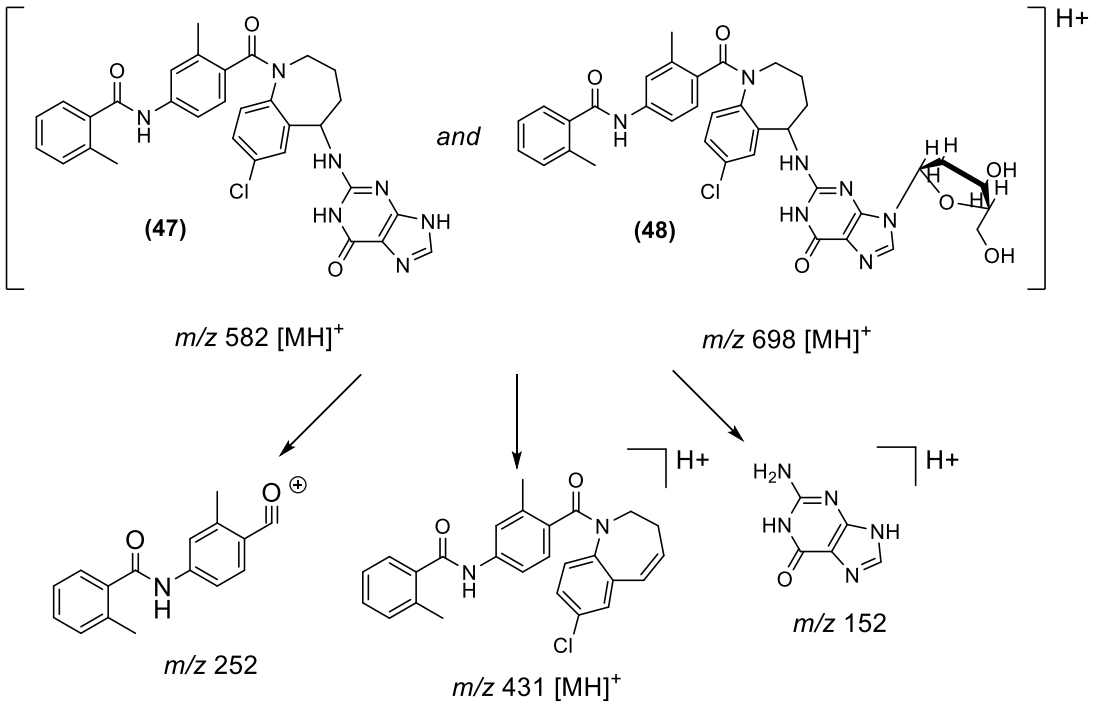

Figure 2.22 Fragmentation patterns of TVP.G (**47**) and TVP•dG (**48**) adducts with *m/z* 582 and *m/z* 698, respectively.

2.2 Reaction of tolvaptan electrophilic metabolites with DNA

Despite the fact that no products were detected upon reaction of tolvaptan's reactive metabolites, 5'-*O*-sulfonate-tolvaptan (TVP•SO_3^-, **10**) and 5'-*O*-acetyl-tolvaptan (TVP•Ac, **11**), with the nucleosides dG and dA, reaction of this metabolites with DNA was performed since the chemical environment experienced by the electrophiles when in contact with DNA's nucleophilic centers is much more complex than the one experienced with 2'-deoxynucleosides, therefore the result obtained can be distinct from the one observed with nucleosides. Indeed, steric constraints and the local electronic environment within the double helix often supersede the intrinsic reactivity of each nucleophilic site at determining the major binding positions of alkylating agents in DNA.

Apart from the phosphodiester bonds which connect nucleotides to one another, the hydrogen bonds between the complementary base pairs, which hold together the two polynucleotide strands, intertwining them into a helical duplex, and the London dispersion forces and hydrophobic effects that stabilize the base pair stacking, there are the glycosidic bonds connecting the base pair to its sugar rings, which are not directly opposite to each other, leading to an uneven spacing of the two sugar-phosphate backbones of the double helix along the helical axis.[34], [53], [54]

Thus, the grooves formed between the backbones are irregular, one is larger the *major groove*, and one smaller the *minor groove* (**Figure 2.23**) The major and minor groove differ in the projection of

their base pair nitrogen and oxygen atoms, that project inward from their sugar-phosphate backbones toward the center of the DNA for the major groove, and outward toward the outer edge of the DNA for the minor groove. The two grooves create two different nucleophilic environments, making it even more peculiar for the required conditions for nucleophilic attack on the electrophilic reactive metabolites to happen. It would be expected that the minor groove presents better nucleophilic features, compared to the major groove, despite its larger steric hindrance, since its nitrogen and oxygen atoms of the base pairs project outward from their sugar-phosphate backbones toward the outer edge of the DNA, being more exposed to electrophilic contact.[34], [54]

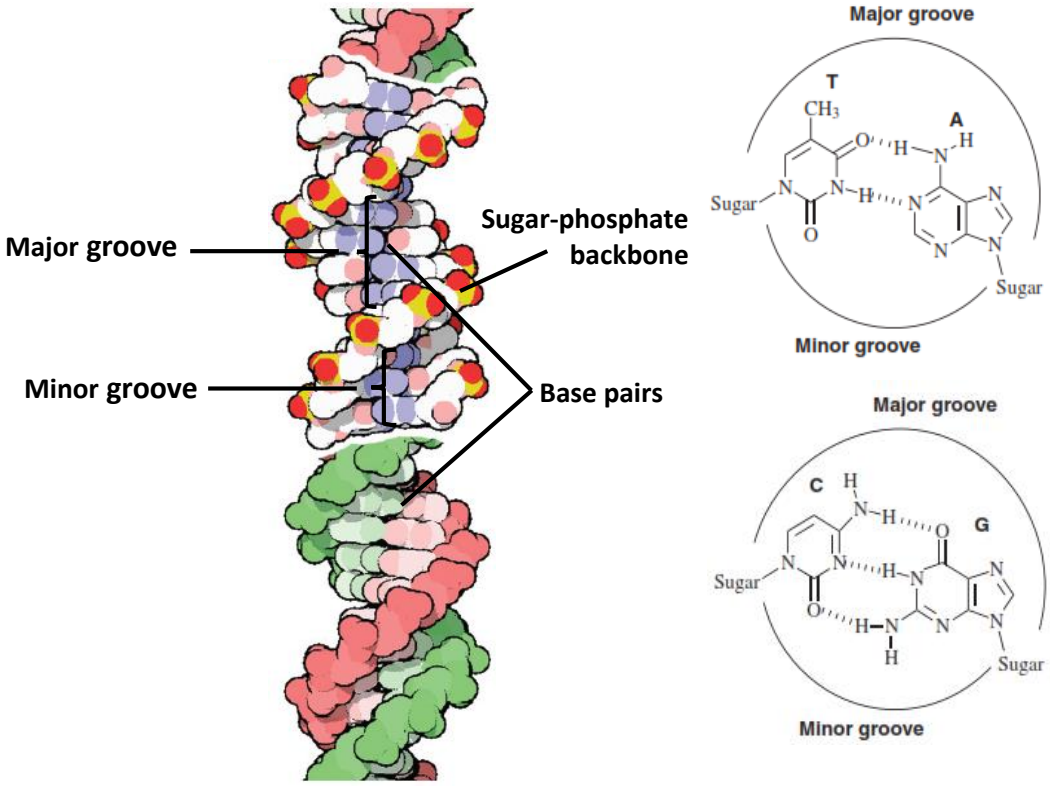

Figure 2.23 B-DNA features that lead to major and minor groove formation. B-DNA, the structure found under typical conditions of living cells, is one of the three DNA possible structures, along with A-DNA, found under dehydrating conditions and having a deep major groove (adapted from [34], [54]).

5'-*O*-sulfonate-tolvaptan (TVP•SO_3^-, **10**) and 5'-*O*-acetyl-tolvaptan (TVP•Ac, **11**) were reacted with salmon testes DNA. The reaction mixture obtained upon enzymatic and thermal hydrolysis were subsequently analyzed by LC-ESI-HRMS (**Figure 2.24**).

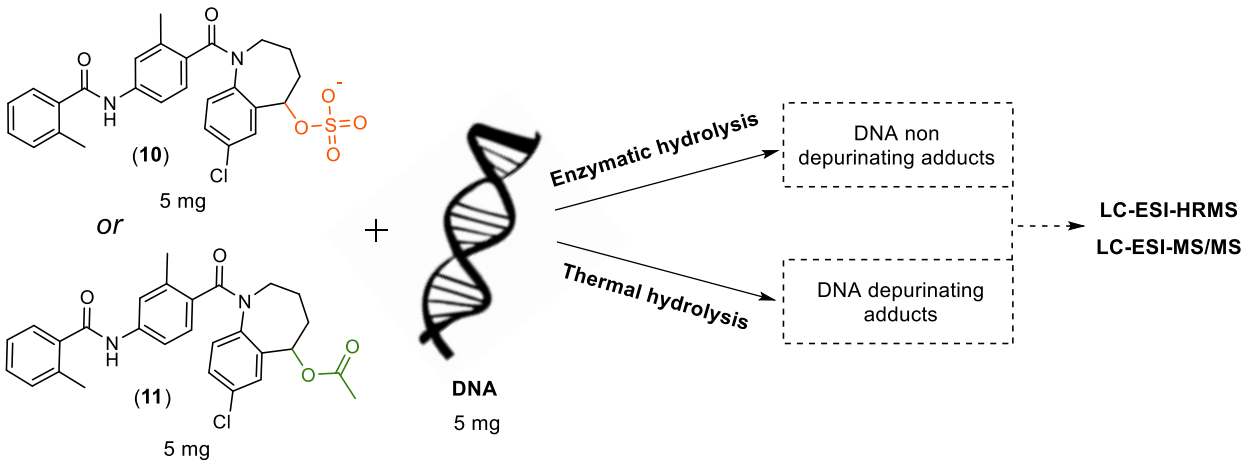

Figure 2.24 Schematic representation of 5'-*O*-sulfonate-tolvaptan (TVP•SO_3^-, **10**) and 5'-*O*-acetyl-tolvaptan (TVP•Ac, **11**) reaction with salmon testes DNA, followed by enzymatic and thermal hydrolysis of the reactional mixtures, and finally LC-ESI-HRMS and LC-ESI-MS/MS of the resulting solutions.

The experimental conditions for the reaction of 5'-*O*-sulfonate-tolvaptan (TVP•SO_3^-, **10**) and 5'-*O*-acetyl-tolvaptan (TVP•Ac, **11**) with DNA, involved the addition of a DMF or THF solution of the metabolite (5 mg) to a solution of salmon testes DNA (5 mg) in Bis-Tris and EDTA buffer (pH 7.24). Following, an incubation period of 10 days at 37˚C, the non-bonded metabolite was extracted with ethyl acetate. The DNA was subsequently precipitated by addition of NaCl (5M) and absolute ethanol. The DNA pellets were washed with ice-cold 70% ethanol and redissolved in the previous buffer. One aliquot of the DNA solution was hydrolyzed enzymatically, in order to obtain non depurinating adducts, and the other subjected to neutral thermal hydrolysis, in order to obtain depurinating adducts. However the LC-ESI-HRMS analysis of hydrolysates thus afforded did not allowed the identification of any TVP-DNA adduct. The putative formation of acetylated 2'-deoxunucleobases was also searched. Indeed, when reacting 5'-*O*-acetyl-tolvaptan (TVP•Ac, **11**) with DNA, the acetylation of nucleophilic positions of 2'-deoxynucleobases is plausible, which in turn may have implications in tolvaptan's toxicity. In fact, preliminary LC-ESI-MS/MS analysis evidenced the formation of a product with *m/z* 294.1176 (**Figure 2.25**) and a fragmentation pattern described in **Figure 2.26**, consistent with deoxyadenosine acetylation.

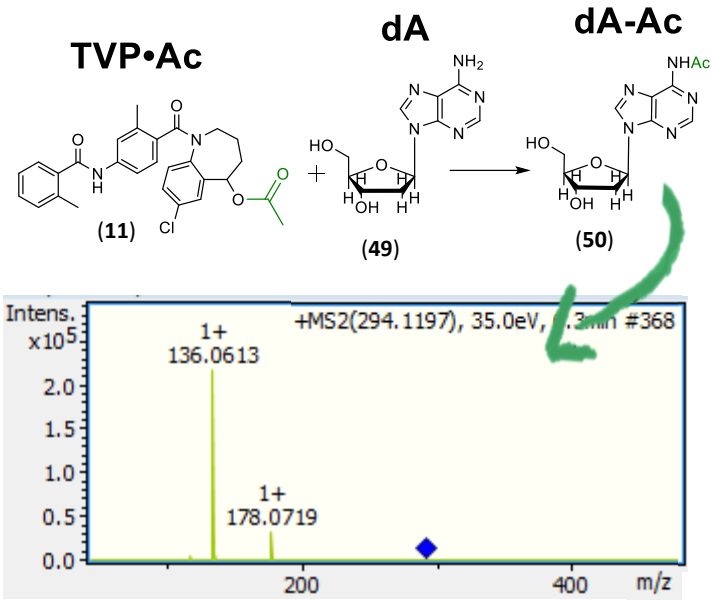

Figure 2.25 MS/MS spectrum of the putative dA•Ac (**50**) product with *m/z* 294, detected in the reaction of 5'-*O*-acetyl-tolvaptan (TVP•Ac, **11**) with DNA.

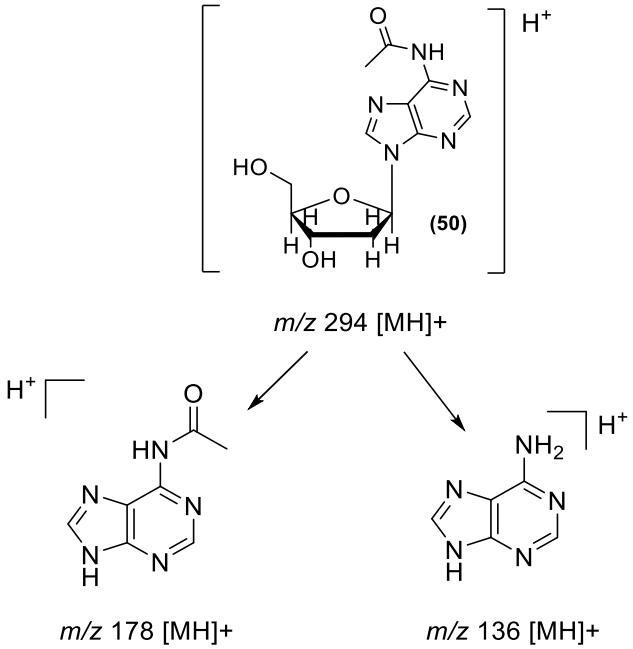

Figure 2.26 Fragmentation pattern of the putative dA•Ac (**50**) product with *m/z* 294, detected in the reaction of 5'-*O*-acetyl-tolvaptan (TVP•Ac, **11**) with DNA.

This prompted us to synthesize the N^6-acetyl-2'-deoxyadenosine **(50)** standard, by the synthetic methodology displayed in **Figure 2.27**.

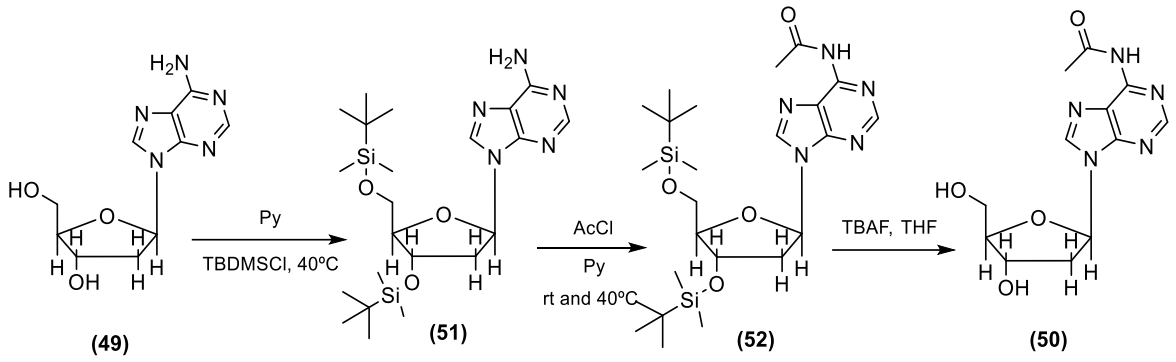

Figure 2.27 Synthetic strategy followed for the synthesis of N^6-acetyl-2'-deoxyadenosine **(50)** standard.

This strategy involved first, the protection of dA (**49**) hydroxyl groups with *tert*-butyldimethylsilyl chloride, followed by the primary amine acetylation, yielding N^6-acetyl- 3',5'-O-bis(*tert*-butyldimethylsilyl)-2'-deoxyadenosine **(52).** Following cleavage of the silylated protection groups, N^6-acetyl-2'-deoxyadenosine **(50)** was isolated from the white yellow solid fraction, and analyzed by LC-ESI-MS/MS (**Figure 2.28**). By analyzing the full scan spectrum, it is visible the presence of a product with *m/z* 294.1183 compatible with the protonated molecule of **50**, having an associated error of Δ = 4.69 ppm. Although fragment ions at *m/z* 178.0707 and 136.0622 obtained upon MS/MS analysis (**Figure 2.28**) are similar with the ones obtained upon MS/MS analysis of DNA enzymatic hydrolysate from reaction with 5'-*O*-acetyl-tolvaptan (TVP•Ac, **11**) (**Figure 2.25** and **2.26**), both products have distinct rt. This may exclude the possibility of 5'-*O*-acetyl-tolvaptan induced acetylation of DNA or suggest distinct acetylation positions between DNA and the synthetic standard prepared. In fact, this subject needs further clarifications.

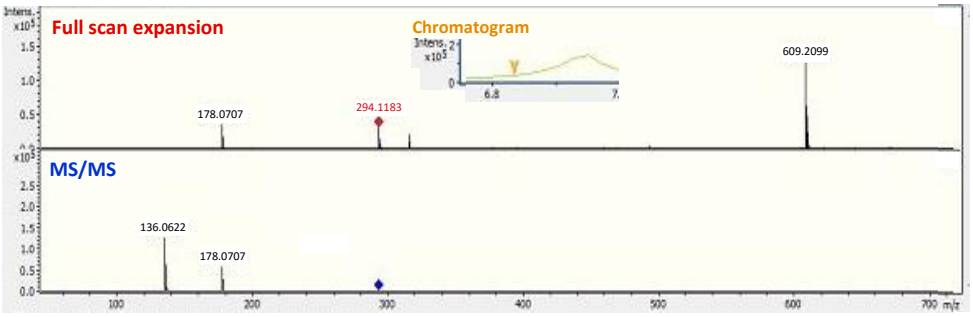

Figure 2.28 N^6-acetyl-2'-deoxyadenosine **(50)** LC-ESI-HRMS and LC-ESI-MS/MS spectra.

3 Conclusions and Prospects

Since tolvaptan-induced liver injury remain to be elucidated, and preliminary results obtained in CYP-deficient liver cell lines have shown evidence of tolvaptan-induced DNA damage without the need for Phase I metabolism, the main goal of this thesis was to investigate whether the observed DNA damage could stem from the formation of DNA adducts with the two metabolic plausible tolvaptan Phase II metabolites: 5'-*O*-sulfonate-tolvaptan (**10**) and 5'-*O*-acetyl-tolvaptan (**11**).

To test this hypothesis several preliminary results were obtained:

1. The two putative tolvaptan Phase II metabolites 5'-*O*-sulfonate-tolvaptan (**10**) and 5'-*O*-acetyl-tolvaptan (**11**) were synthesized and characterized by NMR and MS.
2. Mesylation of tolvaptan, followed by NAC reaction allowed the identification of an NAC conjugate, stemming from nucleophilic attack at the tolvaptan benzamide carbonyl. This product was characterized by NMR.
3. Two tolvaptan-DNA adduct standards were synthesized by a non-biomimetic strategy involving a palladium-catalyzed coupling reaction. This strategy involved the synthesis of 5'-chloro-tolvaptan derivative that was subsequently coupled with 3',5'-*O*-bis(tertbutyldimethylsilyl)-2'-deoxyguanosine, under palladium catalysis. Following deprotection and LC-ESI-HRMS analysis of the mixture afforded two adducts were identified based on exact mass, isotopic pattern and MS/MS fragmentation pattern: One depurinating adduct, and one non-depuritaning adduct. Nonetheless, based on data obtained it was not possible the establishment of the site of adduction to the guanine base.
4. A synthetic standard of *N*-{4''-[(7'-chloro-2',3'-dihydro-1*H*-benzo[*b*]azepine-1'-yl)carbonyl]-3-methylphenyl}-2-methylbenzamide (**42**) (tolvaptan olefin) was prepared and characterized by NMR and mass spectrometry. This compound was consistently identified in all reaction performed with the electrophilic derivatives **10** and **11**.
5. A synthetic standard of N^6-acetyl-2'-deoxyadenosine (49) was prepared and characterized by NMR and MS. The preparation of this standard was determinant to investigate if acetylation of DNA bases could occur upon reaction with 5'-*O*-acetyl-tolvaptan (**11**).

However, following LC-ESI-MS analysis of reaction mixtures, obtained upon reaction of the two putative tolvaptan Phase II metabolites 5'-*O*-sulfonate-tolvaptan (**10**) and 5'-*O*-acetyl-tolvaptan (**11**) with 2-deoxiguanosides (e.g. 2'-deoxyguanosine and 2´-deoxyadeosine) or DNA, any evidence was obtained for the formation of tolvaptan-DNA adducts or for the occurrence of DNA acetylation (by 11). These results suggest that the tolvaptan-induced DNA damage, observed in CYP-deficient cell lines, do not stem from the reaction of the tolvaptan Phase II metabolites, **10** and **11**, with DNA, as initially

hypothesized. Taking into consideration that the formation of covalent adducts with proteins can constitute a pathway of liver toxicity, the reactivity of **10** and **11** towards model amino acids bearing nucleophilic side chains was also investigated. However, this hypothesis can also be ruled out due to the lack of products obtained. DNA damage via acetylation upon reaction with 5'-*O*-acetyl-tolvaptan (**11**) was one additional hypothesis investigated. However, based on distinct rt of product identified in DNA hydrolysate and the synthetic standard N^6-acetyl-2'-deoxyadenosine (**50**), it was possible to attest that acetylation positions of the synthetic product and DNA were distinct. Nonetheless, the possibility of occurrence of other acetylation positions needs further investigations.

Interestingly, *N*-{4''-[(7'-chloro-2',3'-dihydro-1*H*-benzo[*b*]azepine-1'-yl)carbonyl]-3-methylphenyl}-2-methylbenzamide (**42**) (tolvaptan olefin) was consistently identified, by LC-ESI-MS, in reaction mixtures obtained from reactions with the electrophilic derivatives **10** and **11**, based on the comparison with the synthetic standard prepared. This suggests that if acetylation and/or sulfonation of tolvaptan occurs *in vivo*, the formation of this olefinic derivative is a plausible event, which may have toxicological implications due to the possibility of bioactivation via epoxidation.

The synthetic standards prepared in this work (**10**, **11**, **42**, **43, 47, 48** and **50**) are now available to investigate their formation in CYP-deficient cell lines exposed to tolvaptan. In fact the formation of NAC covalent adduct **43**, upon mesylation of tolvaptan amide moiety, suggests that the *in vivo* sulfonation and/or acetylation at the secondary amide shouldn't be ruled out, and could constitute an potential pathway for DNA and protein adducts formation.

4 Experimental Procedure

4.1 Materials and Methods

Tolvaptan was purchased from Sequoia Research Products. All other commercially available reagents were acquired from Sigma-Aldrich Química and Fluka, unless specified otherwise, and were used as received. All amino acids used were (*L*)-*α*-amino acids. Whenever necessary, solvents were purified and dried according to standardized methods.[55]

Molecular Sieves 4Å were activated upon heating at 280˚C for 3 h under vacuum. Preparative and analytical Thin Layer Chromatography (PTLC and TLC, respectively) were carried out using silica gel 60 G/UV254 Macherey-Nagel plates with 0.5 mm and 0.20 mm, respectively.

^{1}H NMR spectra were recorded on Bruker Avance III 300, 400 or 500 spectrometers operating at 300, 400 and 500.16 MHz, respectively. ^{13}C NMR spectra were recorded on the same instruments, operating at 75.43, 100.6 and 125.77 MHz, respectively.[56] Chemical shift (δ) are reported in ppm downfield from TMS and the data for ^{1}H NMR spectra was presented by the following order: deuterated solvent used, chemical shift, relative intensity, spin multiplicity (s – singlet, d – doublet, t – triplet, m – multiplet, dd – doublet of duplets), coupling constant (*J*, in Hz) and molecule attribution, when possible. ^{13}C NMR data was presented as follows: deuterated solvent, chemical shift and molecule attribution, when possible.

LC-DAD was conducted on an Ultimate 3000 Dionex system consisting of an LPG-3400A quaternary gradient pump and a diode array spectrophotometric detector. HPLC analysis were performed with a Luna C18 (2) column (250 mm x 4.6 mm; 5 mm; Phenomenex, Torrance, CA), at a flow rate of 1.0 mL•min^{-1}. Semipreparative HPLC separations were conducted with a Luna C18 (2) column (250 mm x 10 mm; 5 mm; Phenomenex) at a flow rate of 3.0 mL•min^{-1}. Unless specified, a 30.0-min linear gradient from 5 to 70% acetonitrile (B) in 0.1% aqueous formic acid (A), followed by a 2.0-min linear gradient to 100% acetonitrile and an 8.0-min isocratic elution with acetonitrile, was used in all instances (**Figure 4.1**).

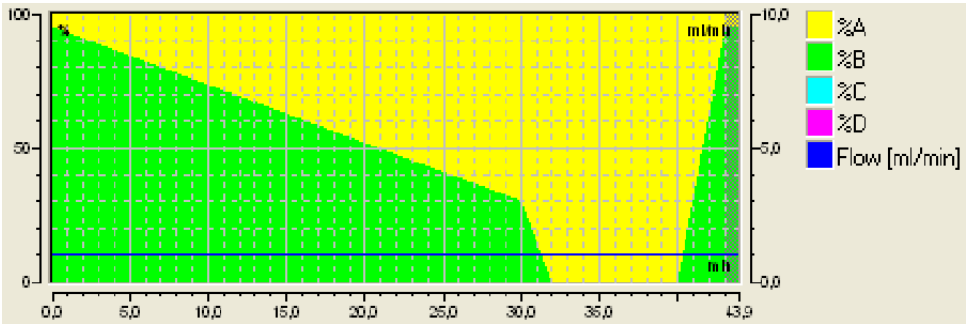

Figure 4.1 LC-DAD and semipreparative HPLC eluent profile.

The low resolution mass spectra (MS) were acquired on an Ion trap LC-ESI-MS device, with an electrospray source, consisting of two 210-LC chromatographic pumps, an automatic ProStar 410 injector, a 20 µL loop and a ProStar 335 Photodiode Array detector, coupled with a mass spectrometer LCQ FleetTM Ion trap from Thermo Scientific. The employed column was a Luna C18 (2) 100A (150 mm x 2.0 mm, i.d., particle size 3 µm, Phenomenex, Torrance, CA), at a flow rate of 0.2 $mL.min^{-1}$. The column oven temperature was 30˚C. A 30.0-min linear gradient from 95 to 30 % 0.1 % aqueous formic acid, followed by a 5.0-min linear gradient to 0 % 0.1 % aqueous formic acid, next a 5.0-min isocratic elution with 100 % acetonitrile, and finally a linear gradient to 5 % of 0.1 % aqueous formic acid, was used in all instances (**Table 4.1**). The mass spectrometer was handled both in positive and negative mode, and the optimized parameters were: 300˚C for capilar temperature; capilar voltage of 28 V; ion spray voltage of 4.5 kV; sweeping gas flow of 5 a.u.; auxiliary gas flow of 10 a.u., cooling gas flow of 35 a.u..

Table 4.1 Gradient program used during the LC –MS analysis.

Retention (min)	Flow (mL/min)	% HCOOH (0.1 %)	%CH_3CN
0.000	0.200	95.0	5.0
0.000	0.200	95.0	0.0
30.000	0.200	30.0	0.0
35.000	0.200	0.0	100.0
40.000	0.200	0.0	100.0
45.000	0.200	5.0	95.0

The high resolution mass spectra (HRMS) were performed on a Q-TOF Impact II Mass Spectrometer from Bruker, with an electrospray source, a capillary voltage of 4.5 kV and a scan range of 50-1000 *m/z.* The chromatographic separation was conducted on a Dionex Ultimate 3000 RSLC nano system using a Kinetex C18 100A (150 mm x 2.1 mm, i.d., particle size 1.7 µm) column at a flow rate of 150 $\mu L.min^{-1}$. A 2.0-min linear gradient of 5 % of acetonitrile/0.1 % formic acid, followed by a 13.0-min linear gradient to 100 % acetonitrile/0.1 % formic acid, next a 5.0-min isocratic elution with 100 % acetonitrile/0.1 % formic acid, next a 2.0-min linear gradient to 5 % acetonitrile/0.1 % formic acid, and finally a 8.0-min linear gradient of 5 % of acetonitrile/0.1 % formic acid, was used in all instances.

Solid Phase Extraction

In order to perform solid phase extraction, cartridges Strata C18-E (55um, 70A), 500 mg/3 mL, Phenomenex were used. For the C18 column conditioning, activation with methanol (5.0 mL) was performed, followed by the equilibration step with water (2 x 5.0 mL), and then sample loading in an appropriate solvent, as a diluted solution. Next, the washing step (to remove pyridine) with water (3 x 5.0 mL), and finally product elution with acetonitrile (1.0 mL) (**Figure 4.2**).

Figure 4.2 Summarized solid phase extraction steps.

4.2 Synthesis of tolvaptan derivatives

4.2.1 Strategies for the mesylation of tolvaptan (41)

Method I

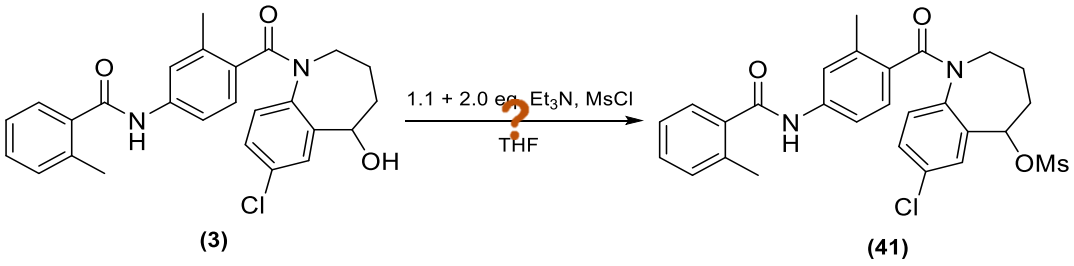

(3) (41)

Figure 4.3 Representation of strategy used for the mesylation of tolvaptan (**3**) by Method I.

To a solution of tolvaptan (**3**) (1.0 eq., 50.0 mg, 111.4 µmol) in THF (4.0 mL), under a nitrogen atmosphere in an ice-cold water bath, triethylamine (1.1 eq., 17.0 µL, 122.0 µmol) was added, followed by methanesulfonyl chloride (1.1 eq., 9.5 µL, 122.7 µmol). The reaction mixture was stirred overnight, and monitored by TLC [CH_2Cl_2/AcOEt (8:2), silica]. An additional 2.0 eq. of both triethylamine and methanesulfonyl chloride were added (**Figure 4.3**). Following 1 h of stirring at r.t., the reaction was stopped upon addition of water (10.0 mL), and extracted with dichloromethane (4 x 5.0 mL). The combined organic layers were dried over anhydrous magnesium sulfate and the solvent was then evaporated under vacuum conditions. The mixture was purified by PTLC [*n*-Hex/AcOEt (9:1), silica], and the resulting fractions stored for further analysis.

Method II

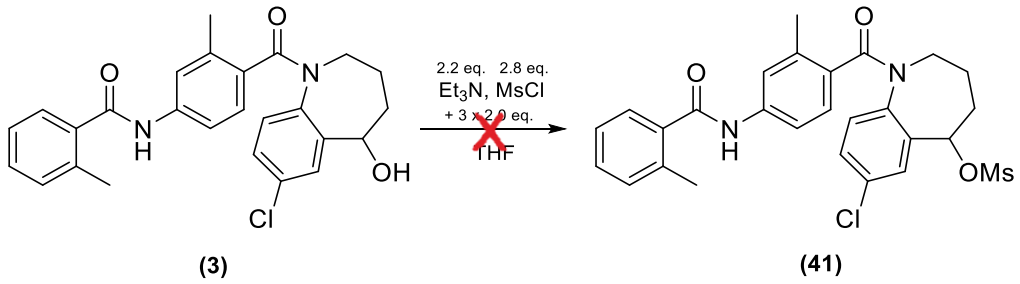

(3) **(41)**

Figure 4.4 Representation of strategy used for the mesylation of tolvaptan (**3**) by Method II.

To a solution of tolvaptan (**3**) (1.0 eq., 20.0 mg, 44.6 µmol) in THF (4.0 mL), in a bath of ice-cold water, was added triethylamine (2.2 eq., 13.6 µL, 97.6 µmol) followed by methanesulfonyl chloride (2.8 eq., 9.6 µL, 124.0 µmol), under a nitrogen atmosphere, the reaction mixture was stirred at 0˚C. Additional 2.0 eq. of triethylamine and methanesulfonyl chloride were added after 2 h, 5 h 40 min and the overnight period of the first addition (**Figure 4.4**). An aliquot from the "overnight + 2.0 eq." reaction was analyzed by LC-DAD, and only the starting material, tolvaptan, was detected.

Method III

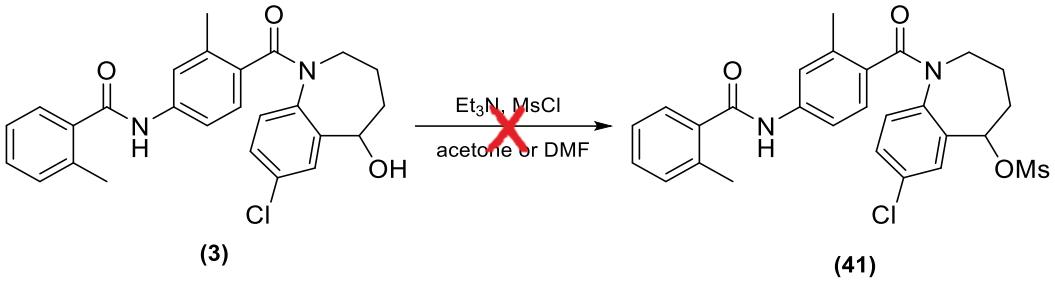

(3) (41)

Figure 4.5 Representation of strategy used for the mesylation of tolvaptan (**3**) by Method III.

To a solution of tolvaptan **(3)** (1.0 eq., 10.0 mg, 22.3 µmol) in a suitable anhydrous solvent (5 mL), in ice-cold water bath, triethylamine (1.0 eq., 3.1 µL, 22.3 µmol) and methanesulfonyl chloride (1.0 eq., 9.6 µL, 22.3 µmol) was added, under nitrogen atmosphere (**Figure 4.5**). The reaction was left stirring at r.t., and after 1h only starting material was observed in the TLC plate [*n*-Hex/AcOEt (1:1), silica]. The reaction was left stirring overnight, after which no changes were detected. One more equivalent of triethylamine and methanesulfonyl chloride was added, and 1 h later no changes were seen (see **Table 4.2**). The reaction was stopped upon addition of H_2O and was subsequently extracted with CH_2Cl_2. The combined organic layers were dried over anhydrous magnesium sulfate and the solvent was then evapored under vacuum conditions. The remaining TVP was recovered.

Table 4.2 Experimental conditions of tolvaptan (**3**) mesylation used by Method III.

Entry	Et_3N (eq.)	MsCl (eq.)	Solvent
1[a]	2.0	2.0	Acetone
2[a]	2.0	2.0	DMF

[a] At the beginning of the reaction 1.0 equivalent of both Et_3N and MsCl were added. One more equivalent of both Et_3N and MsCl was added after the overnight period. Addition of Et_3N and MsCl was done at 0˚C, the mixture was sitirred at r.t.

Method IV

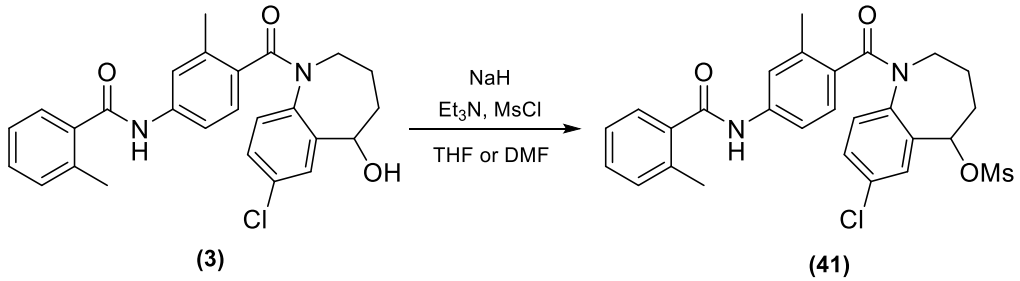

Figure 4.6 Representation of strategy used for the mesylation of tolvaptan (**3**) by Method IV.

To a solution of tolvaptan **(3)** (1.0 eq., 20.0 mg, 44.5 µmol) in a suitable anhydrous solvent (5.0 mL), in ice-cold water bath and under nitrogen atmosphere, sodium hydride (anhydrous, 95 %) (2.0 eq., 14.0 µL, 89.1 µmol) was added. The mixture was allowed to stirred for 5.0 min, whereupon triethylamine and methanesulfonyl chloride, were added (**Figure 4.6**). A second addition of triethylamine and methanesulfonyl chloride was performed and the mixture was stirred overnight at r.t. (see **Table 4.3**). The reaction was stopped upon addition of H_2O and was subsequently extracted with CH_2Cl_2. The combined organic layers were dried over anhydrous magnesium sulfate and the solvent was then evaporated under vacuum. The reaction was monitored by TLC [*n*-Hex/AcOEt (1:1), silica], LC-DAD and LC-ESI-MS. A signal compatible with mesylated tolvaptan was detected with rt = c.a. 29.0 min: **MS (ESI+):** 529 $[^{37}Cl\text{-}MH]^+$, 527 $[^{35}Cl\text{-}MH]^+$.

Table 4.3 Experimental conditions of tolvaptan (**3**) mesylation applied through method IV.

Entry	NaH (eq.)	Et_3N (eq.)	MsCl (eq.)	Solvent	Duration
1[a]	1.0	3.0	3.0	THF	2 days
2[b]	1.0	3.1	3.1	DMF	2 days

[a] One equivalent of both Et_3N and MsCl were added at the beginning of the reaction, and two more equivalents were added after one day. The one day aliquot was analyzed by LC-DAD and LC-ESI-MS/MS.

[b] At the beginning of the reaction 1.1 equivalent of both Et_3N and MsCl were added, and two more were added on the second day, 1.0 eq. in the morning and 1.0 eq. at the end of the day. The 1.5 h aliquot was analyzed by LC-DAD and LC-ESI-MS/MS. DMF was evaporated under vacuum conditions at 40˚C.

Method V

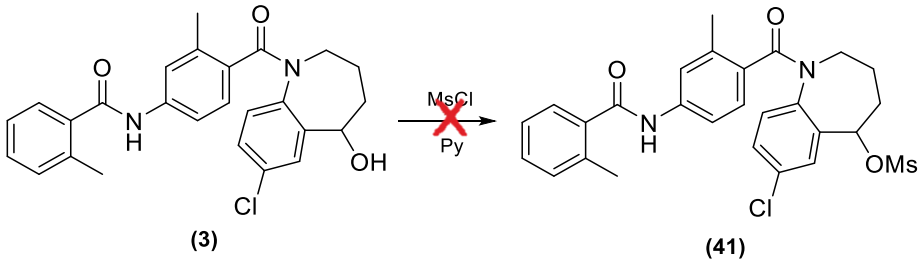

Figure 4.7 Representation of tolvaptan (**3**) mesylation reaction by Method V.

To a solution of tolvaptan **(3)** (1.0 eq., 50.0 mg, 111.4 µmol) in pyridine (5.0 mL, anhydrous), was added methanesulfonyl chloride (1.0 eq., 8.6 µL, 111.4 µmol), in ice-cold water, resulting in a color change from light red brown to very light yellow (**Figure 4.7**). The reaction was left stirring at r.t., and after 1h a new spot was observed in the TLC plate [*n*-Hex/AcOEt (1:1), silica], an aliquot was analyzed by LC-DAD. The reaction was stirred at r.t. overnight. Following 4 more hours at r.t., the reaction was stopped upon the addition of ice-cold water (6.0 mL) and extracted with AcOEt (4 x 10.0 mL). The combined organic layers were washed with HCl (6.0 mL, 1N) and Brine (6.0 mL) and were subsequently dried over anhydrous magnesium sulfate and the solvent was then evaporated under vacuum. The resulting mixture was purified by PTLC [*n*-Hex/AcOEt (1:1), silica]. Upon LC-ESI-MS analysis, the product tolvaptan olefin (**41**) was detected: **MS (ESI+):** 433 $[^{37}Cl\text{-}MH]^+$, 431 $[^{35}Cl\text{-}MH]^+$.

4.2.2 Synthesis of *N*-{4''-[(7'-chloro-2',3'-dihydro-1*H*-benzo[*b*]azepine-1'-yl)carbonyl]-3-methylphenyl}-2-methylbenzamide (42) (tolvaptan olefin)

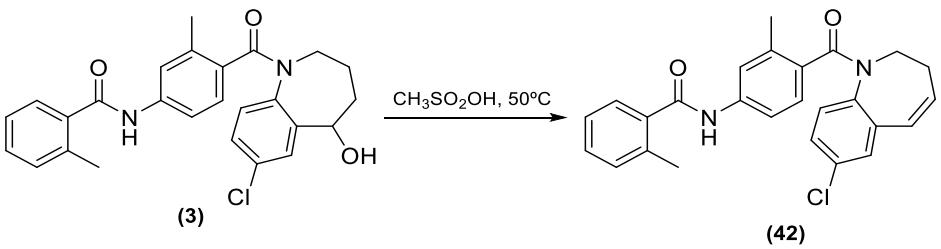

Figure 4.8 Experimental conditions used for the preparation of tolvaptan derivative **42**.

A solution of tolvaptan (**3**) (1.0 eq., 30.0 mg, 66.8 µmol) in methanesulfonic acid (115.4 eq., 500.0 µL, 7.7 mmol) was stirred at 50˚C overnight (**Figure 4.8**), and monitored by TLC [*n*-Hex/AcOEt (1:1), silica]. The reaction was stopped upon addition of H_2O (5.0 mL) and was subsequently extracted with ethyl acetate (3 x 5.0 mL). The combined organic layers were dried over anhydrous magnesium sulfate

and the solvent was then evaporated under vacuum. The crude mixture was purified by PTLC [*n*-Hex/AcOEt/ (6:4), silica]. Compound **42** was obtained in 89 % (16.3 mg) yield, as a very light yellow oil.

HRMS (ESI+) *m/z*: 433.1489 $[^{37}Cl\text{-}MH]^+$, 431.1512 $[^{35}Cl\text{-}MH]^+$, 252.1008 $[C_8H_7O]^+$, 206.0352 $[C_{16}H_{14}NO_2]^+$, 119.0549 $[C_{11}H_9ClNO]^+$.

4.2.3 Synthesis of 7'-chloro-1'-[2'-methyl-4''-(2-methylbenzamido)benzoyl)-2',3',4',5'-tetrahydro-1*H*-benzo[*b*]azepin-5'-yl sulfate (10) (5'-*O*-sulfonate-tolvaptan)

4.2.3.1 Optimization of the synthetic methodology

Method I

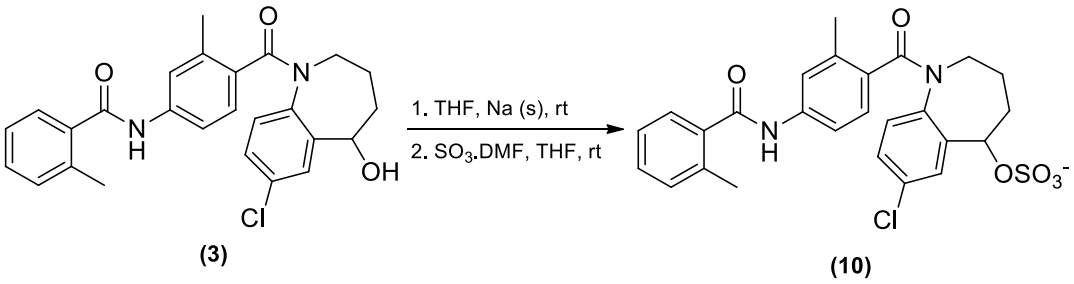

(3) **(10)**

Figure 4.9 Representation of a "two step" tolvaptan's (**3**) sulfonation reaction by Method I.

To a solution of tolvaptan **(3)** (1.0 eq., 100.0 mg, 222.3 µmol) in THF (15 mL) under N_2, sodium (1.1 eq.) was added. The mixture was stirred at r.t. overnight. In a two-necked flask, under nitrogen atmosphere, was prepared a second solution of SO_3•DMF (2.2 eq., c.a. 76.0 mg, 496.2 µmol) in THF (c.a. 2.0 mL). To the second solution it was added dropwise the first solution (1 x 5.0, 1 x 6.0, 1 x 2.5 mL) (**Figure 4.9**). The resulting mixture presented a very light yellow color. The mixture was stirred at r.t. for 0.5 h and was analyzed by LC-DAD[1], only tolvaptan was detected.

[1]Eluent B: 1 M CH_3COONH_4 pH 8.0. Linear gradient of 30.0 min. 5-70 % of acetonitrile in 0.1 M Ammonium Acetate Buffer, followed by a linear gradient of 2.0 min. 70-100% of acetonitrile in 0.1 M Ammonium Acetate Buffer, next a isocratic gradient of 8.0 min. acetonitrile, finishing with a linear column stabilizing gradient of 3 min. 100-5 % of acetonitrile in 0.1 M Ammonium Acetate Buffer.

Method II

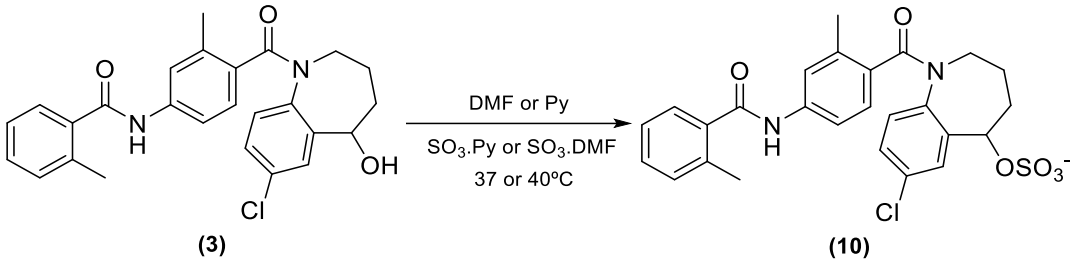

Figure 4.10 Representation of tolvaptan's (**3**) sulfonation reaction by Method II.

To a solution of tolvaptan (**3**) (1.0 eq., 10.0 mg, 22.3 µmol) in an appropriately chosen anhydrous solvent, under a nitrogen atmosphere, was added a sulfate complex either with pyridine or dimethylformamide (SO_3•Pyr or SO_3•DMF, respectively). When SO_3•DMF was used it was also added pyridine (**Figure 4.10**). The reaction mixture was stirred at 37 or 40˚C, for 1 or 2 h (see **Table 4.4**). After 1 or 2 h, the reaction was stopped, upon precipitation with ethyl ether, and centrifuged. The supernatant and the pellet (ressuspended in DMF) were subsequently analyzed by LC-DAD[2].

Table 4.4 Experimental conditions for tolvaptan sulfonation used with method II.

Entry	SO_3•pyr (eq.)	SO_3•DMF (eq.)	Py (eq.)	Solvent	Temperature (˚c)	Duration (h)
1[a]	-	1.1	1.1	DMF	40	2
2[b,d,g]	4.0	-	-	Py	37	1
3[d,e,h]	4.0	-	-	Py	40	2
4[c,e,h]	4.0	-	-	Py	37	2
5[g,h]	4.0	-	-	Py	40	1
6[e,h]	4.0	-	-	Py	37	1

[a]To the starting material, tolvaptan, were added 22.3 µL of dimethylformamide. Aliquots of 1 and 2h of reaction were collected. Although, due to HPLC difficulties, it was not possible to analyzed them, and they were stored at low temperature.

[b]The 1h aliquot was analyzed by LC-DAD, only tolvaptan was detected.

[c]The 1 h 25 min and 2 h aliquots were analyzed by LC-DAD, only tolvaptan was detected.

[d]To the starting material was added first the sulfate complex, and finally the chosen solvent, pyridine.

[2]Eluent B: 1 M CH_3COONH_4 pH 8.0. Linear gradient of 30.0 min. 5-70 % of acetonitrile in 0.1 M Ammonium Acetate Buffer, followed by a linear gradient of 2.0 min. 70-100% of acetonitrile in 0.1 M Ammonium Acetate Buffer, next a isocratic gradient of 8.0 min. acetonitrile, finishing with a linear column stabilizing gradient of 3 min. 100-5 % of acetonitrile in 0.1 M Ammonium Acetate Buffer.

[e]To the starting material, tolvaptan, were added 250.0 µL of pyridine.
[f]The intended temperature was of 37˚C, however, the heating plate did not stabilize properly the temperature and hence the excess 3˚C.
[g]After precipitation, the resulting pellet was resuspended in THF.
[h]After precipitation, the resulting pellet was resuspended in DMF.

Method III

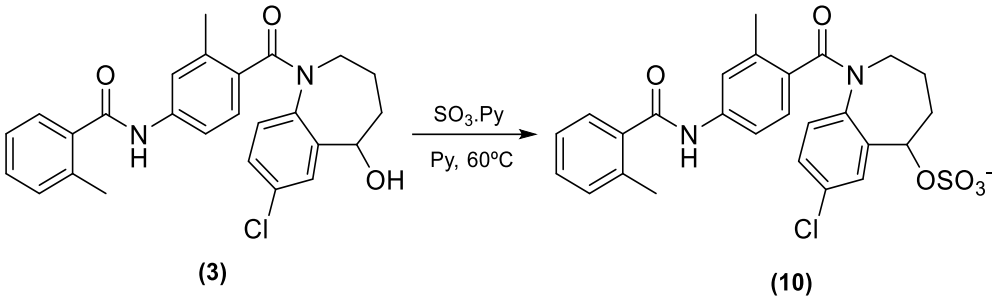

(3) (10)

Figure 4.11 Representation of tolvaptan's (**3**) sulfonation reaction by Method III.

To a solution of anhydrous tolvaptan (**3**) (1.0 eq., 10.0 mg, 22.3 µmol) in anhydrous pyridine, under a nitrogen atmosphere, SO_3•Pyr (**Table 4.5**) was added. The reaction mixture was stirred at 60˚C for a variable period of time (**Figure 4.11**). The reaction was monitored by analytic TLC [CH_3Cl/MeOH (95:5), silica] and LC-DAD[3]. Once the reaction was finished, the mixture was precipitated with diethyl ether (2 x 2.0 mL), and centrifuged between each addition. The pellet was resuspended in DMF and purified by SPE (as described in subsection 4.1). Compound **10** was obtained as a translucent beige oil.

Table 4.5 Experimental conditions of tolvaptan's (**3**) sulfonation applied through method III.

Entry	SO_3•Pyr (eq.)	Py (µL)	Duration (h/day)	R (%)
1[a,b]	31.0	404.0	3 days (71h)	77
2[c,d]	5.1	250.0	1 day (23h)	85
3[d]	5.1	404.0	overnight (21.7h)	84
4	5.0	404.0	7h	88
5	5.0	404.0	overnight	87

[3]Eluent B: 1 M CH_3COONH_4 pH 8.0. Linear gradient of 30.0 min. 5-70 % of acetonitrile in 0.1 M Ammonium Acetate Buffer, followed by a linear gradient of 2.0 min. 70-100% of acetonitrile in 0.1 M Ammonium Acetate Buffer, next a isocratic gradient of 8.0 min. acetonitrile, finishing with a linear column stabilizing gradient of 3 min. 100-5 % of acetonitrile in 0.1 M Ammonium Acetate Buffer.

[a] Aliquots were collected following 6, 24, 48 and 72 h of reaction and analyzed by LC-DAD.
[b]The ressuspended pellet was purified by SPE and the product removed with methanol from the cartridge.
[c]Aliquots were collected following 2, 4, 5 and 6 h of reaction and analyzed by LC-DAD.
[d]The pellet was purified by semipreparative HPLC.

4.2.3.2 Optimized synthetic methodology

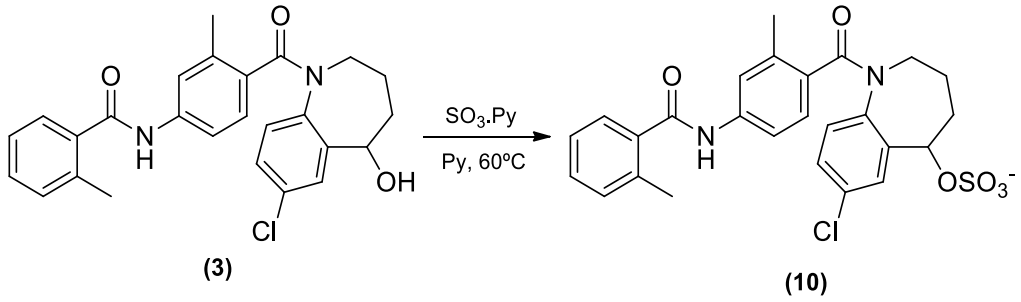

Figure 4.12 Representation of optimized tolvaptan's (**3**) sulfonation methodology.

To a solution of anhydrous tolvaptan (**3**) (1.0 eq., 15.0 mg, 33.4 µmol) in pyridine (604.8 µL), under a nitrogen atmosphere, SO_3•Py (5.0 eq., 26.6 mg, 167.1 µmol) was added. The reaction mixture was stirred at 60˚C overnight (**Figure 4.12**). In the next morning, the reaction was stopped, the mixture was precipitated with ethyl ether (1 x 1.5 and 2 x 2.0 mL), and centrifuged between each addition. The pellet was resuspended in DMF (750.0 µL) and was subsequently purified by SPE. Compound **10** was obtained as a translucent light beige oil, with 89 % yield, and was analyzed by NMR and LC-ESI-HRMS.

500 MHz ^{1}H NMR (CD_3CN): *δ* 1.68-1.68 (1H, m, C*H*$_2$), 1.72-1.78 (1H, m, C*H*$_2$), 2.09 (1H, m, C*H*2), 2.38-2.39 (1H, m, C*H*$_2$), 2.42-2.43 (6H, m, C*H*$_3$), 2.83 (1H, m, C*H*$_2$), 4.67-4.70 (1H, m, C*H*$_2$), 5.57-5.59 (1H, m, C*H*OSO3), 7.00 (1H, m, r*H*), 7.06-7.08 (1H, m, Ar*H*), 7.16 (1H, m, r*H*), 7.26-7.30 (1H, m, ArC*H*), 7.36-7.37 (1H, m, Ar*H*), 7.46-7.48 (1H, m, Ar*H*), 7.53-7.54 (1H, m, Ar*H*), 7.57 (1H, s, Ar*H*), 6.69 (1H, m, Ar*H*), 7.72 (1H, s, Ar*H*), 6.77 (1H, d, *J* = 5, Ar*H*), 8.65 (1H, s, N*H*).

125.7 MHz ^{13}C NMR (CD_3CN): *δ* 18.85 (CH_3), 19.11(CH_3), 25.37 (CH_2), 33.21(CH_2), 45.90 (CH_2),, 75.46 (CH), 116.33 (Ar*C*H), 121.05 (Ar*C*H), 125.00 (Ar*C*H), 127.00 (Ar*C*H), 127.11 (Ar*C*H), 127.34 (Ar*C*H), 129.40 (Ar*C*H), 130.00 (Ar*C*H), 130.75 (Ar*C*H), 131.96 (Ar*C*quat), 132.39 (Ar*C*quat), 136.04 (Ar*C*quat), 136.56 (Ar*C*quat), 136.74(Ar*C*quat), 138.58(Ar*C*quat), 139.22(Ar*C*quat), 142.43(Ar*C*quat), 168.34(C=O), 169.08 (C=O).

HRMS (ESI+): 531.1173 $[^{37}Cl\text{-}MH]^+$, 529.1195 $[^{35}Cl\text{-}MH]^+$, 431.1519 $[C_{26}H_{24}{}^{35}ClN_2O_2]^+$, 433.1498 $[C_{26}H_{24}{}^{37}ClN_2O_2]^+$, 252.1014 $[C_8H_7O]^+$.

4.2.4 Synthesis of 7'-chloro-1'-(2-methyl-4''-(2-methylbenzamido)benzoyl)-2',3',4',5'-tetrahydro-1*H*-benzo[*b*]azepin-5'-yl acetate (11) (5'-*O*-acetyl-tolvaptan)

4.2.4.1 Optimization of the synthetic methodology

Method I

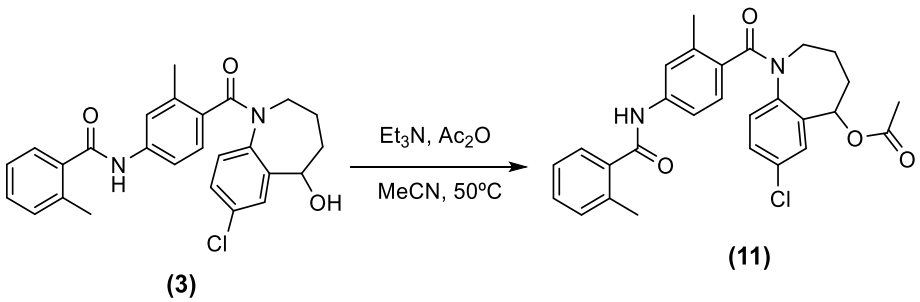

Figure 4.13 Representation of tolvaptan's (**3**) acetylation reaction by Method I.

To a solution of anhydrous tolvaptan **(3)** (1.0 eq., 10.0 mg, 22.3 µmol) in acetonitrile (100.0 µL, anhydrous), triethylamine (1.2 eq., c.a. 5.0 µL, 26.7 µmol) and acetic anhydride (1.2 eq., c.a. 5.0 µL, 26.7 µmol) were added. The reaction was stirred at 50˚C for 24 h (**Figure 4.13**) and monitored by TLC [*n*-Hex/AcOEt (1:1), silica] and LC-DAD. The reaction was stopped upon addition of H_2O (5 mL) and was subsequently extracted with ethyl acetate (3 x 5.0 mL). The combined organic layers were dried over anhydrous magnesium sulfate and the solvent was then evaporated under vacuum. A chromatographic signal, less polar than tolvaptan's, supposed to be tolvaptan acetate was detected upon LC-DAD analysis.

Method II

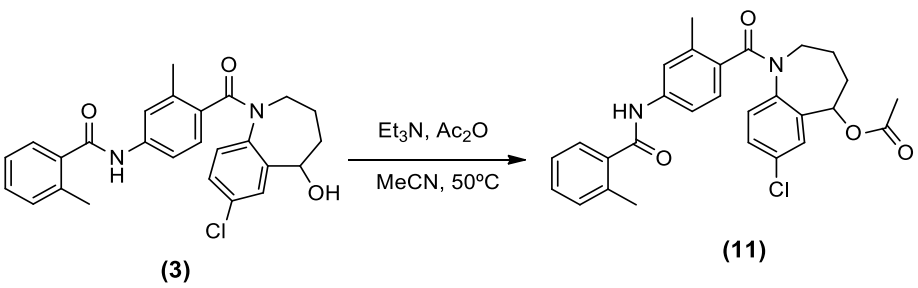

Figure 4.14 Representation of tolvaptan's (**3**) acetylation reaction by Method II.

To a solution of anhydrous tolvaptan **(3)** (1.0 eq., 30.0 mg, 66.8 µmol) in acetonitrile (3.0 mL, anhydrous) was added triethylamine (36.6 eq., 341.0 µL, 2.5 mmol) followed by acetic anhydride (11.9 eq., 75.0 µL, 793.4 µmol), the reaction mixture was stirred at 50˚C for 5 h, and monitored by TLC [*n*-Hex/AcOEt (1:1), silica]. After 4.7 h, a second addition of Et_3N (2.0 eq.) and Ac_2O (2.0 eq.) was performed (**Figure 4.14**). Following 5 h, the reaction was stopped upon addition of H_2O (5 mL) and was subsequently extracted with ethyl acetate (3 x 5.0 mL). The combined organic layers were dried over anhydrous magnesium sulfate and the solvent was then evaporated under vacuum. The organic layer was monitored by TLC and LC-DAD. Compound **11** was obtained as a translucent caramel color solid, in 72 % yield.

500 MHz ^{1}H NMR (CD_3CN): δ 1.73-1.74 (1H, m, C*H*$_2$), 1.75-1.83 (1H, m, C*H*$_2$), 1.99/2.00 (3H, s, C*H*$_3$), 2.06-2.14 (1H, m, C*H*$_2$), 2.11-2.14 (1H, m, C*H*$_2$), 2.20 (3H, s, C*H*$_3$), 2.42 (3H, s, C*H*$_3$), 2.82-2.87 (1H, m, *CH*$_2$), 4.70-4.74 (1H, m, C*H*$_2$), 6.04-6.07 (1H, m, C*H*OAc), 5.98 (1H, d, C*H*$_2$), 6.80 (1H, d, *ArH*), 7.02-7.06 (1H, m, *ArH*), 7.23-7.24 (1H, m, *ArH*), 7.26-7.32 (1H, m, A*rH*), 7.33-7.35 (1H, m, *ArH*), 7.37-7.39 (1H, d, *ArH*), 7.40-7.44 (1H, m, *ArH*), 7.45-7.47 (1H, d, *ArH*), 7.51-7.55 (1H, m, *ArH*), 7.66-7.69 (1H, m, *ArH*), 8.50 (1H, s, N*H*).

125.7 MHz ^{13}C NMR (CD_3CN): δ 18.82 (*C*H$_3$), 19.10 (*C*H$_3$), 20.32 (OC*C*H$_3$), 22.96, 25.13 (*C*H$_2$), 29.76, 31.54 (*C*H$_2$), 45.77 (*C*H$_2$), 72.37 (*C*OAc), 115.99 (Ar*C*H), 120.99 (Ar*C*H), 123.94 (Ar*C*H), 125.59 (Ar*C*H), 127.05 (Ar*C*H), 127.24 (Ar*C*H), 127.52 (Ar*C*H), 130.00 (Ar*C*H), 130.76 (Ar*C*H), 131.80 (Ar*C*quat), 132.66 (Ar*C*quat), 136.03 (Ar*C*quat), 136.58 (Ar*C*quat), 136.98 (Ar*C*quat), 139.03 (Ar*C*quat), 139.40 (Ar*C*quat), 140.42 (Ar*C*quat), 168.15 (C=O), 168.82 (C=O), 169.91 (C=O).

HRMS (ESI): 493.1732 $[^{37}Cl\text{-}MH]^+$, 491.1751 $[^{35}Cl\text{-}MH]^+$, 431.1533 $[C_{26}H_{24}{}^{35}ClN_2O_2]^+$, 433.1513 $[C_{26}H_{24}{}^{37}ClN_2O_2]^+$, 252.1023 $[C_8H_7O]^+$.

Method III

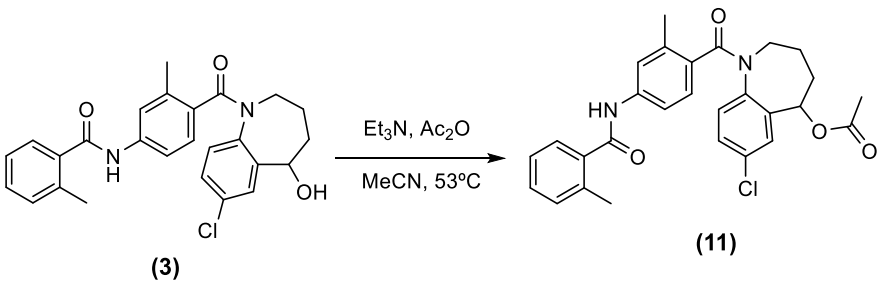

Figure 4.15 Representation of tolvaptan's (**3**) acetylation reaction by Method III.

To a solution of anhydrous tolvaptan **(3)** (1.0 eq., 50.0 mg, 111.4 µmol) in acetonitrile (500.0 µL, anhydrous) triethylamine and acetic anhydride were added (**Table 4.6**). The reaction mixture was stirred at 53˚C for 3.5 h (**Figure 4.15**), and monitored by TLC [*n*-Hex/AcOEt (1:1), silica] and LC-DAD. The reaction was stopped upon addition of H_2O (5.0 mL) and was subsequently extracted with ethyl acetate (3 x 5.0 mL). The combined organic layers were dried over anhydrous magnesium sulfate and the solvent was then evaporated under vacuum. The residue obtained was analyzed by TLC and LC-DAD. Compound **11** was obtained as a translucent caramel color solid.

Table 4.6 Experimental conditions used for tolvaptan acetylation reactions by Method III.

Batch	Et_3N (eq.)	Ac_2O (eq.)	R (%)
1	1.2	1.2	59
2	3.7	1.2	74

Method IV

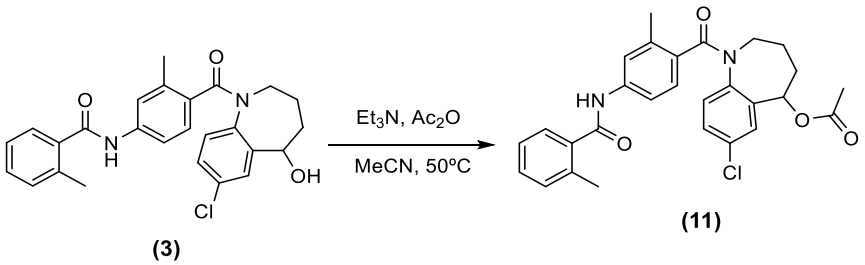

Figure 4.16 Representation of tolvaptan's (**3**) acetylation reaction by Method IV.

To a solution of anhydrous tolvaptan **(3)** (1.0 eq., 55.0 mg, 122.5 µmol) in a variable volume of acetonitrile, was added triethylamine followed by acetic anhydride (**Table 4.7**), the reaction mixture was stirred at 50˚C for 4h (**Figure 4.16**), and monitored by TLC [*n*-Hex/AcOEt (1:1), silica] and LC-DAD.

Elapsed the 4h, the work-up: H_2O addition (5.0 mL) and extraction with ethyl acetate (3 x 5.0 mL) was performed. The organic phases were gathered and concentrated/dried under vacuum conditions. The organic phase was analyzed by TLC and LC-DAD. Compound **11** was obtained as a translucent caramel colored solid.

Table 4.7 Experimental conditions of tolvaptan acetylation reactions by Method IV.

Batch	Et_3N (eq.)	Ac_2O (eq.)	Solvent (µL)	R (%)
1	1.2	1.2	245.0	75
2	3.3	1.1	500.0	79

4.2.4.2 Optimized conditions

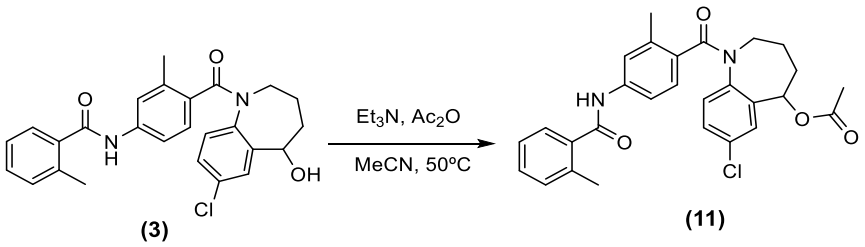

Figure 4.17 Representation of optimized tolvaptan's (**3**) acetylation reaction.

To a solution of anhydrous tolvaptan **(3)** (1.0 eq., 132.6 mg, 295.4 µmol) in acetonitrile (1.3 mL, anhydrous), triethylamine (3.7 eq., 150.6 µL, 1.1 mmol) and acetic anhydride (1.2 eq., 34.0 µL, 351.2 µmol) were added. The reaction mixture was stirred at 50˚C for 5 h (**Figure 4.17**), and monitored by TLC [*n*-Hex/AcOEt (1:1), silica] and LC-DAD. The reaction was stopped upon addition of H_2O (5.0 mL) and was subsequently extracted with ethyl acetate (3 x 5.0 mL). The combined organic layers were dried over anhydrous magnesium sulfate and the solvent was then evaporated under vacuum. Compound **11** was obtained as a translucent rust color solid, in 80 % yield.

4.2.5 Synthesis of *N*-{4''-[(5',7'-dichloro-2',3',4',5'-tetrahydro-1*H*-benzo[*b*]azepine-1'-yl)carbonyl]-3''-methylphenyl}-2-methylbenzamide (46) (5'-chloro-tolvaptan)

Method I

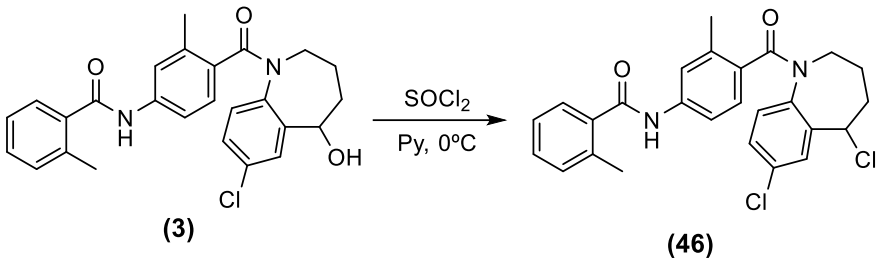

Figure 4.18 Representation of tolvaptan's (**3**) chlorination reaction by Method I.

To a solution of anhydrous tolvaptan **(3)** (1.0 eq., 4.0 mg, 8.9 µmol) in anhydrous pyridine (1.0 mL) was added dropwise thionyl chloride (1.7 eq., 5.5 µL, 15.1 µmol), under a nitrogen atmosphere. The mixture was left stirring at 0˚C for 15.0 min (**Figure 4.18**). The solution was cooled to r.t., whereupon water (80.0 µL) was added. The precipitated formed was filtered and subsequently washed with iced water and methanol. The reaction was monitored by analytic TLC [*n*-Hex/AcOEt (1:1), silica]. Only tolvaptan was detected upon LC-DAD analysis.

Method II

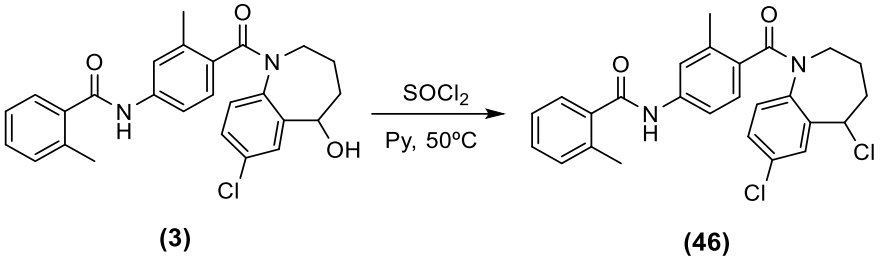

Figure 4.19 Representation of tolvaptan's (**3**) chlorination reaction by Method II.

To a solution of anhydrous tolvaptan **(3)** (1.0 eq., 20.0 mg, 44.6 µmol) in anhydrous pyridine (c.a. 5.0 mL), under a nitrogen atmosphere, thionyl chloride (1.7 eq., 5.5 µL, 75.7 µmol), was added dropwise. The mixture was stirred at 50˚C for 2 h and monitored by TLC [*n*-Hex/AcOEt (1:1), silica]. The solution was cooled to r.t., whereupon water (30.0 mL) and ethyl ether (30 mL) were added. The precipitated formed was filtered and subsequently washed with iced water and methanol. The resulting product was analyzed by LC-DAD, and only tolvaptan was detected.

Method III

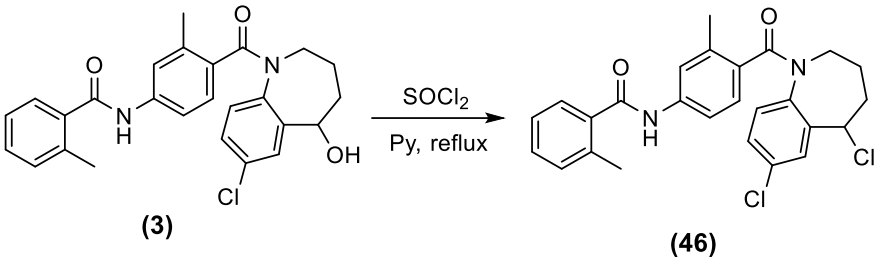

(3) **(46)**

Figure 4.20 Representation of tolvaptan's (**3**) chlorination reaction by Method III.

A solution of anhydrous tolvaptan (**3**) (1.0 eq.) in a variable volume of thionyl chloride, under a nitrogen atmosphere, was refluxed under magnetic stirring for a variable period of time. The reaction was monitored by TLC [*n*-Hex/AcOEt (1:1), silica] (**Table 4.8**). After a variable period of time, the reaction was stopped and the remaining $SOCl_2$ evaporated under vacuum conditions with temperature. The reactional mixture was purified by PTLC, and compound **44** was obtained as a translucent light beige oil and was analyzed by LC-ESI-MS/MS.

Table 4.8 Experimental conditions of tolvaptan's (**3**) chlorination reactions by Method III.

Entry	TVP (µmol)	$SOCl_2$ (mL)	Duration (h)
1	11.1	3	5
2	44.6	12	7

HRMS (ESI+): 471.1215 $[MH+4]^+$, 469.1236 $[MH+2]^+$, 467.1268 $[MH]^+$, 252.1008 $[C_8H_7O]^+$.

4.3 Synthesis of N^6-acetyl-2′-deoxyadenosine (50)

4.3.1 3′,5′-*O*-Bis(*tert*-butyldimethylsilyl)-2′-deoxyadenosine (51)

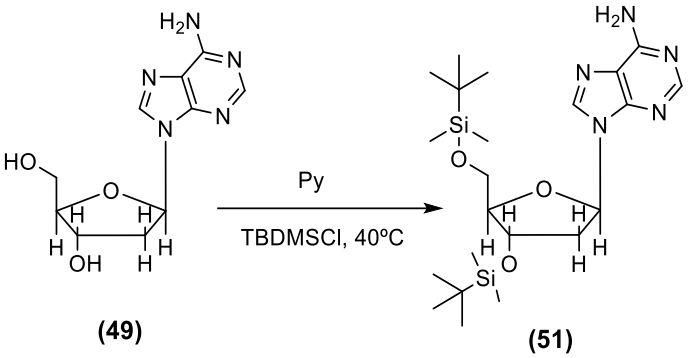

Figure 4.21 Representation of dA's (**49**) silylation reaction.

To a solution of 2'-deoxyadenosine (**50**) (1.0 eq., 200.0 mg, 748.3 µmol) in dried pyridine (5.0 mL), under a nitrogen atmosphere, *t*-butyldimethylsilyl chloride (10 eq., 1.1998 g, 8.0 mmol), was added. The mixture was stirred at 40˚C for 22 h (**Figure 4.21**) and monitored by TLC [CH_2Cl_2/MeOH (10:1), silica]. The reaction was stopped upon the addition of H_2O (10.0 mL) and extracted with CH_2Cl_2 (3 x 15.0 mL). The combined organic layers were dried over anhydrous magnesium sulfate and the solvent was then evaporated under vacuum. The DMF residues were removed upon co-evaporation with toluene. The resulting product was washed with ethyl ether, in order to remove the TBDMSCl in excess, and evaporated/dried under vacuum conditions. A white solid compound was obtained. Since the di-silylation was not complete, both the mono- and di-silylated compounds were obtained, based on the TLC (**Figure 4.22**).

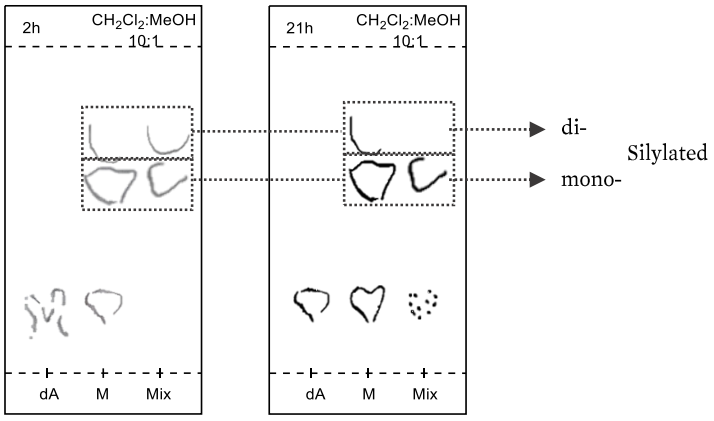

Figure 4.22 Thin Layer Chromatography (TLC) representation of an incomplete dA (**49**) di-silylation reaction.

The white solid was redissolved in pyridine (5.0 mL), under a nitrogen atmosphere, and TBDMSCl (5.0 eq., 599.9 mg, 4.0 mmol) was added. The mixture was stirred at 40˚C, and was monitored by TLC [CH_2Cl_2/MeOH (10:1), silica]. Following 6 h, 10 more equivalents of TBDMSCl were added. The reaction was stopped upon addition of H_2O (5.0 mL) and was subsequently extracted with CH_2Cl_2 (3 x 5.0 mL). The combined organic layers were dried over anhydrous magnesium sulfate and the solvent was then evaporated under vacuum. The pyridine was co-evaporated with toluene under vacuum. The resulting solid was washed with ethyl ether and grinded into smaller fractions. Compound **52** was obtained as a white amorphous solid in 5 % yield, and analyzed through TLC by comparison with a 2'-deoxyadenosine standard.

4.3.2 N^6-acetyl- 3',5'-*O*-bis(*tert*-butyldimethylsilyl)-2'-deoxyadenosine (52)

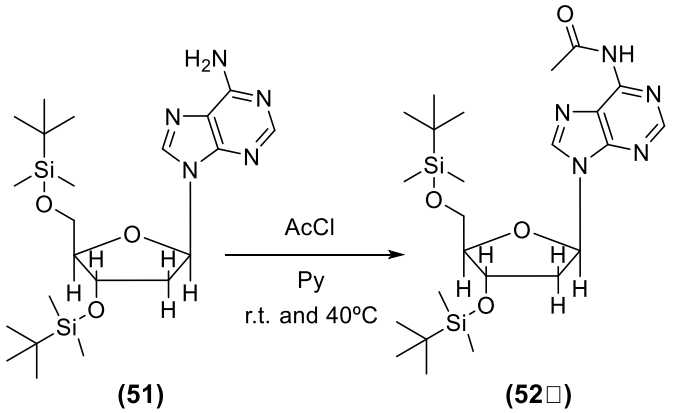

Figure 4.23 Representation of compound **51** acetylation reaction.

To a solution of compound **51** (1.0 eq., 18.8 mg, 74.9 µmol) in pyridine (423.0 µL), acetyl chloride (3.0 eq., 16.0 µL, 224.5 µmol) was added. The mixture was stirred at r.t. and was monitored by TLC [CH_2Cl_2/MeOH (10:0.1), silica]. The temperature was changed to 40˚C after 6 h. Two more equivalents of acetyl chloride (10.5 µL) were added after 8 h and stirred overnight (**Figure 4.23**). The mixture was washed with a saturated solution of $NaHCO_3$, and extracted three times with CH_2Cl_2. The combined organic layers were dried over anhydrous magnesium sulfate and the solvent was then evaporated under vacuum. Compound **52** was obtained as a beige amorphous solid and used in the next synthetic step.

4.3.3 N^6-acetyl-2′-deoxyadenosine (50)

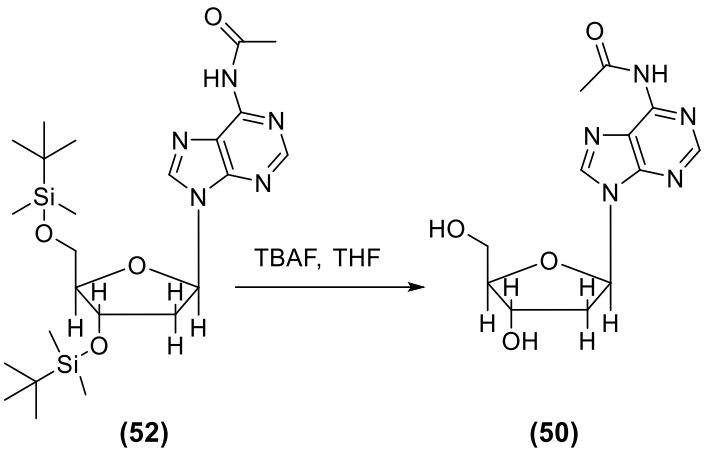

Figure 4.24 Representation of the methodology used for cleavage of the silylated protection groups of compound **52** affording compound **50**.

To a solution of compound **53** (c.a. 21.3 mg) in toluene (1.1 mL), tetrabutylammonium fluoride (TBAF) (c.a. 78.5 μL in THF) was added. The mixture was stirred at r.t. for 1 h, whereupon 4.0 more equivalents of TBAF were added (**Figure 4.24**). Following 20 h, the reaction mixture was decanted, affording and oil and a solution fraction. The oil was washed with THF, affording a brown caramel oil; the solution was concentrated/dried under vacuum conditions, resulting in a white yellow solid. Both the oil and the solid were analyzed by LC-DAD and LC-ESI-MS/MS. N^6-acetyl-2′-deoxyadenosine **(50)** was isolated from the white yellow solid fraction.

HRMS (ESI+): 294.1126 $[MH]^+$, 178.0704 $[MH\text{-}dR]^+$, 136.0617 $[BH]^2$.

4.4 Palladium-Mediated Coupling of *N*-{4''-[(5',7'-dichloro-2',3',4',5'-tetrahydro-1*H*-benzo[*b*]azepine-1'-yl)-carbonyl]-3-methylphenyl}-2-methylbenzamide (45) with 3',5'-*O*-Bis(*tert*-butyldimethylsilyl)-2'-deoxyguanosine (dG•Si, 46)

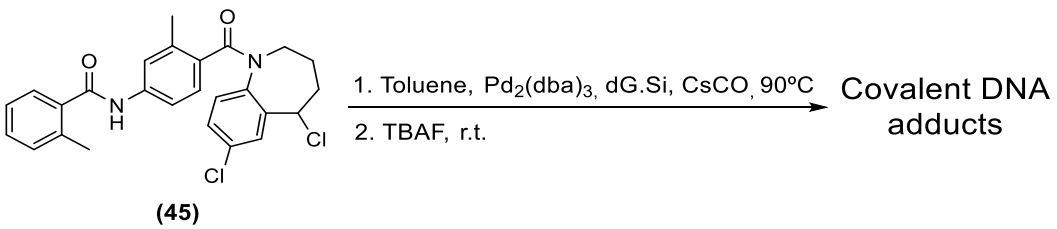

Figure 4.25 Schematic representation of the strategy for the formation of covalent adduct formation between 5'-chloro-tolvaptan (**45**) and dG•Si (**46**).

To a suspension of compound **45** (1.0 eq., 4.5 mg, 6.5 µmol) in toluene (144.0 µL) was prepared in a conic vial, tris-(dibenzylideneacetone)dipalladium (0) [$Pd_2(dba)_3$] (0.1 eq., 0.6 mg, 655.2 nmol) was added. The mixture was stirred at r.t., for 10.0 minutes, whereupon a solution of dG•Si (1.5 eq., 4.8 mg, 9.7 µmol, **46**) and $CsCO_3$ (1.5 eq, 3.2 mg, 9.67 µmol) in toluene (144.0 µL) was added. The resulting mixture was stirred at 90˚C for 3.5 h (**Figure 4.25**) and was monitored by TLC [*n*-Hex/AcOEt (1:1), silica]. Following cooling to r.t. tetrabutyl ammonium fluoride (TBAF) (5.0 eq., 9.31 µL, 32.2 µmol) was added. The resulting solution was stirred at c.a. 38˚C, for 1.5 h. The mixture was transferred to an Eppendorf and centrifuged. After toluene's removal, the remaining residue was dissolved in methanol (1.0 mL) and then centrifuged in order to precipitate the palladium. Both fractions, toluene and methanol, were analyzed by LC-ESI-HRMS and LC-ESI-MS/MS, and 2'-deoxyguanosine adducts were detected in the methanolic fraction.

4.5 Reaction of Tolvaptan and its metabolic plausible electrophiles with bionucleophiles

4.5.1 Reaction with aminoacids

4.5.1.2 Reaction of tolvaptan (3) with *N*-acetyl-cysteine (NAC)

To a solution of tolvaptan (1.0 eq., 11.0 mg, 24.4 µmol) in acetonitrile (300.0 µL) a solution of NAC (3.8 eq., 15.0 mg, 91.9 µmol) in phosphate buffer (pH 7.4 or 10, 50 mM, 1.0 mL) was added. The reaction mixture was incubated at 37˚C for 27 h. Control assays were performed using the same conditions in the absence of NAC. To each solution was added an extra 1.5 mL of phosphate buffer, pH 7 and pH 10, respectively, in order to facilitate homogenization. The reaction mixtures were monitored by LC-DAD and LC-ESI-MS/MS.

4.5.1.3 Reaction of 5'-*O*-sulfonate-tolvaptan (10) with *N*-acetyl-cysteine (NAC)

To a solution of NAC (4.0 eq., 9.9 mg, 60.6 µmol) in phosphate buffer (pH 7.4, 50 mM) was added a solution of 5'-*O*-sulfonate-tolvaptan **(10)** (1.0 eq., 8.0 mg, 15.2 µmol) (obtained as described in subsection 4.2.3.1, method III) in THF, MeCN or DMF (**Table 4.9**). Control assays were performed using the same conditions in the absence of NAC. The reaction mixtures were incubated at 37˚C, and periodically analyzed by LC-DAD[4] (2, *n*24 h).

[4]Eluent B: 1 M CH_3COONH_4 pH 8.0. Linear gradient of 30.0 min. 5-70 % of acetonitrile in 0.1 M Ammonium Acetate Buffer, followed by a linear gradient of 2.0 min. 70-100% of acetonitrile in 0.1 M Ammonium Acetate Buffer, next a isocratic gradient of 8.0 min. acetonitrile, finishing with a linear column stabilizing gradient of 3 min. 100-5 % of acetonitrile in 0.1 M Ammonium Acetate Buffer.

Table 4.9 Experimental conditions of adduct formation between sulfonate derivative of tolvaptan (**10**) and NAC.

Entry	TVP•SO_3^-(10) (eq.)	Solvent	NAC (eq.)	Phosphate Buffer (µL)	LC-DAD
1[a,b]	1.0	DMF	2.0	300.0	periodically
2[c]	1.0	THF	4.0	800.0	2, *n*24 until 72 h, and then 194 and 264 h
3[c]	1.0	MeCN	4.0	1000.0	

[a]A solution of 5'-*O*-sulfonate-tolvaptan was prepared in 100.0 µL of DMF.
[b]To a solution of 5'-*O*-sulfonate-tolvaptan in DMF was added a solution of NAC in phosphate buffer.
[c]A solution of 5'-*O*-sulfonate-tolvaptan was prepared in 200.0 µL of the organic solvent of choice.

4.5.1.4 Reaction of 5'-*O*-acetyl-tolvaptan (11) with *N*-acetyl-cysteine (NAC)

To a solution of NAC (4.0 eq., 9.9 mg, 60.6 µmol) in phosphate buffer (pH 7.4, 50 mM, 1.0 mL) a solution of 5'-*O*-acetyl-tolvaptan **(11)** (1.0 eq., 8.0 mg, 16.3 µmol) (obtained as described in 4.2.4.1, method II/III/IV) in THF (200.0 µL) was added. A blank solution was also prepared. The reaction mixtures were incubated at 37˚C for 72 h, and periodically analyzed by HPLC (2, 24, 48 and 72 h).

4.5.1.5 Reaction of 5'-*O*-sulfonate-tolvaptan (10) with *N*-acetyl-lysine

A solution of 5'-*O*-sulfonate-tolvaptan **(10)** (1.0 eq., 5.0 mg, 9.5 µmol) (obtained as described in 4.2.3.2) in DMF (80 µL) was added to a solution of *N*-acetyl-lysine (4 eq., 7.1 mg, 37.9 µmol) in phosphate buffer (pH 7.4, 50 mM, 1.0 mL). The reaction mixture was incubated at 37˚C, and periodically analyzed by LC-DAD[5] after 2 and 20 h.

4.5.1.6 Reaction of 5'-*O*-sulfonate-tolvaptan (10) and 5'-*O*-acetyl-tolvaptan (11) with Ethyl Valinate

To a solution of ethyl valinate hydrochloride (1.3 eq., 5.0 mg, 27.5 µmol) in phosphate buffer (pH7.4, 50 mM, 400.0 µL for compound **10** or 137.0 µL for compound **11**), was added sodium hydrogenocarbonate and the mixture was stirred at r.t. for 30 min. A solution of 5'-*O*-sulfonate-tolvaptan **(10)** (obtained as described in 4.2.3.2) (1.0 eq., 11.2 mg, 21.2 µmol) or 5'-*O*-acetyl-tolvaptan

[5]Eluent B: 1 M CH_3COONH_4 pH 8.0. Linear gradient of 30.0 min. 5-70 % of acetonitrile in 0.1 M Ammonium Acetate Buffer, followed by a linear gradient of 2.0 min. 70-100% of acetonitrile in 0.1 M Ammonium Acetate Buffer, next a isocratic gradient of 8.0 min. acetonitrile, finishing with a linear column stabilizing gradient of 3 min. 100-5 % of acetonitrile in 0.1 M Ammonium Acetate Buffer.

(**11**) (obtained as described in 4.2.4.1) (1.0 eq., 10.4 mg, 21.2 µmol) in DMF (80.0 µL) or THF (80.0 µL), respectively, was then added to the mixture. The solutions were incubated at 37˚C. The mixtures were periodically analyzed by LC-DAD.

4.5.2 Reaction with 2'-deoxynucleosides

4.5.2.1 Reactions of 5'-*O*-sulfonate-tolvaptan (10) with 2'-deoxyguanosine

Method I

To a solution of 2'-deoxyguanosine (4.0 eq.) in a variable volume of DMF/H_2O (2:1, 187.0 µL or 1000.0 µL, respectively) was added a solution of 5'-*O*-sulfonate-tolvaptan **(10)** (obtained as described in 4.2.3.2) (1.0 eq.) in acetonitrile (500.0 µL) or DMF (100.0 or 376.0 µL). The reaction mixture was incubated at 37˚C, and periodically analyzed by LC-DAD[6].

Method II

A solution of 5'-*O*-sulfonate-tolvaptan **(10)** (obtained as described in 4.2.3.2) (1.2 eq., 18.9 mg, 35.9 µmol) in THF (50.0 µL) was added to a solution of 2'-deoxyguanosine (1.0 eq., 8.0 mg, 29.9 µmol) in DMF/H_2O (2:1, V_T = 250.0 µL). The reaction mixture was incubated at 37˚C and periodically analyzed by LC-DAD[6]. A blank solution, without 2'-deoxyadenine, was prepared. The reaction mixture was purified by semipreparative HPLC and the collected fraction was subsequently analyzed by LC-ESI-MS.

4.5.2.2 Reaction of 5'-*O*-acetyl-tolvaptan (11) with 2'-deoxyguanosine

Method I

A solution of 5'-*O*-acetyl-tolvaptan **(11)** (obtained as described in 4.2.4.2) (1.0 eq.) in THF was added to a solution of 2'-deoxyguanosine (1.8 eq.) in DMF/H_2O (2:1) (**Table 4.10**). A blank solution, without 2'-deoxyguanosine, was prepared. The reaction mixtures were incubated at 37˚C, and periodically analyzed by LC-DAD and LC-ESI-MS/MS.

[6]Eluent B: 1 M CH_3COONH_4 pH 8.0. Linear gradient of 30.0 min. 5-70 % of acetonitrile in 0.1 M Ammonium Acetate Buffer, followed by a linear gradient of 2.0 min. 70-100% of acetonitrile in 0.1 M Ammonium Acetate Buffer, next a isocratic gradient of 8.0 min. acetonitrile, finishing with a linear column stabilizing gradient of 3 min. 100-5 % of acetonitrile in 0.1 M Ammonium Acetate Buffer.

Table 4.10 Experimental conditions of adduct formation between acetate modified tolvaptan (**11**) and dG.

Entry	TVP•Ac (11) (μmol)	THF (μL)	dG (μmol)	DMF/H_2O (μL)
1	4.1	150	7.5	42.0
2	10.2	67.0	18.7	166.0

Method II

A solution of 5'-*O*-acetyl-tolvaptan **(11)** (obtained as described in 4.2.4.2) (1.2 eq., 17.6 mg, 35.9 μmol) in THF was added to a solution of 2'-deoxyguanosine (1.0 eq., 8.0 mg, 29.9 μmol) in 250.0 μL of DMF/H_2O (2:1). A control assay was prepared in the same condition in the absence of 2'-deoxyguanosine. The reaction mixture was incubated at 37˚C, and periodically analyzed by LC-DAD and LC-ESI-MS. The final mixture was purified by semipreparative HPLC.

4.5.2.3 Reaction of 5'-*O*-sulfonate-tolvaptan (10) with 2'-deoxyadenosine

Method I

To a solution of 2'-deoxyadenosine (4.0 eq., 12.8 mg, 95.0 μmol, **49**) in DMF/H_2O (2:1, V_T = 187.0 μL) Next, was added a solution of 5'-*O*-sulfonate-tolvaptan **(10)** (obtained as described in 4.2.3.2) (1.0 eq., 12.5 mg, 23.8 μmol) in acetonitrile (500.0 μL). The reaction mixture was incubated at 37˚C, and periodically analyzed by LC-DAD[7] (0.83, 20.5, 187.6 h).

Method II

A solution of 5'-*O*-sulfonate-tolvaptan **(10)** (obtained as described in 4.2.3.2) (1.2 eq., 18.9 mg, 35.9 μmol) in THF (50.0 μL) was added to a solution of 2'-deoxyadenosine (1.0 eq., 7.5 mg, 29.9 μmol, **49**) in DMF/H_2O (2:1, V_T = 250.0 μL). The reaction mixture was incubated at 37˚C and periodically analyzed
by LC-DAD[7]. A blank solution, without 2'-deoxyadenine, was prepared. The reaction mixture was purified by semipreparative HPLC.

[7]Eluent B: 1 M CH_3COONH_4 pH 8.0. Linear gradient of 30.0 min. 5-70 % of acetonitrile in 0.1 M Ammonium Acetate Buffer, followed by a linear gradient of 2.0 min. 70-100% of acetonitrile in 0.1 M Ammonium Acetate Buffer, next a isocratic gradient of 8.0 min. acetonitrile, finishing with a linear column stabilizing gradient of 3 min. 100-5 % of acetonitrile in 0.1 M Ammonium Acetate Buffer.

4.5.2.4 Reaction of 5'-*O*-acetyl-tolvaptan (11) with 2'-deoxyadenosine

Method I

A solution of 5'-*O*-acetyl-tolvaptan **(11)** (obtained as described in 4.2.4.2) (1.0 eq., 5.0 mg, 10.2 µmol) in THF (150.0 µL) was added to solution of 2'-deoxyadenosine (1.7 eq., 4.3 mg, 17.1 µmol, **49**) in DMF/H_2O (2:1, V_T = 144.0 µL). The reaction mixture was incubated at 37˚C, and periodically analyzed by HPLC (121 h, 188 h).

Method II

A solution of 5'-*O*-acetyl-tolvaptan **(11)** (obtained as described in 4.2.4.2) in a variable volume of THF was added to a solution of 2'-deoxyadenosine (1.0 eq., **49**) in a variable volume of DMF/H_2O (2:1) (**Table 4.11**). The reaction mixtures were incubated at 37˚C, and periodically analyzed by LC-DAD (2, *n*24 h).

Table 4.11 Experimental conditions of adduct formation between sulfate modified tolvaptan (**3**) and dA (**49**).

Entry	TVP•Ac (11) (eq.)	THF (µL)	dA (µmol)	DMF/H_2O (µL)
1	1.1	67.0	6.0	48.0
2[a]	1.2	50.0	29.9	250.0

[a]Two blank solutions were prepared, one without 2'-deoxyadenine and one without 5'-*O*-acetyl-tolvaptan.

4.5.3 Reactions with DNA

4.5.3.1 Reaction of 5'-*O*-sulfonate-tolvaptan (10) with DNA

A solution of 5'-*O*-sulfonate-tolvaptan **(10)** (obtained as described in 4.2.3.2) (5 mg, 9.5 µmol) in DMF (1.0 mL) was added to a solution of salmon testes DNA (5.0 mg) in 5 mM Bis-Tris and 0.1 mM EDTA buffer (pH7.24, 4.0 mL). The reaction mixture was incubated at 37˚C for 10 days. Following removal of non-bonded material by extraction with ethyl acetate (2 x 2.0 mL), DNA was precipitated by addition of 5 M NaCl (90.0 µL) and ethanol (3.0 mL), at -21˚C. After centrifugation, the DNA pellet was washed with ice-cold 70 % ethanol (1 x 3.0 mL) and redissolved in 5.0 mL of 5 mM Bis-Tris and 0.1 mM EDTA (pH 7.24). One aliquot was hydrolyzed enzymatically as described in **4.6.1**, and the other subjected to neutral thermal hydrolysis as described in **4.6.2**.

4.5.3.2 Reaction of 5'-*O*-acetyl-tolvaptan (11) with DNA

A solution of 5'-*O*-acetyl-tolvaptan **(11)** (obtained as described in 4.2.4.2) (5.0 mg, 10.2 µmol) in THF (1.0 mL) was added to a solution of salmon testes DNA (5.0 mg) in 5 mM Bis-Tris and 0.1 mM EDTA buffer (pH 7.24, 4.0 mL). The reaction mixture was incubated at 37˚C for 4 days. Following removal of non-bonded material by extraction with ethyl acetate (2 x 2.0 mL), DNA was precipitated by addition of 5 M NaCl (90.0 µL) and ethanol (3.0 mL), at -21˚C. After centrifugation, the DNA pellet was washed with ice-cold 70 % ethanol (1 x 3.0 mL) and redissolved in 5.0 mL of 5 mM Bis-Tris and 0.1 mM EDTA (pH 7.24). One aliquot was hydrolyzed enzymatically as described in **4.6.1,** and the other subjected to neutral thermal hydrolysis as described in **4.6.2**.

4.6 DNA Hydrolysis

4.6.1 *Enzymatic hydrolysis*

The modified DNA solution was hydrolyzed enzymatically, obtaining 2'-deoxynucleosides by adding firstly $MgCl_2$ (1M, 10µL/mg DNA), DNase I (0.1 mg/mg DNA) and 0.1 mL of DNase buffer (150 mM NaCl, 10 mM $MgCl_2$) incubating the solutions at 37˚C for 3 h. Secondly, was added Tris-HCl (pH c.a. 8, 1M, 10 µL/mg DNA), phosphodiesterase I (10 µL/mg DNA) and alkaline phosphatase (4 µL/mg DNA), incubating the solutions at 37˚C overnight (adapted from [35]).

The adducts were then partitioned into *n*-butanol presaturated with water, and the *n*-butanol fractions combined and back-extracted with water presaturated with *n*-butanol. After the *n*-butanol was evaporated, the remaining residue was redissolved and analyzed by LC-ESI-MS/MS (adapted from [35]).

4.6.2 *Neutral Thermal Hydrolysis*

The modified DNA solution undergone thermal hydrolysis, in order to release the depurinating adducts. The DNA solutions were heated at 100˚C for a period of 10 min. and subsequently cooled to room temperature and eluted through a prewashed Amicon Microcon 3 kDa molecular weight cutoff centrifugal size exclusion column, by centrifugation at 15500g, 10 x 15 min ($V_{centrifugation}$ = 500.0 µL), at room temperature (adapted from [57])

The resulting fractions were combined and concentrated, and then analyzed by LC-ESI-MS/MS.

References

[1] C. A. Villabona, "Papel de los vaptanes en el tratamiento de la hiponatremia", Chap 16, in *Actualización en Neuroendocrinología*, J. M. G. Ed. Madrid: Elsevier, **2015**, pp. 251–268.

[2] Vaprisol® (Conivaptan hydrochloride) Prescribing Information. U. S. Food and Drug Adminstration. 2012. http://www.accessdata.fda.gov/drugsatfda_docs/label/2012/021697s003lbl.pdf (acessed Aug 6, 2015).

[3] J. Li and D. Johnson, *Modern Drug Synthesis*. Wiley, **2010**.

[4] Samsca® (tolvaptan) Prescribing Information. U. S. Food and Drug Adminstration. 2014. http://www.otsuka-us.com/products/Documents/Samsca.PI.pdf (acessed Feb 13, 2015).

[5] V. E. Torres, A. B. Chapman, O. Devuyst, R. T. Gansevoort, J. J. Grantham, E. Higashihara, R. D. Perrone, H. B. Krasa, J. Ouyang, and F. S. Czerwiec, "Tolvaptan in patients with autosomal dominant polycystic kidney disease.," *N. Engl. J. Med.*, vol. 367, no. 25, pp. 2407–18, **2012**.

[6] Drug Safety Communication: Samsca (tolvaptan). U. S. Food and Drug Admnistration. 2013. http://www.fda.gov/downloads/Drugs/DrugSafety/UCM350084.pdf (acessed Aug 18, 2015).

[7] CHMP ASSESSMENT REPORT FOR Samsca. European Medicines Agency: Evaluation of Medicines for Human Use. 2009. http://www.ema.europa.eu/docs/en_GB/document_library/EPAR_-_Public_assessment_report/human/000980/WC500048715.pdf (acessed Aug 18, 2015).

[8] M. Furukawa, K. Miyata, C. Kawasome, Y. Himeda, K. Takeuchi, T. Koga, Y. Hirao,and K. Umehara, "Liquid chromatography–tandem mass spectrometry method for determining tolvaptan and its nine metabolites in rat serum: application to a pharmacokinetic study," *Arch. Pharm. Res.*, vol. 37, no. 12, pp. 1578–1587, **2014**.

[9] W. L. Wan, J. B. Wu, F. Lei, X. L. Li, L. Hai, and Y. Wu, "Synthesis of the major metabolites of Tolvaptan", *Chinese Chem. Lett.*, vol. 23, no. 12, pp. 1343–1346, **2012**.

[10] M. Coleman, *Human Drug Metabolism - An Introduction*, 2nd ed. John Wiley & Sons, Ltd, 2010.

[11] R. B. Silverman and M. W. Holladay, "Chapter 8 - Drug Metabolism," in *The Organic Chemistry of Drug Design and Drug Action*, 3rd ed., Academic Press, **2014**, pp. 357–422.

[12] A. Parkinson, "Chapter 6 - Biotransformation of Xenobiotics" in *Casarett and Doull's Toxicology: The Basic Science of Poisons*, 8th ed, C. K. **2013**, pp. 133-224.

[13] M. J. Zamek-Gliszczynski, K. a. Hoffmaster, K. I. Nezasa, M. N. Tallman, and K. L. R. Brouwer, "Integration of hepatic drug transporters and phase II metabolizing enzymes: Mechanisms of hepatic excretion of sulfate, glucuronide, and glutathione metabolites," *Eur. J. Pharm. Sci.*, vol. 27, no. 5, pp. 447–486, **2006**.

[14] R. Remmel, S. Nagar, and U. Argikar, "Conjugative Metabolism of Drugs," in *Drug Metabolism in Drug Design and Development - Basic Concepts and Practice*, D. Zhang, M. Zhu, and W. G. Humphreys, Eds. Hoboken, NJ, USA: John Wiley & Sons, Inc., **2007**, pp. 37–88.

[15] N. Gamage, A. Barnett, N. Hempel, R. G. Duggleby, K. F. Windmill, J. L. Martin, and M. E. Mcmanus, "Human Sulfotransferases and Their Role in Chemical Metabolism," vol. 90, no. 1, pp. 5–22, **2006**.

[16] K. S. Pang, A. J. Schwab, C. A. Goresky, and M. Chiba, "Transport, binding, and metabolism of sulfate conjugates in the liver," *Chem. Biol. Interact.*, vol. 92, no. 1, pp. 179–207, **1994**.

[17] C. N. Falany, X. Xie, J. Wang, J. Ferrer, and J. L. Falany, "Molecular cloning and expression of novel sulphotransferase-like cDNAs from human and rat brain," *Biochem. J.*, vol. 346, pp. 857–64, **2000**.

[18] R. M. Weinshilboum, D. M. Otterness, I. a Aksoy, T. C. Wood, C. Her, and R. B. Raftogianis, "Sulfation and sulfotransferases 1: Sulfotransferase molecular biology: cDNAs and genes," *FASEB J.*, vol. 11, pp. 3–14, **1997**.

[19] C. Her, T. C. Wood, E. E. Eichler, H. W. Mohrenweiser, L. S. Ramagli, M. J. Siciliano, and R. M. Weinshilboum, "Human hydroxysteroid sulfotransferase SULT2B1: Two enzymes encoded by a single chromosome 19 gene", *Genomics*, vol. 53, no. 3, pp. 284–295, **1998**.

[20] D. M. Otterness and R. Weinshilboum, "Human dehydroepiandrosterone sulfotransferase: molecular cloning of cDNA and genomic DNA", *Chem. Biol. Interact.*, vol. 92, no. 1–3, pp. 145–159, Jun. **1994**.

[21] C. A. Strott, "Sulfonation and molecular action", *Endocr. Rev.*, vol. 23, no. 5, pp. 703–732, 2002.

[22] Y. Yamazoe, K. Nagata, S. Ozawa, and R. Kato, "Structural similarity and diversity of sulfotransferases", *Chem. Biol. Interact.*, vol. 92, no. 1–3, pp. 107–117, Jun. **1994**.

[23] T. C. Wood, I. A. Aksoy, S. Aksoy, and R. M. Weinshilboum, "Human Liver Thermolabile Phenol Sulfotransferase: cDNA Cloning, Expression and Characterization", *Biochem. Biophys. Res. Commun.*, vol. 198, no. 3, pp. 1119–1127, Feb. **1994**.

[24] X. Y. Zhu, M. E. Veronese, L. N. Sansom, and M. E. Mcmanus, "Molecular Characterization of a Human Aryl Sulfotransferase cDNA", *Biochem. Biophys. Res. Commun.*, vol. 192, no. 2, pp. 671–676, Apr. **1993**.

[25] X. Zhu, M. E. Veronese, P. A. T. Iocco, and M. E. Mcmanus, "cDNA Cloning and Expression of a New Form of Human Aryl Sulfotransferase", *Int. J. Biochem. Cell Biol.*, vol. 28, no. 5, pp. 565–571, **1996**.

[26] J. P. Uetrecht and W. Trager, *Drug metabolism : chemical and enzymatic aspects*. New York: Informa healthcare, **2007**.

[27] P. Smith. 2009. "Phase II Metabolism of Drugs". University of North Carolina. 2009 http://www.unc.edu/courses/2009fall/envr/442/001/Phase2Metab,General,9.2009.pdf (acessed Aug 18, 2015).

[28] Absorption, Distribution, Metabolism and Excretion (ADME): NST110: Advanced Toxicology, Lecture 5: Phase II Metabolism. Department of Nutritional Sciences and Toxicology, University of California, Berkeley. http://nature.berkeley.edu/~dnomura/pdf/Lecture5. (acessed Aug 6, 2015).

[29] P. E. Hanna, "*N*-Acetyltransferases, *O*-Acetyltransferases, and *N,O*-Acetyltransferases: Enzymology and Bioactivation," in *Conjugation-Dependent Carcinogenicity and Toxicity of Foreign Compounds*, D. M. W., Anders; W., Ed. Academic Press, **1994**, pp. 401–430.

[30] P. Jančová and M. Šiller, "Phase II Drug Metabolism, Topics on Drug Metabolism", Dr. James Paxton (Ed.), **2012**. Available from: http://www.intechopen.com/books/topics-on-drug-metabolism/phase-ii-dr. (acessed Aug 22, 2015).

[31] M. Blum, D. M. Grant, a Demierre, and U. a Meyer, "N-acetylation pharmacogenetics: a gene deletion causes absence of arylamine N-acetyltransferase in liver of slow acetylator rabbits.", *Proc. Natl. Acad. Sci. U. S. A.*, vol. 86, no. 23, pp. 9554–7, **1989**.

[32] G. Ginsberg, D. Hattis, A. Russ, and B. Sonawane, "Physiologically based pharmacokinetic (PBPK) modeling of caffeine and theophylline in neonates and adults: implications for assessing children's risks from environmental agents.", *J. Toxicol. Environ. Health. A*, vol. 67, no. 4, pp. 297–329, **2004**.

[33] A. Kawamura, J. Graham, A. Mushtaq, S. A. Tsiftsoglou, G. M. Vath, P. E. Hanna, C. R. Wagner, and E. Sim, "Eukaryotic arylamine N-acetyltransferase", *Biochem. Pharmacol.*, vol. 69, no. 2, pp. 347–359, **2005**.

[34] R. B. Silverman and M. W. Holladay, "Chapter 6 - DNA-Interactive Agents", in *The Organic Chemistry of Drug Design and Drug Action*, 3rd ed., R. B. B. T.-T. O. C. of D. D. and D. A. (Second E. Silverman, Ed. San Diego: Academic Press, **2014**, pp. 323–403.

[35] A. M. M. Antunes, M. P. Duarte, P. P. Santos, G. G. Da Costa, T. M. Heinze, F. A. Beland, and M. M. Marques, "Synthesis and characterization of DNA adducts from the HIV reverse transcriptase inhibitor nevirapine", *Chem. Res. Toxicol.*, vol. 21, no. 7, pp. 1443–1456, **2008**.

[36] A. M. M. Antunes, A. L. A. Godinho, I. L. Martins, G. C. Justino, F. a Beland, and M. M. Marques, "Amino acid adduct formation by the nevirapine metabolite, 12-hydroxynevirapine--a possible factor in nevirapine toxicity.", *Chem. Res. Toxicol.*, vol. 23, no. 5, pp. 888–99, **2010**.

[37] A. M. M. Antunes, A. L. A. Godinho, I. L. Martins, M. C. Oliveira, R. A. Gomes, A. V Coelho, F. A. Beland, and M. M. Marques, "Protein adducts as prospective biomarkers of nevirapine

toxicity.", *Chem. Res. Toxicol.*, vol. 23, no. 11, pp. 1714–25, **2010**.

[38] A. M. Sharma, K. Klarskov, and J. Uetrecht, "Nevirapine bioactivation and covalent binding in the skin.", *Chem. Res. Toxicol.*, vol. 26, no. 3, pp. 410–21, **2013**.

[39] G. Gamboa da Costa, L. P. McDaniel-Hamilton, R. H. Heflich, M. M. Marques, and F. a Beland, "DNA adduct formation and mutant induction in Sprague-Dawley rats treated with tamoxifen and its derivatives.", *Carcinogenesis*, vol. 22, no. 8, pp. 1307–1315, **2001**.

[40] G. Gamboa da Costa, M. M. Marques, X. Fu, M. I. Churchwell, Y. P. Wang, D. R. Doerge, and F. A. Beland, "Effect of N,N-didesmethyltamoxifen upon DNA adduct formation by tamoxifen and α-hydroxytamoxifen", *Cancer Lett.*, vol. 257, no. 2, pp. 191–198, **2007**.

[41] S. Y. Kim, Y. R. S. Laxmi, N. Suzuki, K. Ogura, T. Watabe, M. W. Duffel, and S. Shibutani, "Formation of Tamoxifen-Dna Adducts Via O -Sulfonation , Not O -Acetylation , of α-Hydroxytamoxifen in Rat and Human Livers", *Drug Metab. Dispos. Dispos.*, vol. 33, no. 11, pp. 1673–1678, **2005**.

[42] A. Manuscript, "NIH Public Access", *Discovery*, vol. 66, no. 16, pp. 2907–2918, **2011**.

[43] C. Charneira, A. L. A. Godinho, M. C. Oliveira, S. A. Pereira, E. C. Monteiro, M. M. Marques, and A. M. M. Antunes, "Reactive aldehyde metabolites from the anti-HIV drug abacavir: amino acid adducts as possible factors in abacavir toxicity.", *Chem. Res. Toxicol.*, vol. 24, no. 12, pp. 2129–41, **2011**.

[44] C. Charneira, N. M. Grilo, S. A. Pereira, A. L. A. Godinho, E. C. Monteiro, M. M. Marques, and A. M. M. Antunes, "N-terminal valine adduct from the anti-HIV drug abacavir in rat haemoglobin as evidence for abacavir metabolism to a reactive aldehyde in vivo.", *Br. J. Pharmacol.*, vol. 167, no. 6, pp. 1353–61, **2012**.

[45] M. Törnqvist, "Epoxide adducts to N-terminal valine of hemoglobin.", *Methods Enzym.*, vol. 231, pp. 650–657, **1994**.

[46] A. M. M. Antunes, M. Sidarus, D. A. Novais, S. G. Harjivan, P. P. Santos, J. L. Ferreira da Silva, F. A. Beland, and M. M. Marques, "Oxidation of 2-Hydroxynevirapine, a Phenolic Metabolite of the Anti-HIV Drug Nevirapine: Evidence for an Unusual Pyridine Ring Contraction", *Molecules*, vol. 17, no. 12, pp. 2616–2627, **2012**.

[47] M. K. Lakshman, "Synthesis of biologically important nucleoside analogs by palladium-catalyzed C-N bond-formation", *Curr. Org. Synth.*, vol. 2, no. 1, pp. 83–112, **2005**.

[48] J. Tsuji, *Palladium Reagents and Catalysts*. John Wiley & Sons, Ltd, **2004**.

[49] H. W. Kim, Y. S. Lee, D. Shetty, H. J. Lee, D. S. Lee, J. K. Chung, M. C. Lee, K. H. Chung, and J. M. Jeong, "Facile chlorination of benzyl alcohols using 1,8-diazabicyclo[5.4.0]undec- 7-ene (DBU) and sulfonyl chlorides", *Bull. Korean Chem. Soc.*, vol. 31, no. 11, pp. 3434–3436, **2010**.

[50] D. A. Rodriguez and R. Priefer, "Sulfite formation versus chlorination of benzyl alcohols with thionyl chloride", *Tetrahedron Lett.*, vol. 55, no. 19, pp. 3045–3048, **2014**.

[51] A. G. Brenton and A. R. Godfrey, "Accurate Mass Measurement: Terminology and Treatment of Data", *J. Am. Soc. Mass Spectrom.*, vol. 21, no. 11, pp. 1821–1835, **2010**.

[52] M. Holčapek, R. Jirásko, and M. Lísa, "Recent developments in liquid chromatography-mass spectrometry and related techniques", *J. Chromatogr. A*, vol. 1259, pp. 3–15, **2012**.

[53] M. Simonyi, "The concept of chiral conformers and its significance in molecular pharmacology", in *Advances in Drug Research*, vol. 30, B. Testa and U. A. Meyer, Eds. Academic Press, **1997**, pp. 73–110.

[54] Educational Portal of Protein Data Bank, PDB-101, Molecule of the Month: DNA. 2004 http://pdb101.rcsb.org/motm/23. (acessed Aug 22, 2015)

[55] W. L. E. Armarego and C. L. L. Chai, *Purification of Laboratory Chemicals*, 5th ed. Elsevier Science, **2003**.

[56] T. D. W. Claridge, *High-Resolution NMR Techniques in Organic Chemistry*, 1st ed., vol. 19. Oxford: Elsevier Science Ltd, **1999**.

[57] G. G. Da Costa, M. I. Churchwell, L. P. Hamilton, L. S. Von Tungeln, F. a. Beland, M. M. Marques, and D. R. Doerge, "DNA Adduct Formation from Acrylamide via Conversion To Glycidamide in Adult and Neonatal Mice", *Chem. Res. Toxicol.*, vol. 16, no. 10, pp. 1328–1337, **2003**.